

GROWTH PARAMETERS FOR SACCHAROMYCES
CEREVISIAE IN GLUCOSE
CONTAINING MEDIA

by

GLENN CRAIG BOYD, B.S. in Ch.E.

A THESIS

IN

CHEMICAL ENGINEERING

Submitted to the Graduate Faculty
of Texas Tech University in
Partial Fulfillment of
the Requirements for
the Degree of

MASTER OF SCIENCE

IN

CHEMICAL ENGINEERING

Approved

Accepted

August, 1985

AC
805
T3
1985
No. 67
Cop. 2-

ACKNOWLEDGEMENTS

I would like to thank the members of my committee, Dr. Steven R. Beck, Dr. Caryl E. Heintz and Dr. Fred Senatore. Appreciation is extended to Dr. L. D. Clements for his guidance. I would like to thank the faculty of the Department of Chemical Engineering for putting up with me for so long.

I want to especially thank Laurie Wade and my other friends, Steve and Cathy Duran, Dan Baker, Larry File, Gary Baumgarten, Desi MacDonald, Sue Willis and Steve Beck. Also, I want to thank everyone I taught in Process Control Lab and my best student, R. L. Myers.

TABLE OF CONTENTS

	PAGE
ACKNOWLEDGEMENTS.....	ii
LIST OF TABLES.....	vi
LIST OF FIGURES.....	vii
NOMENCLATURE.....	xiii
CHAPTER 1 INTRODUCTION.....	1
CHAPTER 2 LITERATURE REVIEW.....	3
Fermentation of Glucose to Ethanol.....	3
Cell Cycle.....	3
Growth-Cycle for Batch Fermentation.....	7
Lag Phase.....	7
Exponential Growth Phase.....	9
Stationary Phase.....	10
Death Phase.....	12
Exponential Growth Models.....	12
The Effect of Temperature on the Maximum Specific Growth Rate.....	17
CHAPTER 3 EXPERIMENTAL APPARATUS.....	19
Batch Fermenter.....	19
CHAPTER 4 EXPERIMENTAL PROCEDURE.....	23
Preparation of the Media.....	23
Slants.....	23
Broth.....	26

	PAGE
Plates.....	26
Synthetic Media.....	29
Plate Count and Optical Density.....	31
Preparation of Glucose Standards.....	34
Glucose Analysis.....	35
Operation Procedure for the Batch Fermenter.....	38
CHAPTER 5 DISCUSSION OF RESULTS.....	40
Operating Conditions.....	40
Experimental Problems.....	41
Ethanol.....	41
Cell Count Versus Optical Density.....	43
Calculation of the Specific Growth Rate.....	45
Modeling the Specific Growth Rates.....	45
Sensitivity of the Parameter Values.....	52
Temperature Effects on the Specific Growth Rate.....	59
Temperature Effects on the Maximum Specific Growth Rates.....	64
Glucose Analysis.....	65
pH Effects.....	73
CHAPTER 6 CONCLUSIONS AND RECOMMENDATIONS.....	75
Conclusions.....	75
Recommendations.....	75

	PAGE
LIST OF REFERENCES.....	76
APPENDIX A TYPICAL TEMPERATURE PROFILE.....	79
APPENDIX B GENERAL LEAST SQUARES PROGRAM.....	84
APPENDIX C SPECIFIC GROWTH RATE CURVES.....	86
APPENDIX D NLIN PROGRAMS FOR THE MONOD, MOSER AND TEISSER EXPRESSIONS.....	105
APPENDIX E VIABLE CELL CONCENTRATION PROFILE.....	109
APPENDIX F NLIN PROGRAMS FOR THE ARRHENIUS EXPRESSION IN THE MONOD, MOSER AND TEISSER EXPRESSIONS.....	111
APPENDIX G GLUCOSE CONCENTRATION PROFILE.....	114

LIST OF TABLES

		PAGE
Table 1	Typical Specific Growth Rates.....	11
Table 2	Typical Parameter Values for the Monod Expression.....	15
Table 3	Composition of Slant Medium.....	24
Table 4	Composition of Broth Medium.....	27
Table 5	Composition of Plate Medium.....	28
Table 6	Composition of Synthetic Medium.....	30
Table 7	Ethanol Concentration Profile.....	42
Table 8	Summary of Experimental Results.....	46
Table 9	Parameter Values for the Monod, Moser and Teisser Expressions.....	48
Table 10	Sensitivity of Parameter Values.....	56
Table 11	Comparison of Predicted and Actual Growth Rates.....	60
Table 12	Parameter Values for the Modified Monod, Moser and Teisser Expressions.....	66

LIST OF FIGURES

	PAGE
Figure 1. Stage of the Cell Cycle G ₁ , S, G ₂ , and M Phases, Bud Initiation (BI) and Cell Division (CD).....	5
Figure 2. Length of the Cell Cycle Phase Versus the Specific Growth Rate.....	6
Figure 3. Typical Growth Curve for Batch Fermentation.....	8
Figure 4. The Dependence of the Specific Growth Rate on the Concentration of the Growth Limiting Nutrient for the Monod Expression.....	14
Figure 5. A Typical Arrhenius Plot for a Yeast.....	18
Figure 6. Fermenter Vessel.....	20
Figure 7. Fermenter Vessel Cover.....	21
Figure 8. The Slant Media in a Sample Bottle.....	25
Figure 9. Dilution Scheme.....	32
Figure 10. Plating Technique.....	33
Figure 11. The Calculation of Area Under the Response Curve.....	36
Figure 12. Typical Calibration Curve for the HPLC.....	37
Figure 13. Total Viable Cell Count vs. Optical Density.....	44
Figure 14. Specific Growth Rate vs. Concentration of Glucose at 30 ^o C.....	49
Figure 15. Specific Growth Rate vs. Concentration of Glucose at 34 ^o C.....	50

	PAGE
Figure 16. Specific Growth Rate vs. Concentration of Glucose at 37°C.....	51
Figure 17. Lineweaver Plot of $1/\mu$ vs. $1/C_i$ at 37°C.....	53
Figure 18. Lineweaver Plot of $1/\mu$ vs. $1/C_i$ at 30°C.....	54
Figure 19. Lineweaver Plot of $1/\mu$ vs. $1/C_i$ at 34°C.....	55
Figure 20. The Natural Log of the Specific Growth Rate vs. $1/T$	63
Figure 21. A Plot of the Modified Monod Expression.....	67
Figure 22. A Plot of the Modified Moser Expression.....	68
Figure 23. A Plot of the Modified Teisser Expression.....	69
Figure 24. The Natural Log of the Maximum Specific Growth Rate vs. $1/T$ for the Modified Monod Expression.....	70
Figure 25. The Natural Log of the Maximum Specific Growth Rate vs. $1/T$ for the Modified Moser Expression.....	71
Figure 26. The Natural Log of the Maximum Specific Growth Rate vs. $1/T$ for the Modified Teisser Expression.....	72
Figure 27. A Plot of the Specific Growth Rate vs. pH.....	74
Figure C.1. Natural Log of the Number of Cells Versus Time for $T = 30^\circ\text{C}$, $C_i = 23.1$ g/l, pH = 4.5 and $\mu = 0.373 \text{ hr}^{-1}$	87
Figure C.2. Natural Log of the Number of Cells Versus Time for $T = 30^\circ\text{C}$, $C_i = 13.1$ g/l, pH = 5.0 and $\mu = 0.396 \text{ hr}^{-1}$	88

	PAGE
Figure C.3. Natural Log of the Number of Cells Versus Time for $T = 30^{\circ}\text{C}$, $C_i = 23.1$ g/l, pH = 5.0 and $\mu = 0.507 \text{ hr}^{-1}$	89
Figure C.4. Natural Log of the Number of Cells Versus Time for $T = 30^{\circ}\text{C}$, $C_i = 23.1$ g/l, pH = 5.0 and $\mu = 0.500 \text{ hr}^{-1}$	90
Figure C.5. Natural Log of the Number of Cells Versus Time for $T = 30^{\circ}\text{C}$, $C_i = 33.1$ g/l, pH = 5.0 and $\mu = 0.576 \text{ hr}^{-1}$	91
Figure C.6. Natural Log of the Number of Cells Versus Time for $T = 34^{\circ}\text{C}$, $C_i = 13.1$ g/l, pH = 5.0 and $\mu = 0.403 \text{ hr}^{-1}$	92
Figure C.7. Natural Log of the Number of Cells Versus Time for $T = 37^{\circ}\text{C}$, $C_i = 23.1$ g/l, pH = 5.0 and $\mu = 0.534 \text{ hr}^{-1}$	93
Figure C.8. Natural Log of the Number of Cells Versus Time for $T = 34^{\circ}\text{C}$, $C_i = 33.1$ g/l, pH = 5.0 and $\mu = 0.586 \text{ hr}^{-1}$	94
Figure C.9. Natural Log of the Number of Cells Versus Time for $T = 34^{\circ}\text{C}$, $C_i = 33.1$ g/l, pH = 5.0 and $\mu = 0.600 \text{ hr}^{-1}$	95
Figure C.10. Natural Log of the Number of Cells Versus Time for $T = 37^{\circ}\text{C}$, $C_i = 23.1$ g/l, pH = 4.5 and $\mu = 0.143 \text{ hr}^{-1}$	96
Figure C.11. Natural Log of the Number of Cells Versus Time for $T = 37^{\circ}\text{C}$, $C_i = 13.1$ g/l, pH = 5.0 and $\mu = 0.426 \text{ hr}^{-1}$	97
Figure C.12. Natural Log of the Number of Cells Versus Time for $T = 37^{\circ}\text{C}$, $C_i = 13.1$ g/l, pH = 5.0 and $\mu = 0.447 \text{ hr}^{-1}$	98
Figure C.13. Natural Log of the Number of Cells Versus Time for $T = 37^{\circ}\text{C}$, $C_i = 23.1$ g/l, pH = 5.0 and $\mu = 0.564 \text{ hr}^{-1}$	99

	PAGE
Figure C.14. Natural Log of the Number of Cells Versus Time for $T = 37^{\circ}\text{C}$, $C_i = 33.1$ g/l, pH = 5.0 and $\mu = 0.682 \text{ hr}^{-1}$	100
Figure C.15. Natural Log of the Number of Cells Versus Time for $T = 37^{\circ}\text{C}$, $C_i = 40.6$ g/l, pH = 5.0 and $\mu = 0.684 \text{ hr}^{-1}$	101
Figure C.16. Natural Log of the Number of Cells Versus Time for $T = 37^{\circ}\text{C}$, $C_i = 60.6$ g/l, pH = 5.0 and $\mu = 0.677 \text{ hr}^{-1}$	102
Figure C.17. Natural Log of the Number of Cells Versus Time for $T = 37^{\circ}\text{C}$, $C_i = 23.1$ g/l, pH = 5.5 and $\mu = 0.341 \text{ hr}^{-1}$	103
Figure C.18. Natural Log of the Number of Cells Versus Time for $T = 41^{\circ}\text{C}$, $C_i = 23.1$ g/l, pH = 5.0 and $\mu = 0.0 \text{ hr}^{-1}$	104
Figure G.1. Weight Percent Glucose Versus Time for $T = 30^{\circ}\text{C}$, $C_i = 13.1$ g/l, pH = 5.0 and $\mu = 0.396 \text{ hr}^{-1}$	116
Figure G.2. Weight Percent Glucose Versus Time for $T = 30^{\circ}\text{C}$, $C_i = 13.1$ g/l, pH = 5.0 and $\mu = 0.396 \text{ hr}^{-1}$	117
Figure G.3. Weight Percent Glucose Versus Time for $T = 30^{\circ}\text{C}$, $C_i = 23.1$ g/l, pH = 5.0 and $\mu = 0.507 \text{ hr}^{-1}$	118
Figure G.4. Weight Percent Glucose Versus Time for $T = 30^{\circ}\text{C}$, $C_i = 23.1$ g/l, pH = 5.0 and $\mu = 0.500 \text{ hr}^{-1}$	119
Figure G.5. Weight Percent Glucose Versus Time for $T = 30^{\circ}\text{C}$, $C_i = 33.1$ g/l, pH = 5.0 and $\mu = 0.576 \text{ hr}^{-1}$	120
Figure G.6. Weight Percent Glucose Versus Time for $T = 34^{\circ}\text{C}$, $C_i = 13.1$ g/l, pH = 5.0 and $\mu = 0.403 \text{ hr}^{-1}$	121

	PAGE
Figure G.7. Weight Percent Glucose Versus Time for $T = 34^{\circ}\text{C}$, $C_i = 23.1 \text{ g/l}$, $\text{pH} = 5.0$ and $\mu = 0.532 \text{ hr}^{-1}$	122
Figure G.8. Weight Percent Glucose Versus Time for $T = 34^{\circ}\text{C}$, $C_i = 33.1 \text{ g/l}$, $\text{pH} = 5.0$ and $\mu = 0.586 \text{ hr}^{-1}$	123
Figure G.9. Weight Percent Glucose Versus Time for $T = 34^{\circ}\text{C}$, $C_i = 33.1 \text{ g/l}$, $\text{pH} = 5.0$ and $\mu = 0.600 \text{ hr}^{-1}$	124
Figure G.10. Weight Percent Glucose Versus Time for $T = 37^{\circ}\text{C}$, $C_i = 23.1 \text{ g/l}$, $\text{pH} = 4.5$ and $\mu = 0.143 \text{ hr}^{-1}$	125
Figure G.11. Weight Percent Glucose Versus Time for $T = 37^{\circ}\text{C}$, $C_i = 13.1 \text{ g/l}$, $\text{pH} = 5.0$ and $\mu = 0.426 \text{ hr}^{-1}$	126
Figure G.12. Weight Percent Glucose Versus Time for $T = 37^{\circ}\text{C}$, $C_i = 13.1 \text{ g/l}$, $\text{pH} = 5.0$ and $\mu = 0.447 \text{ hr}^{-1}$	127
Figure G.13. Weight Percent Glucose Versus Time for $T = 37^{\circ}\text{C}$, $C_i = 23.1 \text{ g/l}$, $\text{pH} = 5.0$ and $\mu = 0.564 \text{ hr}^{-1}$	128
Figure G.14. Weight Percent Glucose Versus Time for $T = 37^{\circ}\text{C}$, $C_i = 33.1 \text{ g/l}$, $\text{pH} = 5.0$ and $\mu = 0.682 \text{ hr}^{-1}$	129
Figure G.15. Weight Percent Glucose Versus Time for $T = 37^{\circ}\text{C}$, $C_i = 40.6 \text{ g/l}$, $\text{pH} = 5.0$ and $\mu = 0.684 \text{ hr}^{-1}$	130
Figure G.16. Weight Percent Glucose Versus Time for $T = 37^{\circ}\text{C}$, $C_i = 60.6 \text{ g/l}$, $\text{pH} = 5.0$ and $\mu = 0.677 \text{ hr}^{-1}$	131
Figure G.17. Weight Percent Glucose Versus Time for $T = 37^{\circ}\text{C}$, $C_i = 23.1 \text{ g/l}$, $\text{pH} = 5.0$ and $\mu = 0.341 \text{ hr}^{-1}$	132

Figure G.18. Weight Percent Glucose Versus Time for $T = 41^{\circ}\text{C}$, $C_i = 23.1 \text{ g/l}$, $\text{pH} = 5.0$ and $\mu = 0.0 \text{ hr}^{-1}$	133
---	-----

NOMENCLATURE

C_{i0}	initial concentration of the growth limiting nutrient (g/l)
K_i	empirical constant (g/l)
t	time (hr)
t_d	doubling time (hr)
t_{lag}	length of the lag phase (hr)
μ	specific growth rate (hr ⁻¹)
μ_m	maximum specific growth rate (hr ⁻¹)
n	number of viable cells
n_0	number of viable cells at the end of the lag phase

CHAPTER 1

INTRODUCTION

With the oil embargo of 1973-74, Americans have become increasingly aware of the value of energy and the need for the country to become energy self-sufficient. The United States should not have to depend on nonrenewable energy sources from foreign countries, but rely on renewable energy sources from the United States.

On the South Plains of Texas, the main agricultural crop is cotton. For every pound of cotton, there is approximately 1.83 lbs of clean cotton gin residue (11). The result is an annual average cotton gin residue production of approximately 900,000 tons (11). Presently, cotton gin residue has little beneficial use, but it could be converted to fuel grade ethanol. The lint in cotton gin residue is composed mostly of crystalline cellulose. This lint, along with the cellulose in the plant matter, can be hydrolyzed to glucose and fermented to ethanol. The ethanol can then be distilled to 100% ethanol for a fuel source.

The fermentation step was the main area of concern for this research. The purpose of this research was to study the effect of varying glucose concentration on the exponential growth phase of Saccharomyces cerevisiae. The effects of pH and

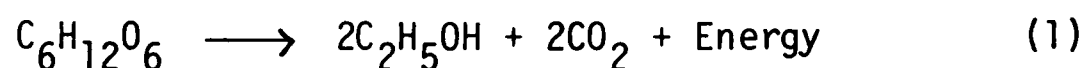
temperature on the exponential growth phase were studied. The growth parameter values for several exponential growth phase models were determined. These expressions were compared with experimental results to determine which one best represented the exponential growth rate of S. cerevisiae.

CHAPTER 2

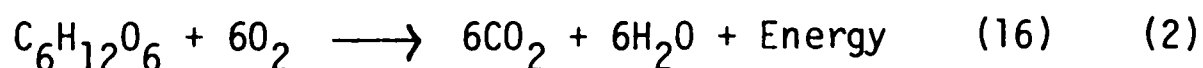
LITERATURE REVIEW

Fermentation of Glucose to Ethanol

The yeast used in this study was Saccharomyces cerevisiae, commonly known as bakers' or brewers' yeast. The yeast was obtained from Dr. Caryl E. Heintz of the Department of Biology at Texas Tech University in Lubbock, Texas. S. cerevisiae utilizes glucose as its carbon source and excretes ethanol as waste. The stoichiometry of the fermentation of glucose to ethanol is:



The reaction occurs when there is a high glucose concentration or when oxygen is absent. If oxygen is added another reaction occurs:



Cell Cycle

S. cerevisiae is an oval diploid yeast and usually exists as small cells about 8 μm long and 5 μm in diameter. In typical batch cultivation, S. cerevisiae reproduces asexually by budding, but under adverse environmental conditions the yeast

can sporulate sexually. The cell cycle is described in five stages, shown in Figure 1 (5).

(1) G1 phase is the period when the cell grows to a larger size and forms a bud before DNA replication.

(2) S phase is the period of DNA replication.

(3) G2 phase is the period after DNA replication and before nuclear division.

⊙ (4) M phase is the period of nuclear migration and division.

(5) G1* is the time after nuclear division and before cell division.

The amount of time for each phase for different specific growth rates can be measured (Figure 2). The S and M phases remain constant regardless of the specific growth rate. The G2 phase remains constant except for low specific growth rates. The sum of the time for the S + M + G2 phases remains constant except for low specific growth rates. The G1 phase is strongly dependent on the specific growth rate (19).

After the cell division has been completed, the process is repeated. A scar will remain on the mother cell where the bud was formed. No new buds can be initiated over the scarred areas (19).

Initiation

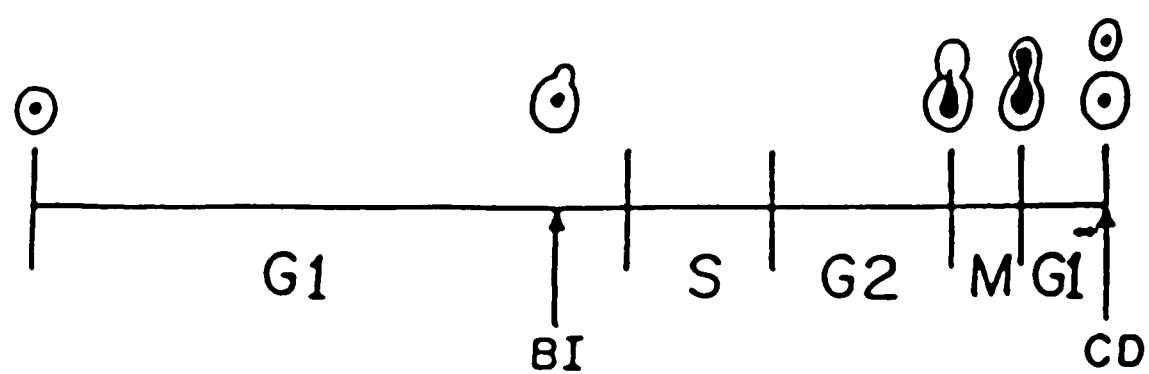


Figure 1. Stage of the Cell Cycle G1, S, G2, and M Phases, Bud Initiation (BI) and Cell Division (CD) (5)

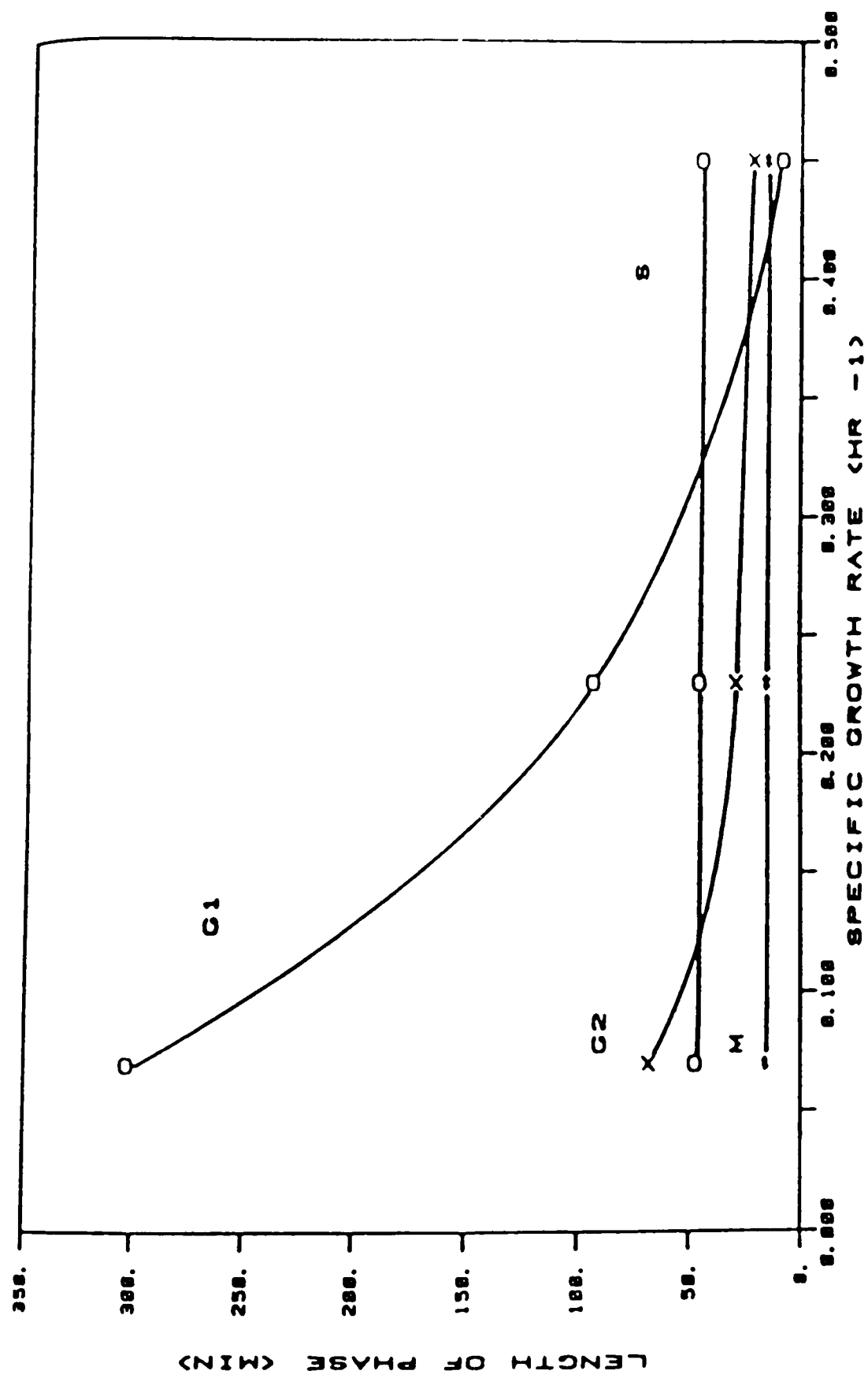


Figure 2. Length of the Cell Cycle Phase Versus the Specific Growth Rate (5)

Growth-Cycle for Batch Fermentation

There are four growth-cycle phases in batch fermentation. They are the lag phase, exponential growth phase, stationary phase and the death phase (Figure 3).

Lag Phase

The lag phase is the period after the medium has been inoculated with yeast and before the exponential growth phase. The length of the lag depends on the change in the nutrient concentration, pH and temperature from the inoculating medium to the fresh medium, and the age and size of the inoculum. A change in nutrient concentration can cause several effects on the yeast. If the new medium is richer in nutrients, the cells must create a larger concentration of metabolizing enzymes. A decrease in the nutrient level may result in no lag phase at all. The exponential growth phase will begin immediately, but at a slower rate. Many of the required vitamins and ions pass easily through the cell membrane (3). Transfer of a small culture inoculum to a large volume of medium could cause outward diffusion of these vitamins and ions. The diffusion is a function of pH, temperature and nutrient concentration. The age of the inoculum has a strong effect on the length of the lag time. Older cells (in a slower growth rate stage due to

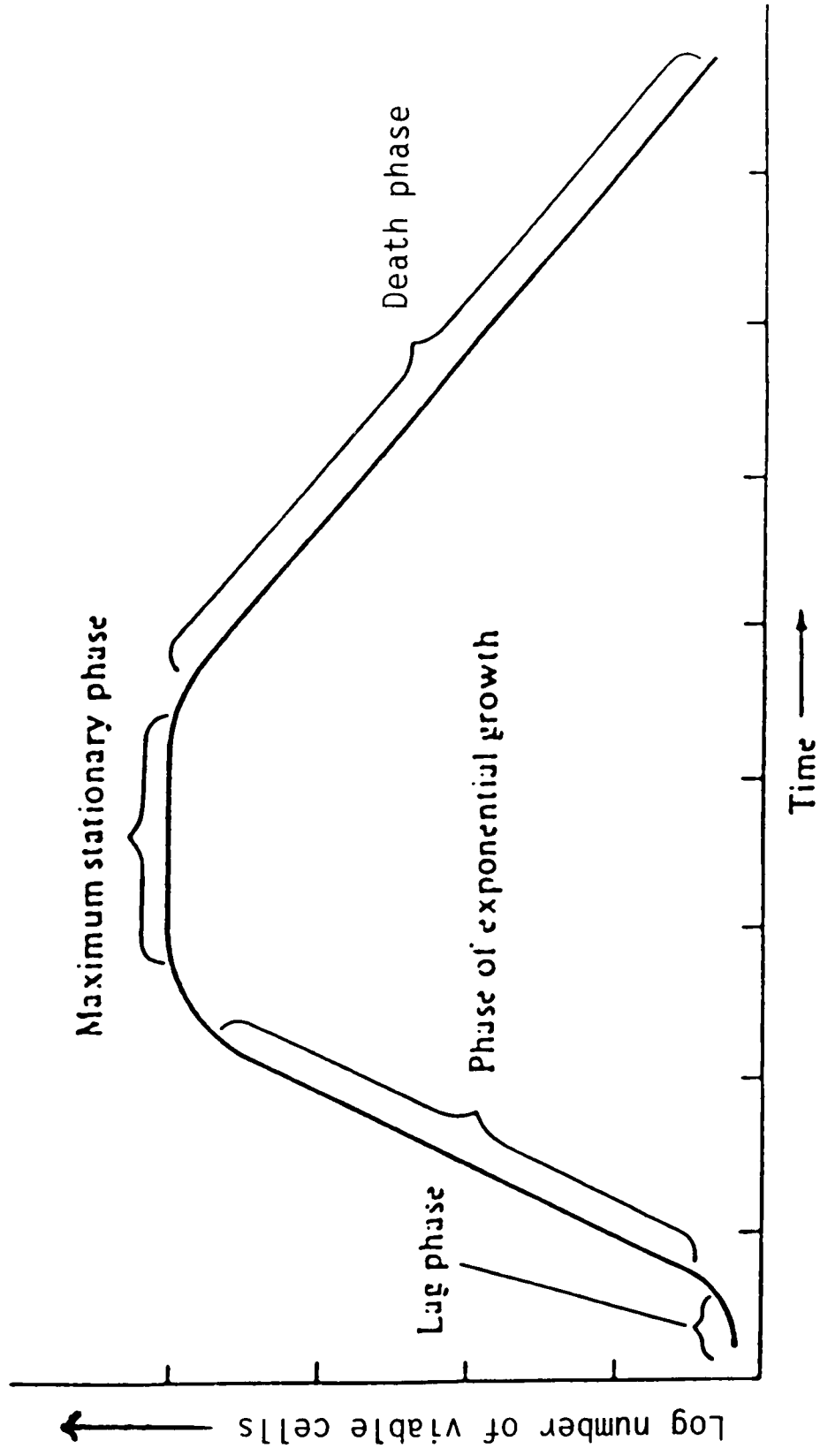


Figure 3. Typical Growth Curve for Batch Fermentation (4)

nutrient depletion and/or toxic metabolic products accumulation) may not survive the shock of being transferred to higher nutrient concentration. Older cells take longer to adjust to the higher concentration medium while its metabolism adjusts to new medium. Also, a deinhibition effect may occur if there is a buildup of toxins in the cell. The toxins could diffuse out when the cells are inoculated into a fresh medium (5).

Exponential Growth Phase

At the end of the lag phase, the cells have become adjusted to their new environment and exponential growth will begin. In the exponential growth phase, the cells multiply rapidly. The number of living cells and the cell mass doubles regularly with time. Equation 3 describes the increase in the cell numbers during exponential growth.

$$\mu = \frac{1}{n} \frac{dn}{dt} \quad (3)$$

Equation 4 is derived by integrating Equation 3 from $n = n_0$, $t = t_{lag}$ to $n = n$ and $t = t$.

$$n = n_0 e^{\mu(t-t_{lag})} \quad t > t_{lag} \quad (4)$$

By plotting natural log of the total cell count versus time, the slope (μ) can be determined (Equation 5).

$$\mu = \frac{\ln \eta_2 - \ln \eta_1}{t_2 - t_1} \quad t > t_{lag} \quad (5)$$

The doubling time, the time required for the number of cells to double, is derived by substituting $2\eta_0$ into Equation 4.

$$t_d = \frac{\ln 2}{\mu} \quad (6)$$

During the exponential growth, only one parameter is needed to describe the growth, μ or t_d . Typical values of the specific growth rate for S. cerevisiae are listed in Table 1. Table 1 shows that the specific growth rate changes with the temperature, pH and glucose concentration.

Stationary Phase

When the nutrient level can no longer support exponential growth and/or the toxic level inhibits the exponential growth, this phase will end and the stationary phase will begin. The stationary phase is when the total viable cell count remains constant. The effect of any particular nutrient of the medium upon the birth rate is dependent on the importance of the nutrient in cell metabolism. Exhaustion of a carbon source or important nutrients will cause a rapid decrease in the birth rate. For non-essential nutrients in the medium, the yeast can

Table 1
Typical Specific Growth Rates

Experiments	Conc. of glucose	Temp. (°C)	pH	$\mu(\text{hr}^{-1})$
erobic? Woehrer and Roehr (35)	0.1	30	4.5	0.18
Bar Bradford and Hall (6)	20.0	30	5.0	0.45
Carter and Jagadish (9)	10	24	5.5	0.24
ation Maxon and Johnson (20)	10	30	5.0	0.41

synthesize the nutrients and little effect on the birth rate will be seen (12).

Death Phase

The death phase is the period when the death rate is greater than the birth rate of the cells. Due to nutrient depletion and/or toxic products, the medium cannot sustain the population and the death phase will begin. In the death phase, the cells will utilize both dead and live cells for food (5, 27).

Exponential Growth Models

Monod (18) studied the relationship between the exponential growth rate and the concentration of the growth limiting nutrient in batch cultures of bacteria. He proposed the empirical expression between these as shown below.

$$\mu = \mu_{\max} \frac{C_{i0}}{K_i + C_{i0}} \quad (7)$$

This is the same form as the Langmuir adsorption isotherm (5) and the standard rate equation for enzyme catalyzed reactions with a single substrate (5). This empirical expression and modification of this expression have no theoretically sound starting point for the development of a kinetic theory (27).

The Monod expression is a great oversimplification, but reasonably expresses the relationship between cell growth and growth limiting nutrient even though the physical meaning is unclear or does not exist.

The maximum specific growth rate occurs when $C_i \gg K_i$. K_i is the concentration of nutrient i where the specific growth rate was half the maximum specific growth rate (Figure 4). Typical parameter values for *S. cerevisiae* are listed in Table 2. The parameter values were determined under the following conditions. Aiba (2) conducted batch experiments with glucose as the growth limiting nutrient. The glucose concentration was 10 and 20 g/l with temperature of 30°C and pH of 4.0. Bardford and Hall (7) conducted batch experiments under aerobic conditions. In this study, K_s was determined by unsteady state balance with cell mass. Bijkerk and Hall (8) did aerobic batch experiments with glucose as the growth limiting nutrient with a temperature of 30°C and pH of 5.5. Lievens (19) conducted two experiments with glucose concentrations of 10 and 20 g/l and calculated the parameter values with a Lineweaver-Burke plot. Peringer (24) conducted batch experiments with 40% air saturation of the medium at a temperature of 30°C and pH of 5.1 with 10 g/l glucose concentration. Novak (23) conducted anaerobic batch experiments with glucose concentration of 80

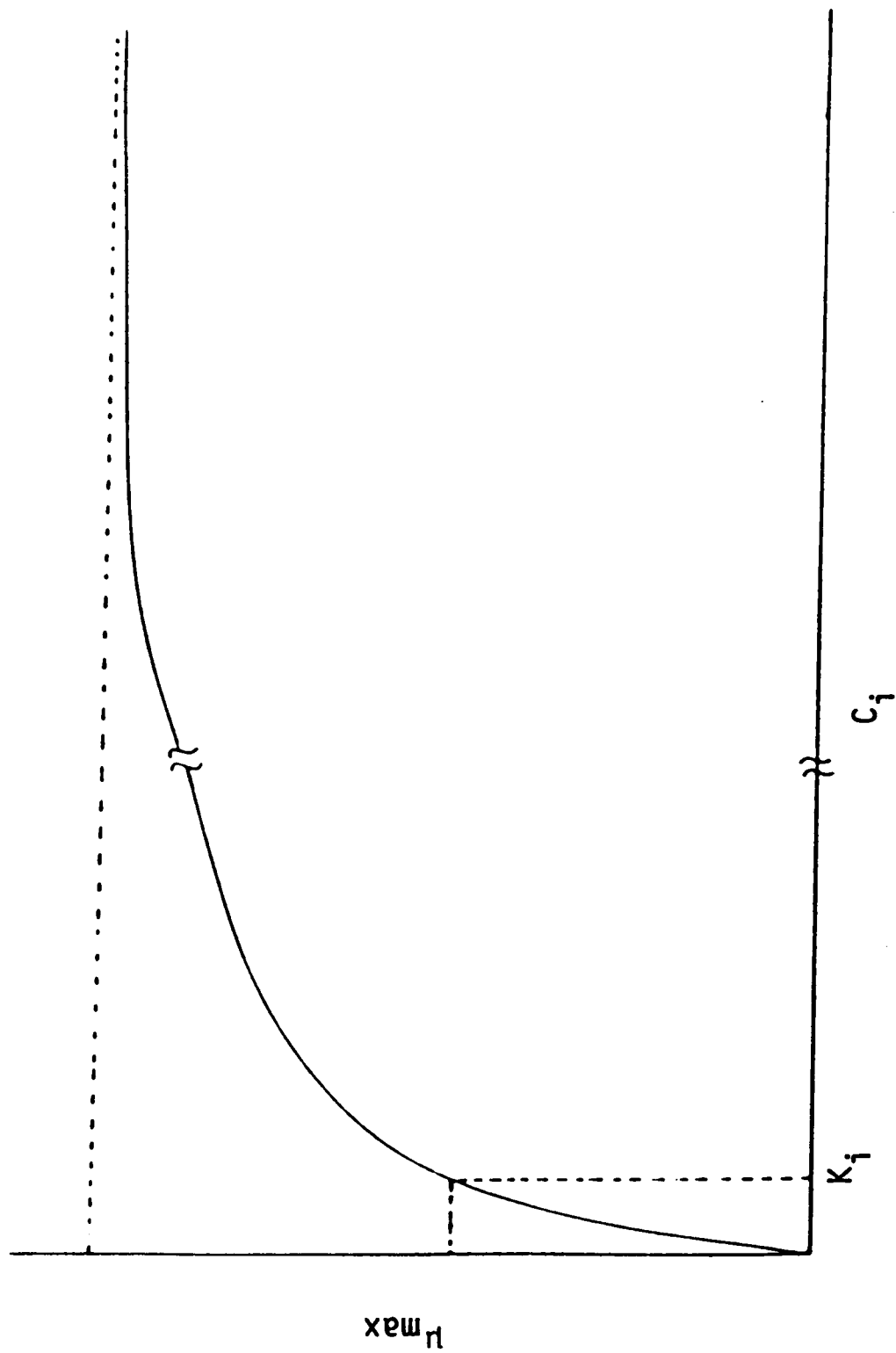


Figure 4. The Dependence of the Specific Growth Rate on the Concentration of the Growth Limiting Nutrient for the Monod Expression

Table 2
Typical Parameter Values for the Monod Expression

Experimenters	$\mu_{\max} (\text{hr}^{-1})$	$K_i (\text{g/l})$
Aiba (2)	0.408	0.22
Barford and Hall (7)	0.283	0.05
Bijkerk and Hall (8)	0.42	0.5
Lievens (19)	0.46	2.0
Peringer (24)	0.307	0.103
<i>Amesbury</i> Novak (23)	0.324	0.172
Yoon (36)	0.33	0.04

and 125 g/l with agitation of 150 rpm. Yoon (36) studied the growth of S. cerevisiae with L-lactate and glucose as the growth limiting substrate at 30°C and pH of 5.0 under anerobic conditions.

Before using the Monod expression, there are several warnings. The expression suggests that if $C_i \neq 0$ then $\mu \neq 0$ which is not always true. Generally the implied behavior for the Monod expression is not well tested for $C_i \gg K_i$. Since the nutrient level is often initially high in a batch medium ($C_i \gg K_i$), a true exponential growth phase will be observed. The most serious limitation of the Monod expression is that there must be true balanced growth. Balanced growth means that over a time interval every extensive property of the growing system increases with the same factor during that interval (5).

In batch fermentation, the growth is sufficiently slow, and the population is not large. Under these conditions, balanced growth is a reasonable approximation during the exponential growth phase (5). With balanced growth, the Monod expression models the growth quite reasonably (5).

The Monod equation is accepted as depicting the general variation of the growth rate with substrate concentration. However, reservations regarding its detailed applicability led Moser (19) to include an additional empirical feature (Equation 8) and Tessier to take in account for slower growth at low

substrate concentrations (Equation 9) (3). These expressions, like the Monod expression, have no theoretical basis.

$$\mu = \mu_{\max} (1 + K_i C_{i0}^{-\lambda})^{-1} \quad (8)$$

$$\mu = \mu_{\max} (1 - e^{-C_{i0}/K_i}) \quad (9)$$

The Effect of Temperature on the Maximum Specific Growth Rate

The specific growth rate is a function of temperature and can be described by an Arrhenius type expression as shown below.

$$\mu = \mu_o e^{-E_a/RT} \quad (10)$$

Since μ is a function of temperature, then μ_{\max} can also be expressed as a function of temperature. If the Arrhenius equation is valid, then $\ln \mu$ versus $1/T$ will form a straight line and have a slope of $-E_a/R$ (Equation 11). For the Arrhenius expression, the temperature range is quite limited for yeast (Figure 5). Typical values of activation energies for micro-organisms are 12.2 kJ/g mole for Penicillium chrysogenum (1) and 16.7 kJ/g mole for Nocardia corallina (19).

$$\ln \mu = \ln \mu_o - (E_a/R)(1/T) \quad (11)$$

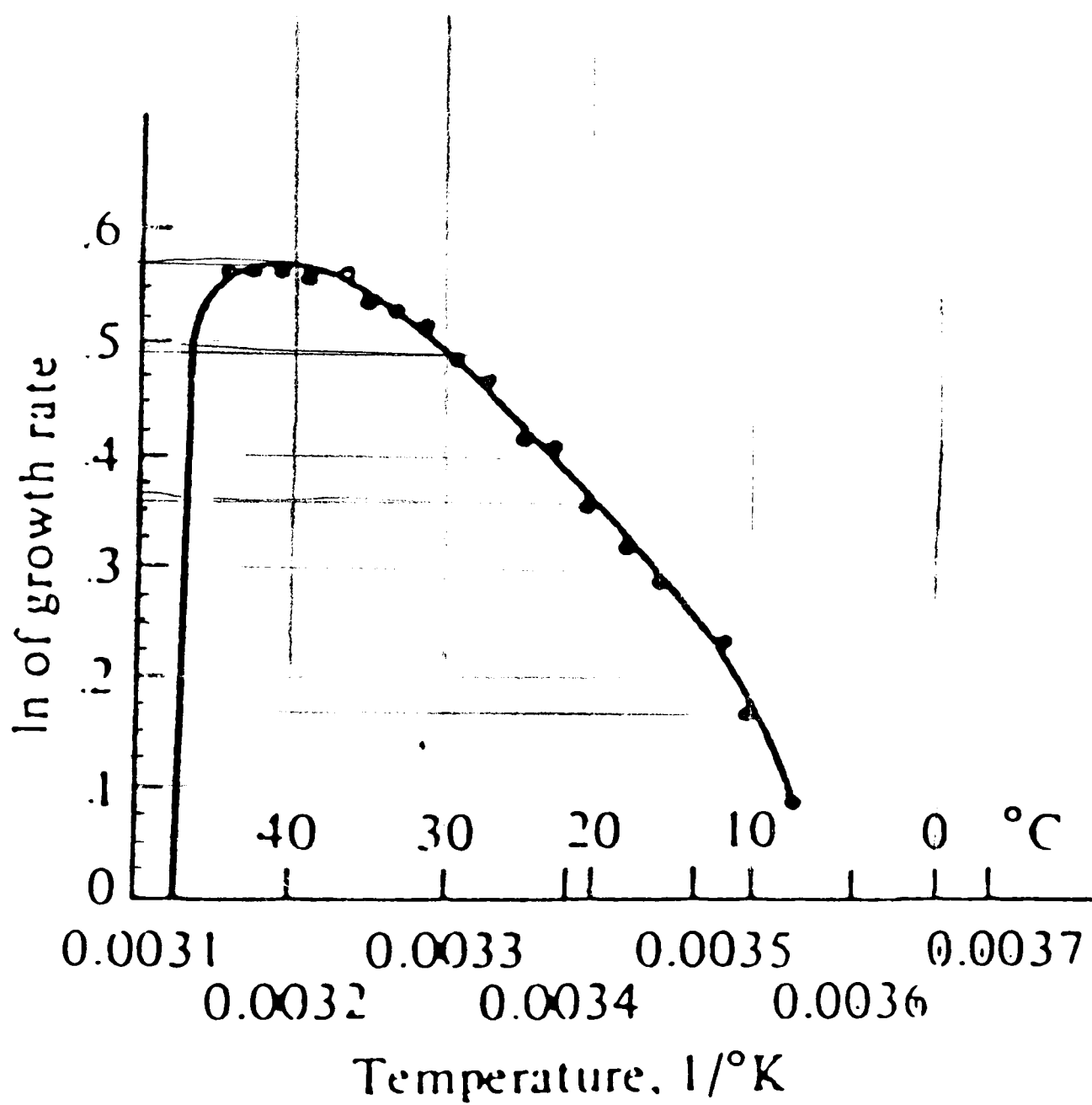


Figure 5. A Typical Arrhenius Plot for a Yeast (4)

CHAPTER 3

EXPERIMENTAL APPARATUS

Batch Fermenter

The experimental apparatus used was a Chemapec p.e.c. Glass Fermenter Type GF0014 (10). The fermenter vessel (Figure 6) has a working volume of 4ℓ with the blade stirrer attachment. The stainless steel cover has 13 entry ports. The entry ports were used for the pH probe, temperature probe, contact thermometer, sample line and pressure release valve (Figure 7).

Steam was used for sterilization of the water in the fermenter. When steam is used, the protection jacket must be in place. Water through a water heater was used to cool or heat the fermenting medium. The steam or water entered at the base of the fermenter, traveled to the top and then to the bottom of the vessel through stainless steel tubing. Fins were attached to the tubing to increase the rate of heat transfer. Temperature control was obtained with a contact thermometer. The contact thermometer regulated the water heater to heat or not to heat the water. A thermometer and the Chemapec recorder were used to record the temperature of the medium. The pH was recorded using a pH probe and the Chemapec FZ-1 with built-in

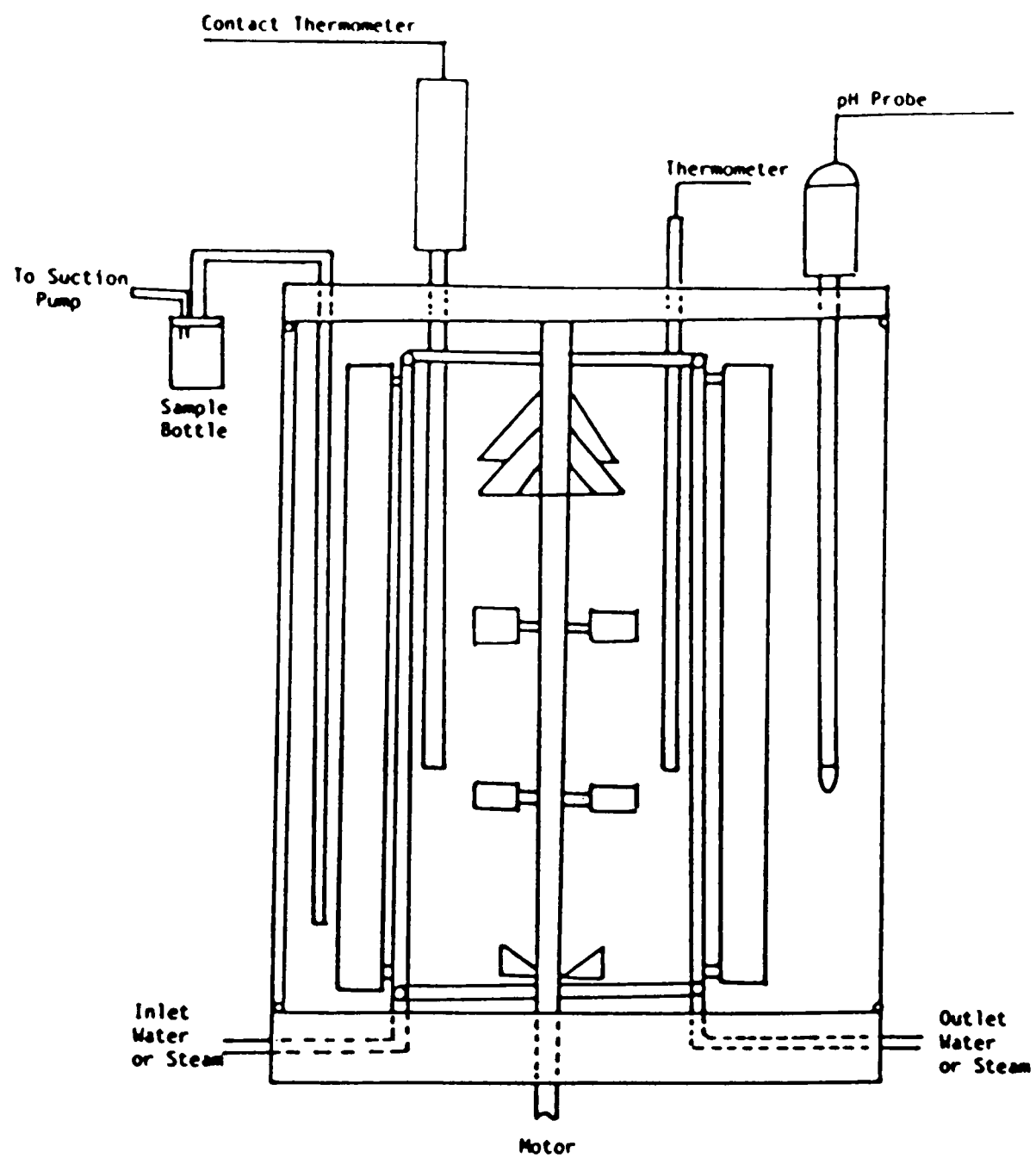


Figure 6. Fermenter Vessel

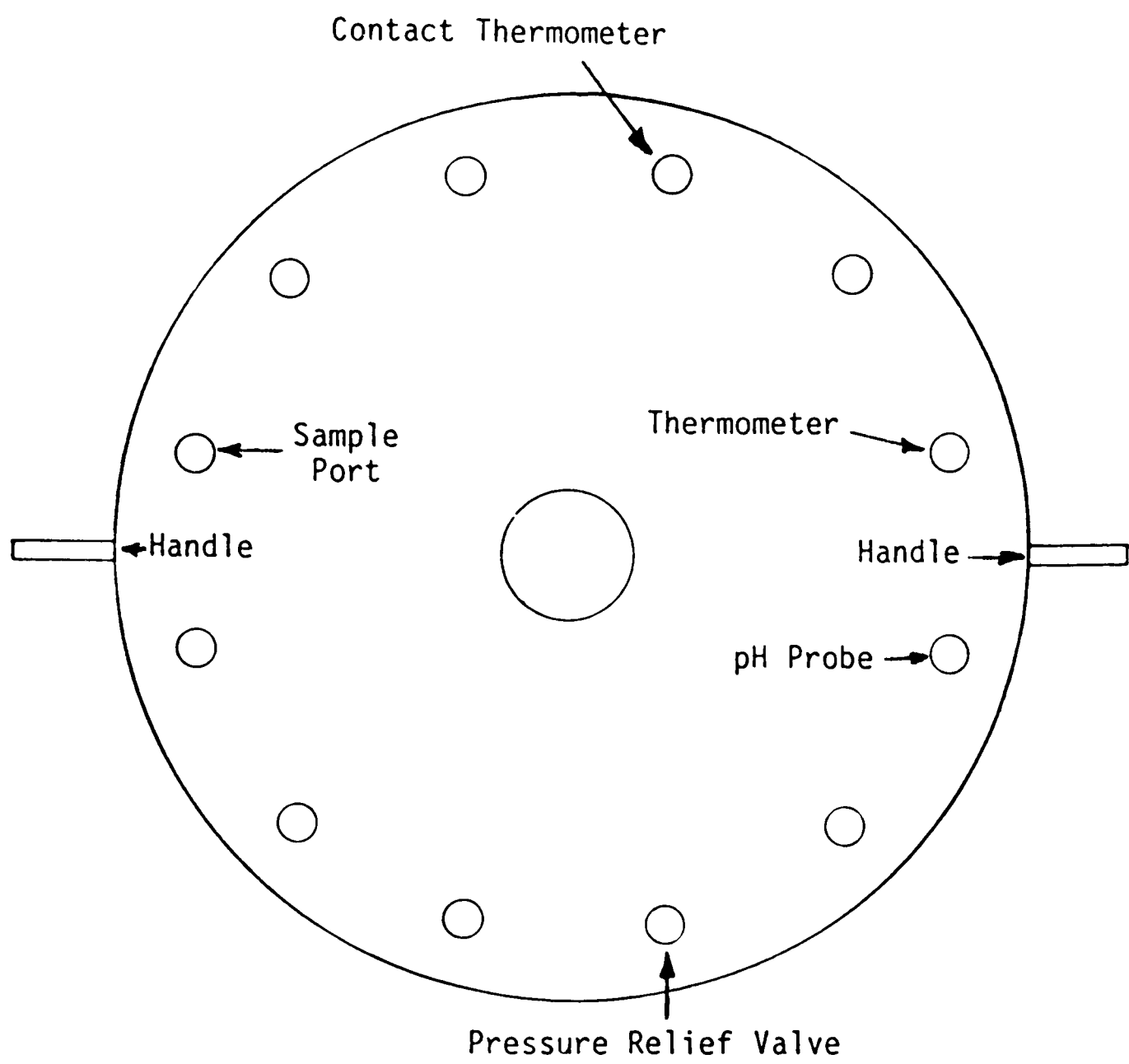


Figure 7. Fermenter Vessel Cover

Speedomax Recorder. Samples were removed by suction to a 50 ml sample bottle using a Guzzler 400 hand pump.

CHAPTER 4

EXPERIMENTAL PROCEDURE

Preparation of the Media

The media used in this study consisted of slants, broth, plates and synthetic media.

Slants

The components in the slant medium are listed in Table 3. The slants were made by slowly mixing the ingredients in deionized water in the order shown. The solution was heated to approximately 70⁰C while adding the agar to help the agar dissolve. The solution was watched carefully to keep it from boiling over. Once the solution was well mixed, it was added to the sample bottles to approximately 1/3 full. Next, the bottle caps were screwed on approximately halfway to keep the inside to outside differential pressure in the glassware to a minimum in the autoclave. The sample bottles were autoclaved for ten minutes at 120⁰C, and allowed to cool slowly. When the autoclave had cooled, the sample bottles were removed and the caps tightly secured. The sample bottles were turned sideways so the solution made an approximate angle of 60⁰ with the side of the sample bottle (Figure 8). The solution was held in this position until it had solidified.

Table 3
Composition of Slant Medium (16)

Yeast Extract	4 g
Malt Extract	0.6 g
Bacto-Peptone	1 g
Glucose	1 g
Bacto-Agar	3 g
Deionized Distilled Water	200 ml

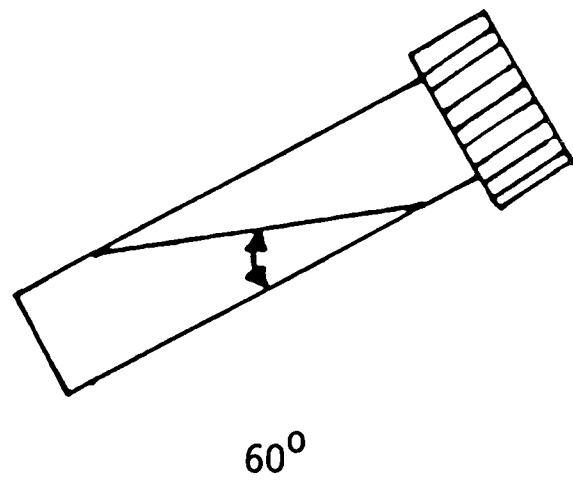


Figure 8. The Slant Media in a Sample Bottle

Broth

The broth medium components are listed in Table 4. The broth was made by mixing the ingredients with water. The broth was then added to test tubes to be used as dilution tubes and/or flasks to be used as the inoculating broth. The container caps were screwed on halfway. The broth was autoclaved for ten minutes at 121°C , and allowed to cool slowly. Once the autoclave had cooled, the caps were tightened to keep out unwanted microorganisms.

Plates

The plate medium components are listed in Table 5. The plate medium was made by mixing the ingredients with water in the order given. The solution was heated while adding the agar to help the agar dissolve. The solution was divided equally into two 1ℓ flasks. The flasks were corked with cotton or with sponge closures. The solution was autoclaved for ten minutes at 121°C , and allowed to cool slowly. The solution made approximately forty plates. Petri dishes were packaged in plastic sleeves with twenty Petri dishes per sleeve. The Petri dishes were removed from the sleeve, and the sleeve was saved. The Petri dishes were laid flat on a table. The cover of the solution container was removed and the lip of the flask was waved over a flame to disinfect the lip. This sterilization was

Table 4
Composition of Broth Medium (16)

Yeast Extract	4 g
Malt Extract	0.6 g
Bacto-Peptone	1 g
Glucose	10 g
Deionized Distilled Water	200 ml

Table 5
Composition of Plate Medium (16)

Yeast Extract	20 g
Malt Extract	3 g
Bacto-Peptone	5 g
Glucose	50 g
Bacto-Agar	15 g
Deionized Distilled Water	1 l

Makes approximately 40 plates.

Slant 100 200 400 600 800 1000
Broth 200 400 600 800 1000
Plate 100 200 400 600 800 1000

done periodically throughout the procedure. The Petri dish lid was barely lifted so the solution could be added, but still keep out unwanted bacteria. The solution was poured into the Petri dish, and the lid was replaced. The plate solution was allowed to solidify. The plate was then turned upside down to keep the condensate on the Petri dish lid from falling onto the plate. When all of the plates had hardened, they were put back into the sleeve and stored upside down in a refrigerator at 7°C.

Synthetic Media

The synthetic media components are listed in Table 6. The glucose and water mixture and the casamino acid and water mixture were sterilized by autoclaving for ten minutes at 121°C. Biotin mixture, folic acid mixture, and trace elements with the rest of the vitamins mixture and amino acid mixture were sterilized by ultrafiltration. Sterilization by ultrafiltration was performed using autoclaved sterile equipment consisting of a filtering flask, a filtering funnel and 0.2 µm cellulose filter paper. The cellulose filter paper was put into a glass Petri dish, sealed with autoclave tape, put in the autoclave with the other glassware, autoclaved for fifteen minutes at 121°C and rapidly cooled. The mixtures were then filtered separately with the sterile equipment. Water was

Table 6
Composition of Synthetic Medium⁽¹⁾ (32)

<u>Carbon Source</u>	<u>Grams</u>
Glucose	Varied
<u>Nitrogen Source</u>	<u>Grams</u>
Casamino Acid ⁽²⁾	2.25
<u>Amino Acid</u>	<u>Milligrams</u>
L-histidine • HCl • H ₂ O	10
L-methionine	10
L-tryptophan	10
<u>Trace Elements</u>	<u>Micrograms</u>
H ₃ BO ₃	500
KI	100
ZnCl	400
<u>Vitamins</u>	<u>Micrograms</u>
Biotin	2
Calcium Pantothenate	400
Folic Acid	2
Inositol	2000
Niocin	400
Para-aminobenzoic Acid	200
Pyridoxine • HCl	400
Riboflavin	200
Thiamine • HCl	400

(1) Per liter of aqueous solution.

(2) Note the reference says 2 grams but a missed calculation led to 2.25 grams.

steam sterilized in the fermenter vessel for twenty minutes. The mixtures were added to the fermenter. Sterile water was then added to obtain the desired volume, and the pH was adjusted to the desired pH with 1 N Na_2CO_3 and 0.86 N HCl (15).

Plate Count and Optical Density

Plate counting technique was performed by diluting the synthetic media with broth, placing a thin film of the sample onto a plate, incubating and counting the number of cell colonies. A 0.1 ml sample of the synthetic media was added to 9.9 ml of the sterile broth. Then 0.1 ml of the diluted sample was added to 9.9 ml of the sterile broth. This was repeated until the desired dilution was obtained (Figure 9). A plate was then taken out of the incubator, and a 0.1 ml of the sample was added to a point halfway from the center to the edge of the plate. An "L" shaped glass rod was then taken out of an alcohol bath and disinfected by placing it over a flame until the alcohol had burned off. The glass rod was waved in the air to allow it to cool. The glass rod was gently placed on the plate but not touching the sample. This made sure that the rod was no longer hot and would not kill the yeast in the sample. The plate was gently rotated so the sample was evenly spread over the plate (Figure 10). All plate counts were done in triplicate (5). The lid was put back on the Petri dish, the plate was

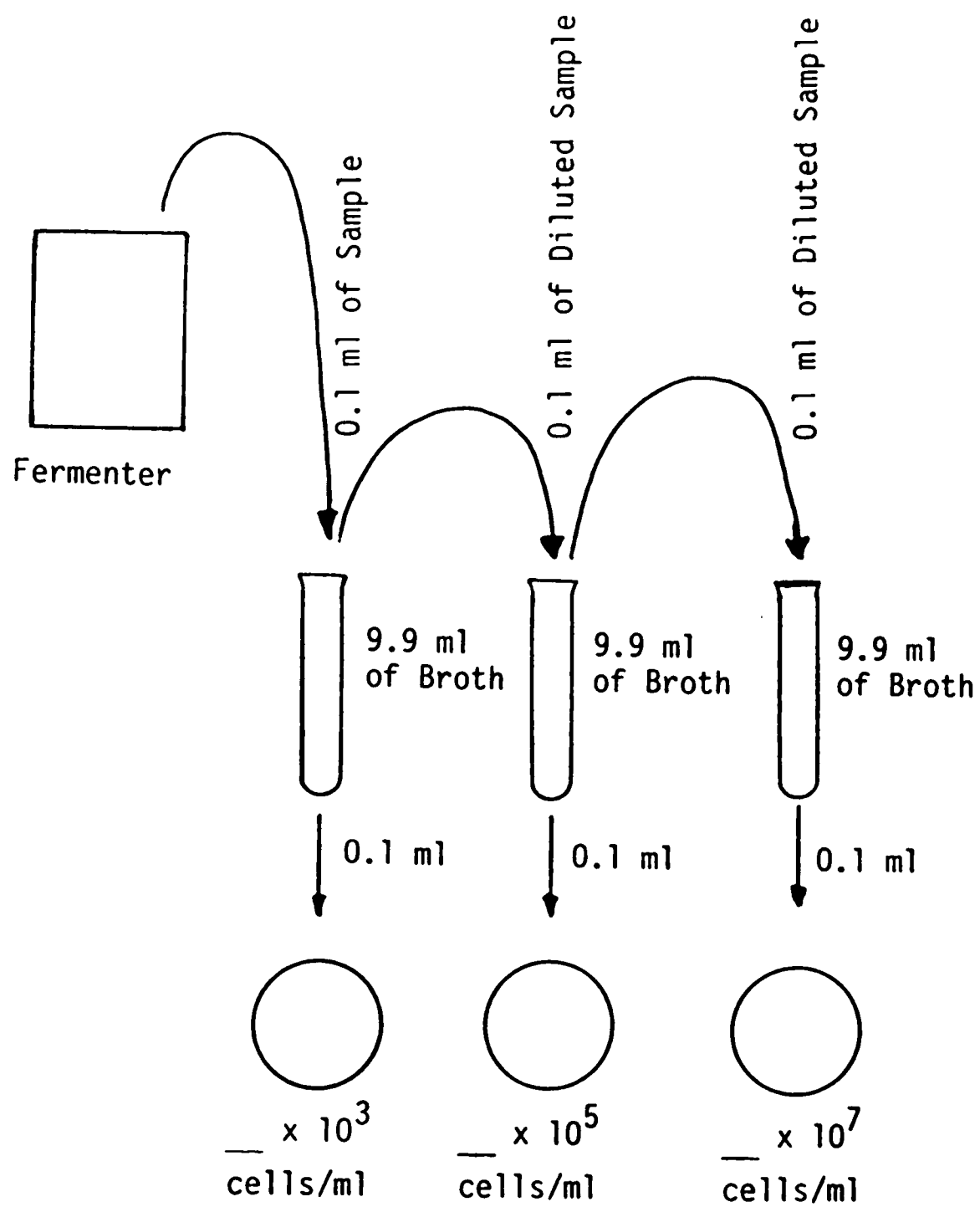


Figure 9. Dilution Scheme

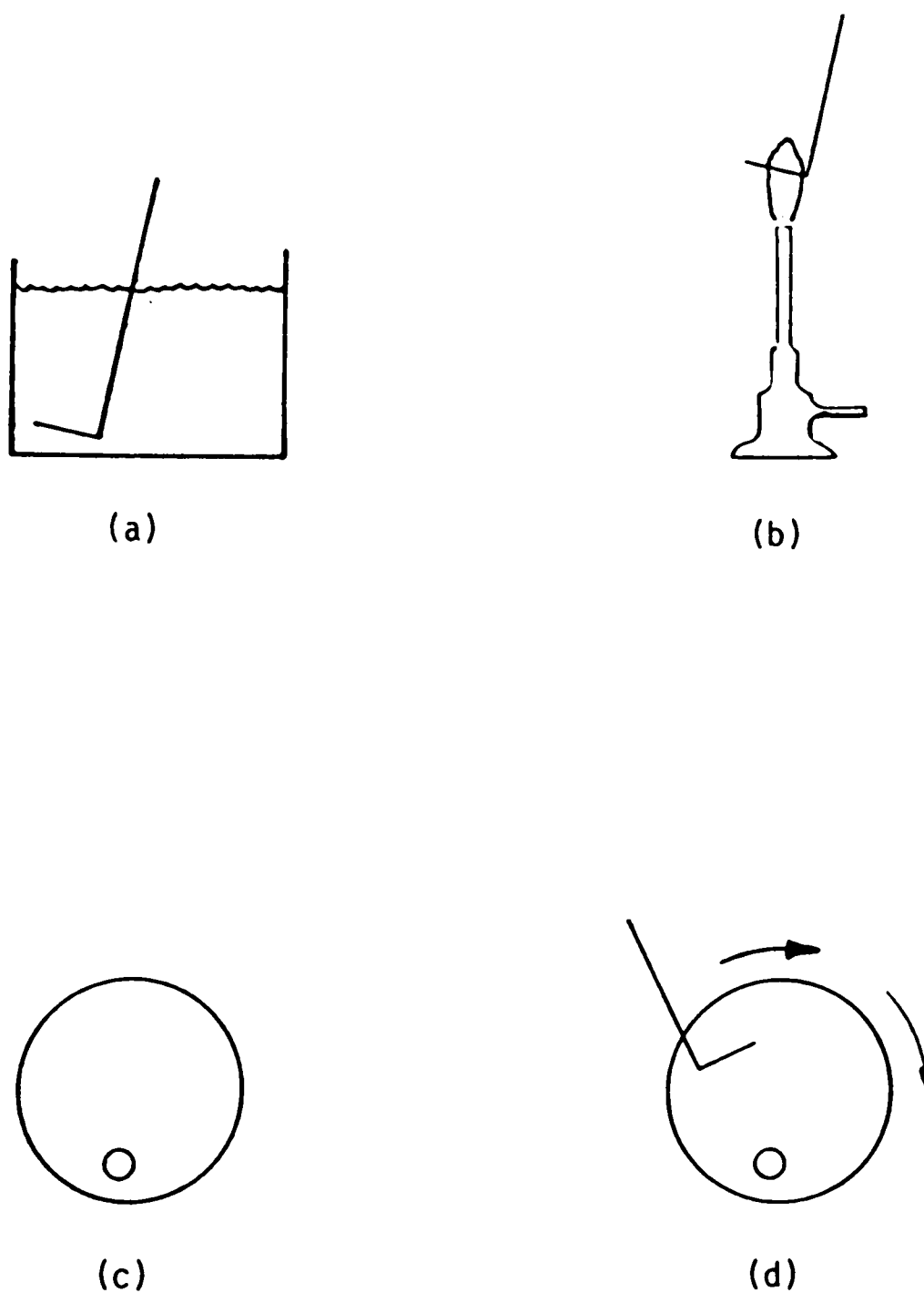


Figure 10. Plating Technique: (a) "L" shaped rod stored in an alcohol bath, (b) "L" shaped rod is sterilized with a flame until the alcohol has been burned off, (c) sample is placed on the plate and (d) sample is spread evenly on the plate

cataloged, and stored upside down in the incubator for twenty-four hours at 34°C. The number of colonies of yeast were calculated and recorded. Each colony of the yeast was assumed to be formed from a single cell (19).

Optical density was measured by using a 3 ml sample of the media in a Bausch and Lomb Spectronic 21 at a wavelength at 620 nm (14). The optical density was measured in ^badsorption ^{ance} or transmittance. In this study, adsorption reading was used (5). Transmittance was obtained by the following relation.

$$\text{Absorption} = -\log_{10} (\text{Transmittance}/100) \quad (12)$$

In the exponential growth phase, the optical ^badsorption is proportional to the cell mass and the number of cells (33).

Preparation of Glucose Standards

Glucose standards were prepared on a wt. % basis (Equation 13). The correct amount of glucose was measured using a Mettler Analytical Balance and mixed with 50 ml of distilled water. The solution was then filtered with a Waters Associates' Sample Clarification Kit (34). The solutions were stored in a freezer until needed (13).

$$\text{wt. \%} = (C_g/C_g + 50) \times 100 \quad (13)$$

The equation assumes the density of water is 1 g/ml.

Glucose Analysis

Glucose analysis was performed using a Waters Associates' High Performance Liquid Chromatograph (HPLC). A carbohydrate column (144234) was used for the glucose analysis. The carrier solvent was 85 vol. % acetonitrile and 15 vol. % water (13). The HPLC was operated at the following settings:

- (1) Solvent Rate: 2.0 ml/min
- (2) Chart Speed: 0.5 in/min
- (3) Polarity: -
- (4) Attenuator: 8X
- (5) Average Column Pressure: 600 psi
- (6) Sample Injection Volume: 15 μ l

Glucose standard solutions were injected into the HPLC. The area under the response curve was calculated as shown in Figure 11 (17). The area of the glucose peak was plotted versus wt. % glucose. A straight line calibration curve was obtained by linear regression (Figure 12). New calibration curves were made every time fresh solvent was added to the solvent carrier vessel. Then the samples were analyzed and an area under the peak was calculated. Glucose concentration was determined using the calibration curve.

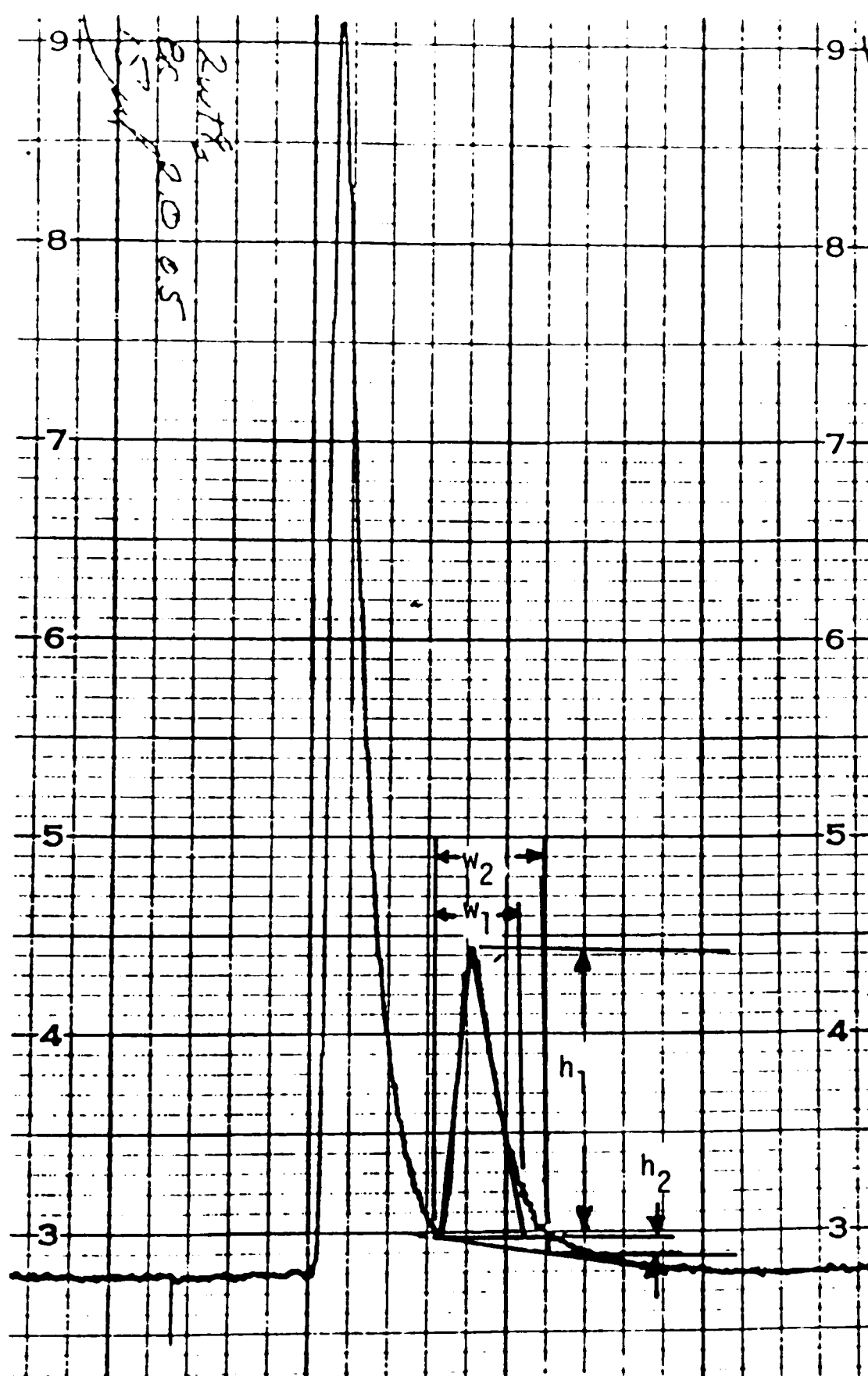


Figure 11. The Calculation of Area Under the Response Curve

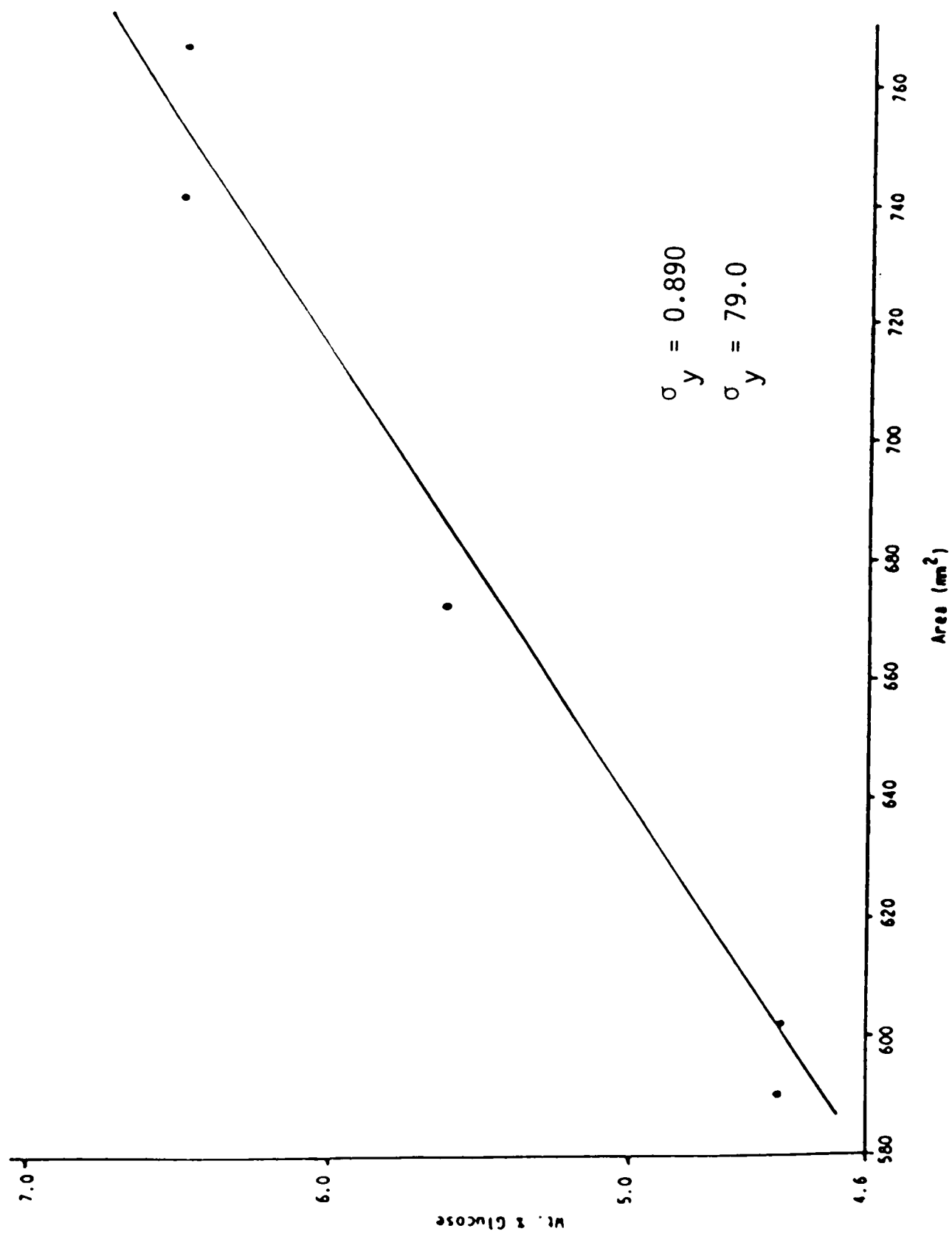


Figure 12. Typical Calibration Curve for the HPLC

Operation Procedure for the Batch Fermenter

An inoculating loop was sterilized by using a flame. The inoculating wire loop was heated until it had a red glow (30). After cooling, the inoculating loop was used to get a loopful of yeast from the slant. Care was taken not to scoop any of the slant medium. The loop of yeast was placed into 100 ml of sterile broth. This was repeated until three loopsful of yeast had been placed into the broth. The inoculating loop was sterilized and stored. The broth was placed in a Precision Scientific Thelco Incubator for 24 hours at 34°C. In the meantime, the glass fermenter was cleaned with soap and water, and rinsed with distilled water. The glass fermenter vessel was assembled and mounted on the fermenter stand (10). Approximately 6 l of distilled water was poured into the fermenter, and the water was sterilized for 20 minutes. The fermenter was allowed to cool to 50°C. The contact thermometer, disinfected with an alcohol dampened cloth, was inserted into the fermenter vessel. The temperature controller was turned on. The water temperature was allowed to stabilize at the desired temperature, usually overnight. The pH electrode was turned on and calibrated. Also, the Spectronic 21 was turned on. The ingredients of the synthetic media were mixed into the fermenter. The stirrer was set at 500 rpm. The pH electrode was

disinfected with an alcohol dampened cloth and inserted into the fermenter. The pH was manually adjusted using 0.86 N HCl or ✓ 1 N Na_2CO_3 . A sample of the medium was taken. The sample was placed into the Spectronic 21 and calibrated to 0 absorption. A sample of the inoculated broth was taken and the plating technique was performed to determine the cell count. The inoculated broth was poured into the fermenter. A sample was taken after 5 minutes and the stirrer was turned off. The sample was placed in the Spectronic 21 and the reading recorded. Both synthetic medium and five minute sample were ultrafiltered. The filtrate was saved in the freezer until ready to be analyzed using the HPLC. Samples were taken every hour. Before each sample was taken the media was stirred at 1500 rpm for five minutes to get a true representation of the media. The Spectronic 21 readings were recorded and the plate counting technique was performed every two hours. The samples were ultrafiltered and the filtrates were stored in the freezer. After the run had been completed, the pH probe and contact thermometer were removed and disinfected with the cloth soaked with alcohol. The protective shield was put in place and the entry ports were plugged. The media was sterilized for 20 minutes at 121°C and was disposed of properly.

CHAPTER 5

DISCUSSION OF RESULTS

Operating Conditions

Experiments were conducted to study the exponential growth phase of S. cerevisiae in a synthetic medium under static aerobic conditions. The medium was stirred periodically before a sample was taken. The experiments were conducted in 8ℓ of media in a 14ℓ batch fermenter over a temperature range of 30 to 41°C, pH range of 4.5 to 5.5, and glucose concentration of 0 to 60.6 g/ℓ. Each experiment was inoculated with yeast incubated for 24 hours at 34°C in 100 ml of broth. The total viable cell count for the inoculum was approximately 2×10^9 cells.

Constant temperature was maintained with a contact thermometer and a water heater. The medium was heated during the growth of the yeast and the fermentation of glucose to ethanol. The temperature could rise 1.5 degrees above the set point before the water heater would turn off and cool down to the inlet water temperature. The medium would then cool down 0.5 degrees below the set point until the water heater would turn back on. The cycle took approximately 30 minutes (Appendix A).

Constant pH control was maintained manually ± 0.2 pH units from the set point. When the fermentation of glucose to ethanol was taking place the pH would decrease as reported in other studies (4, 15, 23). ✓

Experimental Problems

A problem of contamination arose in this research. An inoculum size of 100 ml solved some of the contamination problems. With 100 ml of inoculum, there was enough yeast present to prevent growth of unwanted bacteria.

Another problem was that the yeast lived approximately three weeks on the slant before dying. The dead yeast look just like live yeast on a slant. Yeast had to be transferred to new slants periodically. A problem of mutation occurred when transferring the old yeast to new slants. After five transfers of the yeast to new slants, the yeast were not as white as they once were. A "mother" yeast was kept on a slant with sterile mineral oil and stored in a refrigerator and used periodically to regenerate the yeast.

Ethanol

The conversion of glucose to ethanol did occur. Ethanol was proven to be produced (Table 7) by using a Sigma Ethanol Assay (29). This did prove that the glucose did not metabolize

Table 7

Ethanol Concentration Profile

 $T = 30^{\circ}\text{C}$, $\text{pH} = 5.0$, $C_i = 23.1 \text{ g/l}$

Day	Ethanol w/v %	Yield, % Theoretical
0	0.01	0.002
1	0.035	0.006
2	0.083	0.014
3	0.140	0.024
4	0.170	0.029
5	0.156	0.026
6	0.350	0.059
7	0.340	0.058
8	0.515	0.087

to carbon dioxide and water. This could have occurred since oxygen was present in the gas above the medium, but the yeast lived at the bottom of the fermenter so the oxygen for the yeast had to come from the media. There was no dissolved oxygen probe to measure the dissolved oxygen.

Cell Count Versus Optical Density

A straight line calibration curve of optical absorption versus the total living cell count from the triplicate plate counts was obtained (Figure 13). The total living cells were calculated by multiplying the plate count (cells/ml) by the total volume (8000 ml). The total cell count from the plate count is actually the minimum cell count since some of the cells could die of shock when being transferred from the synthetic medium to the broth in the diluting process. There was no way to determine how many of the cells did die of shock. The slope and intercept were calculated by using the points which gave the best straight line in a SAS General Linear Model (GLM) (25) program (in Appendix B).

The medium had a different optical density with each experiment due to variation in glucose concentrations. The Spectronic 21 was calibrated to 0.0 absorption with the uninoculated synthetic medium giving each experiment a different starting reference point. The broth sometimes had a

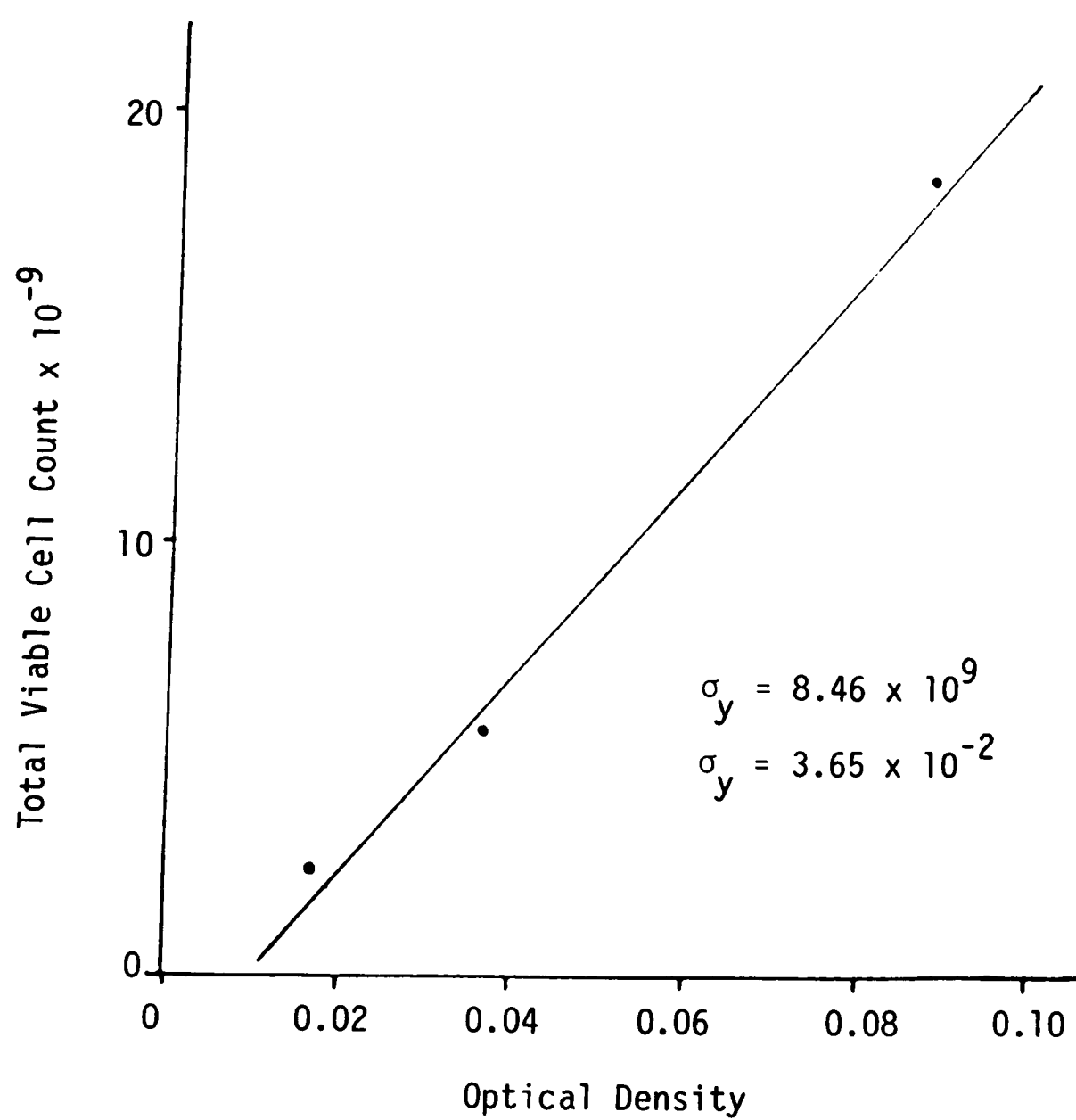


Figure 13. Total Viable Cell Count vs. Optical Density

different optical density because of the autoclaving step which would change the optical density of the inoculated medium. The change in optical density is due to slight caramelization of the glucose.

Calculation of the Specific Growth Rate

The specific exponential growth rate was calculated for every experiment. This was performed by plotting the natural log of the total cell count versus time (Appendix C). From the plot, three of the four points formed a straight line. Using these points, the SAS GLM program determined the slope (μ) of the best straight line through these points (Table 8).

Modeling the Specific Growth Rates

The Monod, Moser, and Teisser expressions were used to model the exponential specific growth rate of S. cerevisiae in a varied glucose medium. The growth parameters for each expression were determined by SAS NLIN programs (Appendix D) (25) using the specific growth rates and their corresponding glucose concentrations. The expressions were compared using the residual sum of squares.

A control experiment was performed to show that there is no growth without glucose. This was performed by using 250 ml of the media without the glucose. The experiment was conducted at 37°C and pH of 5.0, and no growth was detected. Since there

Table 8

Summary of Experimental Results

conc. of growth limit nutrient at start

Temperature ($^{\circ}\text{C}$)	pH	C_i (g/l)	μ (hr $^{-1}$)
30	4.5	23.1	0.373
30	5.0	13.1	0.396
30	5.0	23.1	0.507
30*	5.0	23.1	0.500
30	5.0	33.1	0.576
34	5.0	13.1	0.403
34	5.0	23.1	0.532
34	5.0	33.1	0.586
34*	5.0	33.1	0.600
37	4.5	23.1	0.143
37	5.0	13.1	0.426
37*	5.0	13.1	0.447
37	5.0	23.1	0.564
37	5.0	33.1	0.682
37	5.0	40.6	0.684
37	5.0	60.6	0.677
37	5.5	23.1	0.341
41	5.0	23.1	0.0

*Duplicate Experiments

was no growth at 37°C, it was assumed that there would be no growth without glucose at 30°C or at 34°C. Both the Monod and Teisser expressions predict this behavior. This is not true with the Moser expression since there would be division by zero which is undefined, but as C_i approaches zero, the specific growth rate from the Moser expression approaches zero. The point $C_i = 0.01$, $\mu = 0.0$ was used instead for calculating the parameters of the Moser expression.

An F test analysis was conducted to prove that each of the three expressions were valid over a 95% confidence level and that the Moser expression was calculated to be the best expression of the growth of the yeast based on the residual sum of squares in each case (Table 9 and Figures 14, 15 and 16) which came as no surprise. This is because the Moser expression has three parameters to curve fit the data while the Monod and the Teisser have only two parameters. In general, a three parameter expression will model the data better than a two parameter expression if the three parameter expression is a reasonable model for the data. Two parameter models are more desirable if they adequately represent the data.

The Monod expression represented the data for 30°C and 34°C better than the Teisser expression, while at first the Teisser expression at 37°C appeared to be better than the Monod expression. The parameters were recalculated without using the

Table 9

Parameter Values for the Monod, Moser and Teisser Expressions

T = 30°C		T = 34°C		T = 37°C	
<u>Monod Expression</u>		<u>Monod Expression</u>		<u>Monod Expression</u>	
$\mu_{\max} = 0.817 \text{ hr}^{-1}$		$\mu_{\max} = 0.855 \text{ hr}^{-1}$		$\mu_{\max} = 1.06 \text{ hr}^{-1}$	
$K_i = 14.1 \text{ g/l}$		$K_i = 14.5 \text{ g/l}$		$K_i = 19.0 \text{ g/l}$	
$RSOS = 6.82 \times 10^{-5}$		$RSOS = 1.55 \times 10^{-4}$		$RSOS = 6.34 \times 10^{-4}$	
<u>Moser Expression</u>		<u>Moser Expression</u>		<u>Moser Expression</u>	
$\mu_{\max} = 1.18 \text{ hr}^{-1}$		$\mu_{\max} = 0.715 \text{ hr}^{-1}$		$\mu_{\max} = 2.67 \text{ hr}^{-1}$	
$K_i = 11.6$		$K_i = 30.7$		$K_i = 24.5$	
$\lambda = 0.685$		$\lambda = 1.43$		$\lambda = 0.606$	
$RSOS = 2.54 \times 10^{-5}$		$RSOS = 9.8 \times 10^{-5}$		$RSOS = 3.88 \times 10^{-4}$	
<u>Teisser Expression</u>		<u>Teisser Expression</u>		<u>Teisser Expression</u>	
$\mu_{\max} = 0.670 \text{ hr}^{-1}$		$\mu_{\max} = 0.670 \text{ hr}^{-1}$		$\mu_{\max} = 0.766 \text{ hr}^{-1}$	
$K_i = 13.3 \text{ g/l}$		$K_i = 13.6 \text{ g/l}$		$K_i = 15.9 \text{ g/l}$	
$RSOS = 2.47 \times 10^{-4}$		$RSOS = 1.98 \times 10^{-3}$		$RSOS = 9.60 \times 10^{-4}$	

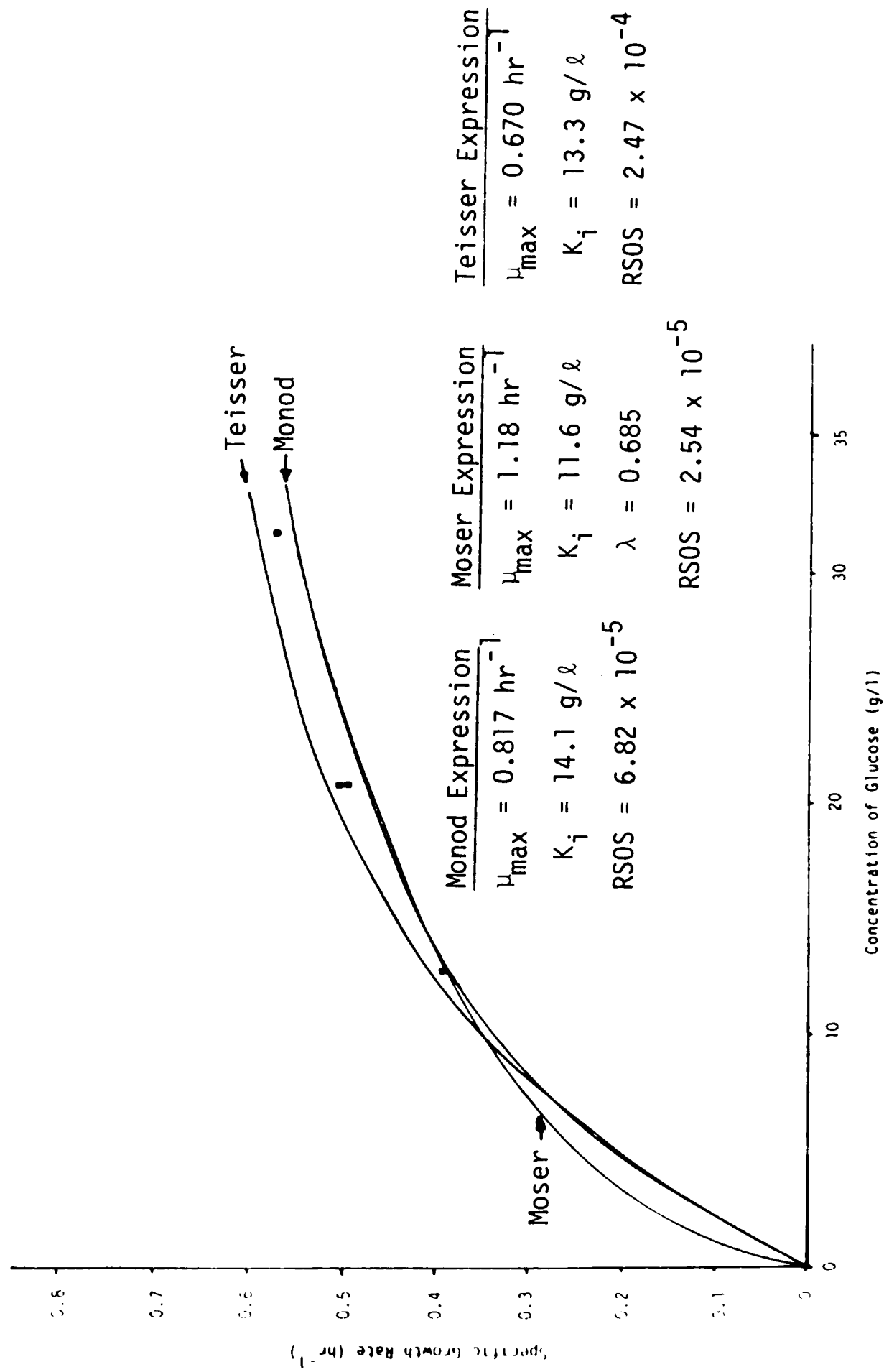


Figure 14. Specific Growth Rate vs. Concentration of Glucose at 30°C

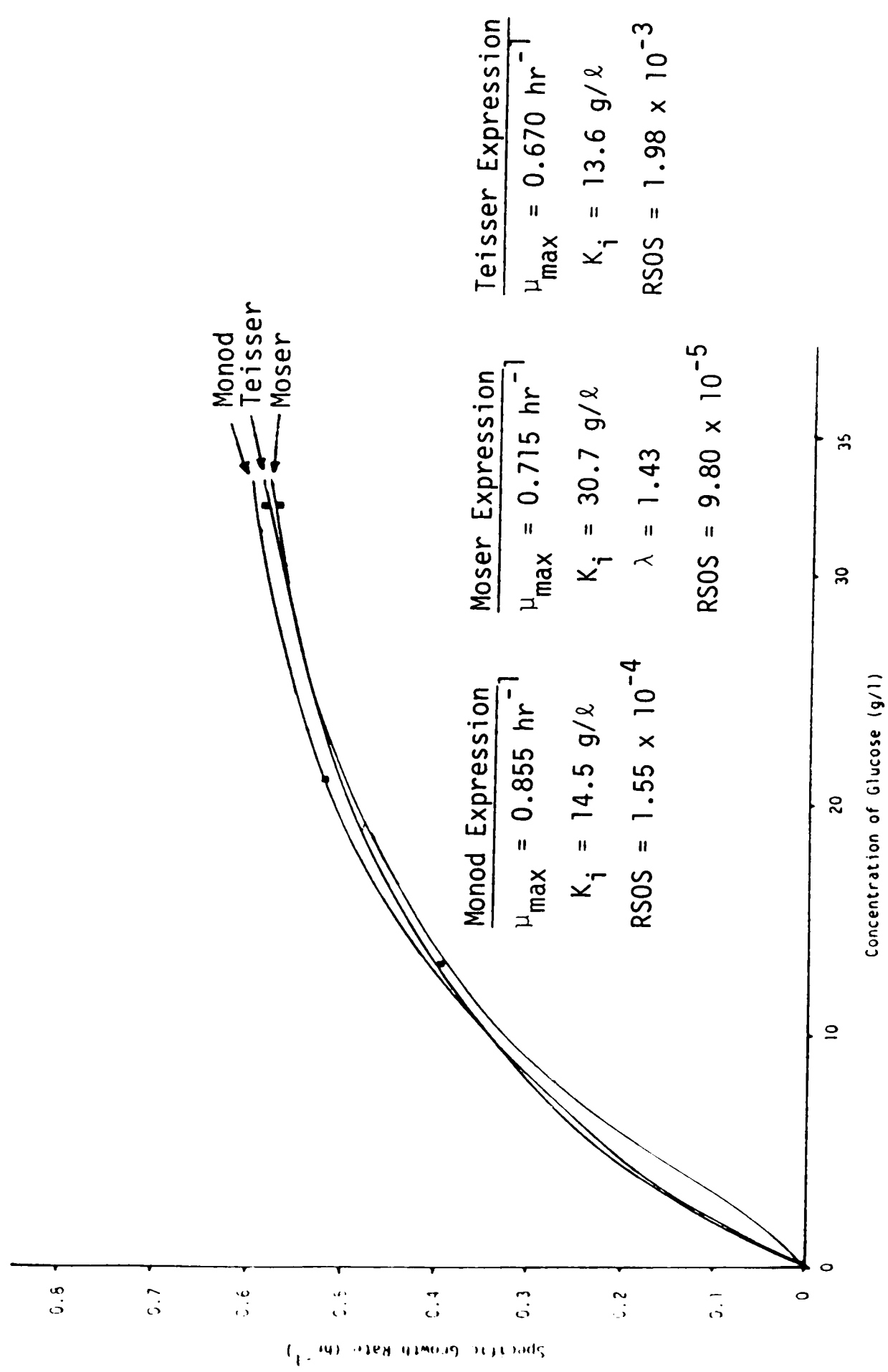


Figure 15. Specific Growth Rate vs. Concentration of Glucose at 34°C

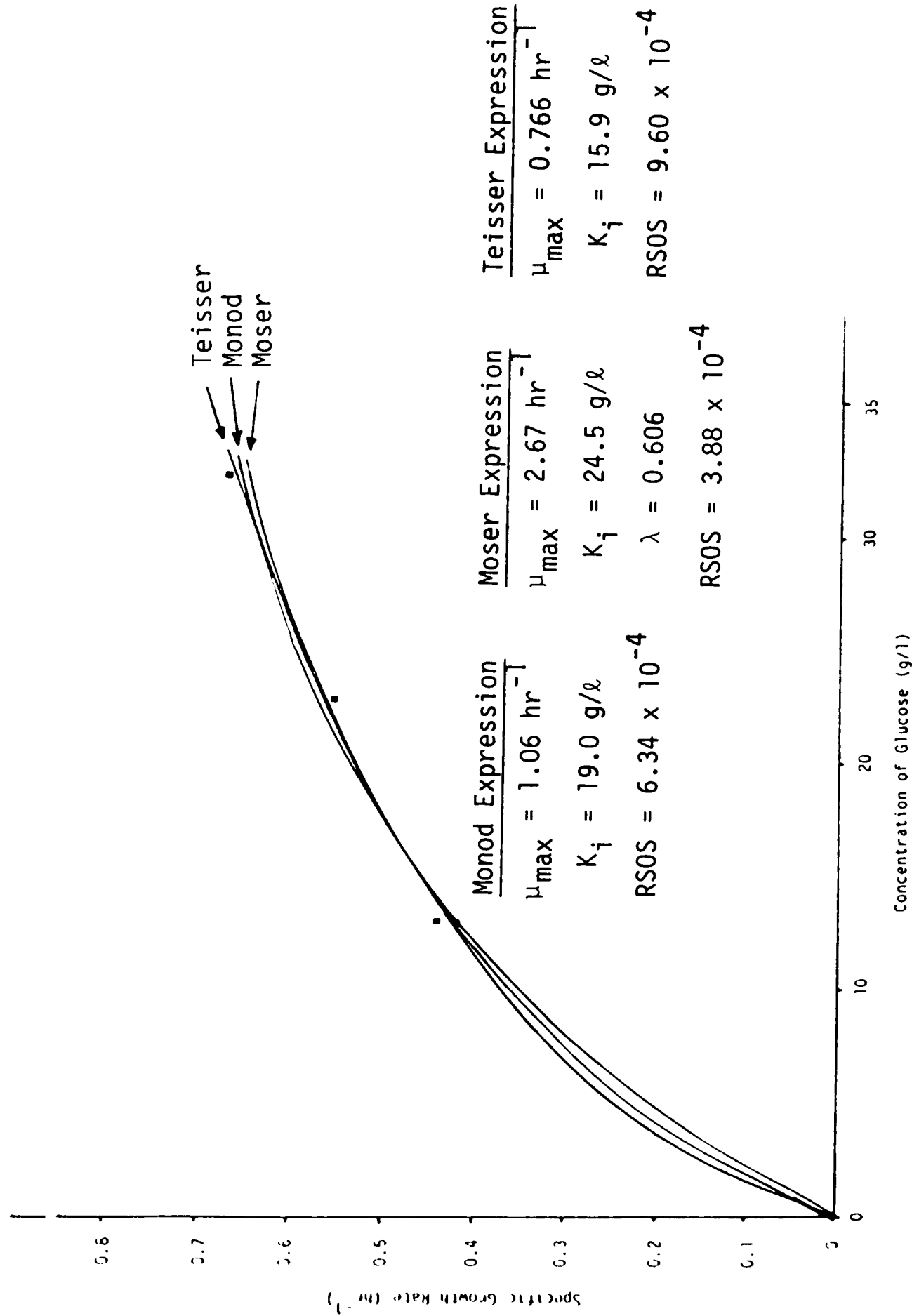


Figure 16. Specific Growth Rate vs. Concentration of Glucose at 37°C

40.6 and 60.6 g/l experiments and the Monod expression worked better. The question rose as to why the Teisser expression worked better than the Monod at 37°C with the higher glucose concentrations but not without the higher glucose concentrations. A Lineweaver plot (Appendix E) (5):

$$(1/\mu) = (1/\mu_{\max}) + (K_m/\mu_{\max})(1/C_{i0}) \quad (14)$$

was performed for each temperature (Figures 17, 18 and 19). It was noticed that it did not form a straight line as did the 30°C and 34°C experiments. The reason for the deviation from the Monod expression is that glucose is no longer the growth limiting nutrient. Therefore, the Monod expression did model the growth better than the Teisser expression

Sensitivity of the Parameter Values

The values of the parameters for each expression were calculated at each temperature without the duplicate experiment. The values of the parameters were then recalculated with the duplicate experiment and without the original experiment (Table 10). This was performed to find out how sensitive the parameters were to the data.

At 30°C and C_i of 23.1 g/l, the specific growth rate changed from 0.507 to 0.500 hr⁻¹. The Monod maximum specific growth rate changed 0.3% without the duplicate experiment and

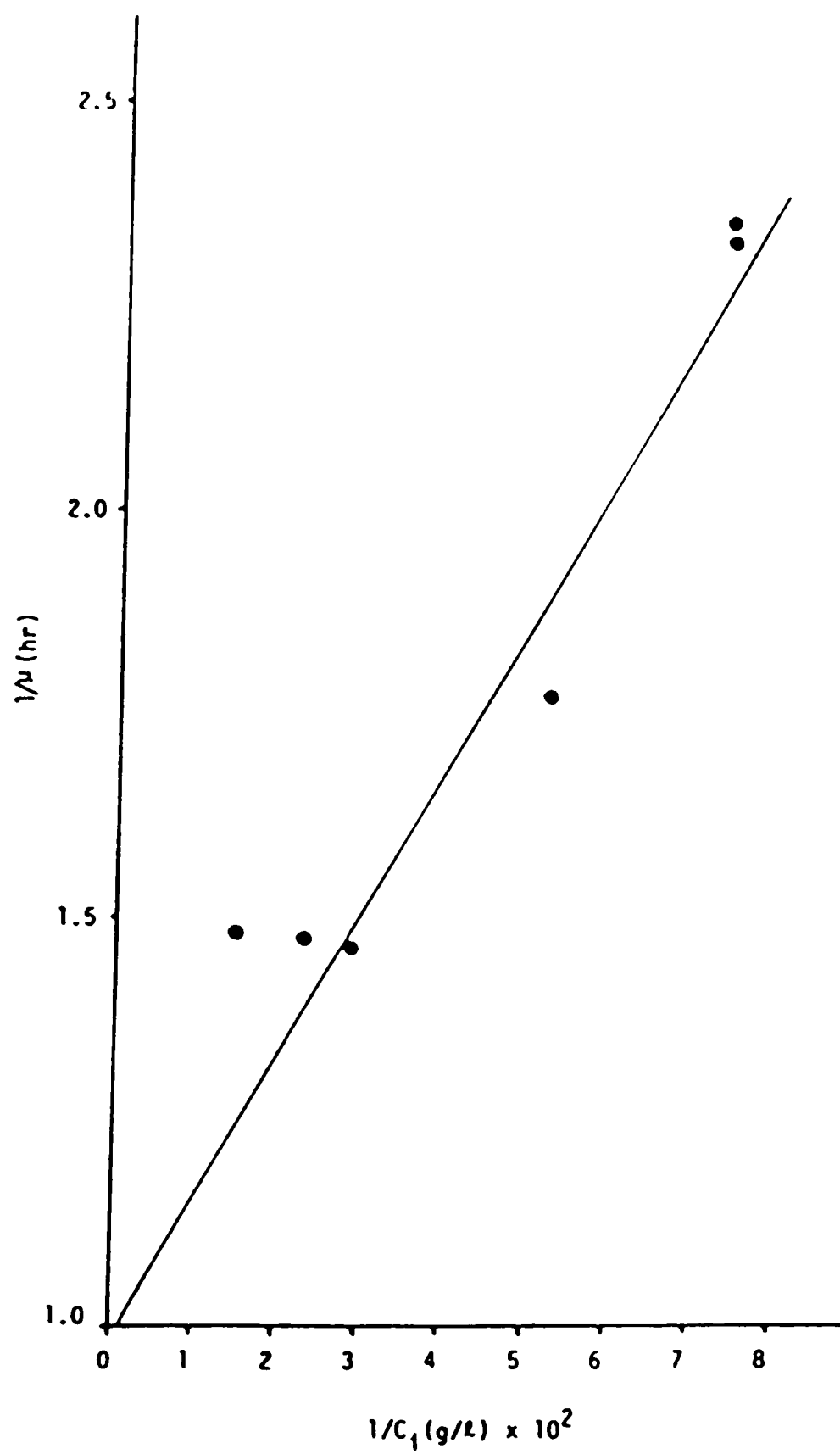


Figure 17. Lineweaver Plot of $1/\mu$ vs. $1/C_i$ at 37°C

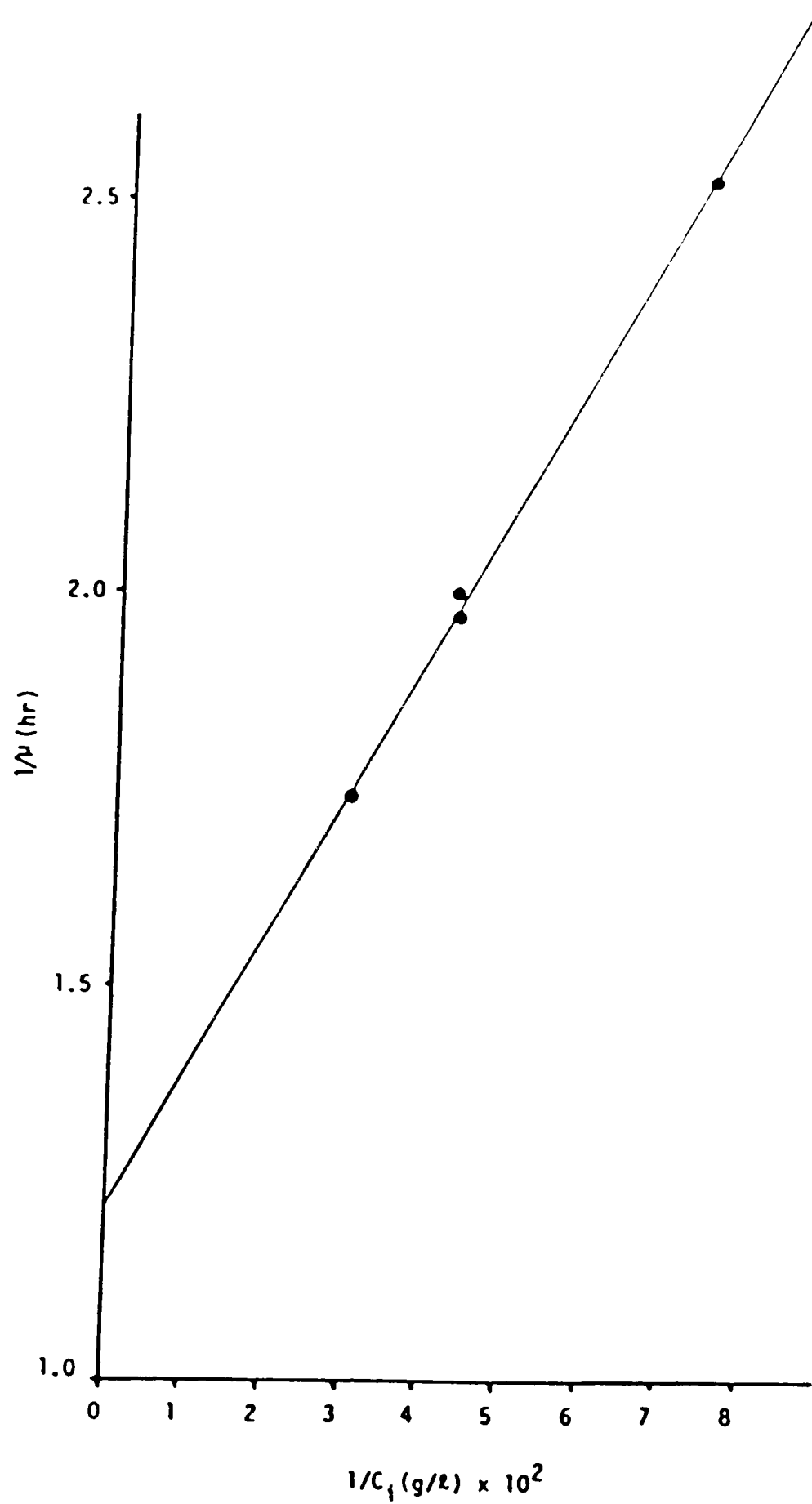


Figure 18. Lineweaver Plot of $1/\mu$ vs. $1/C_i$ at 30°C

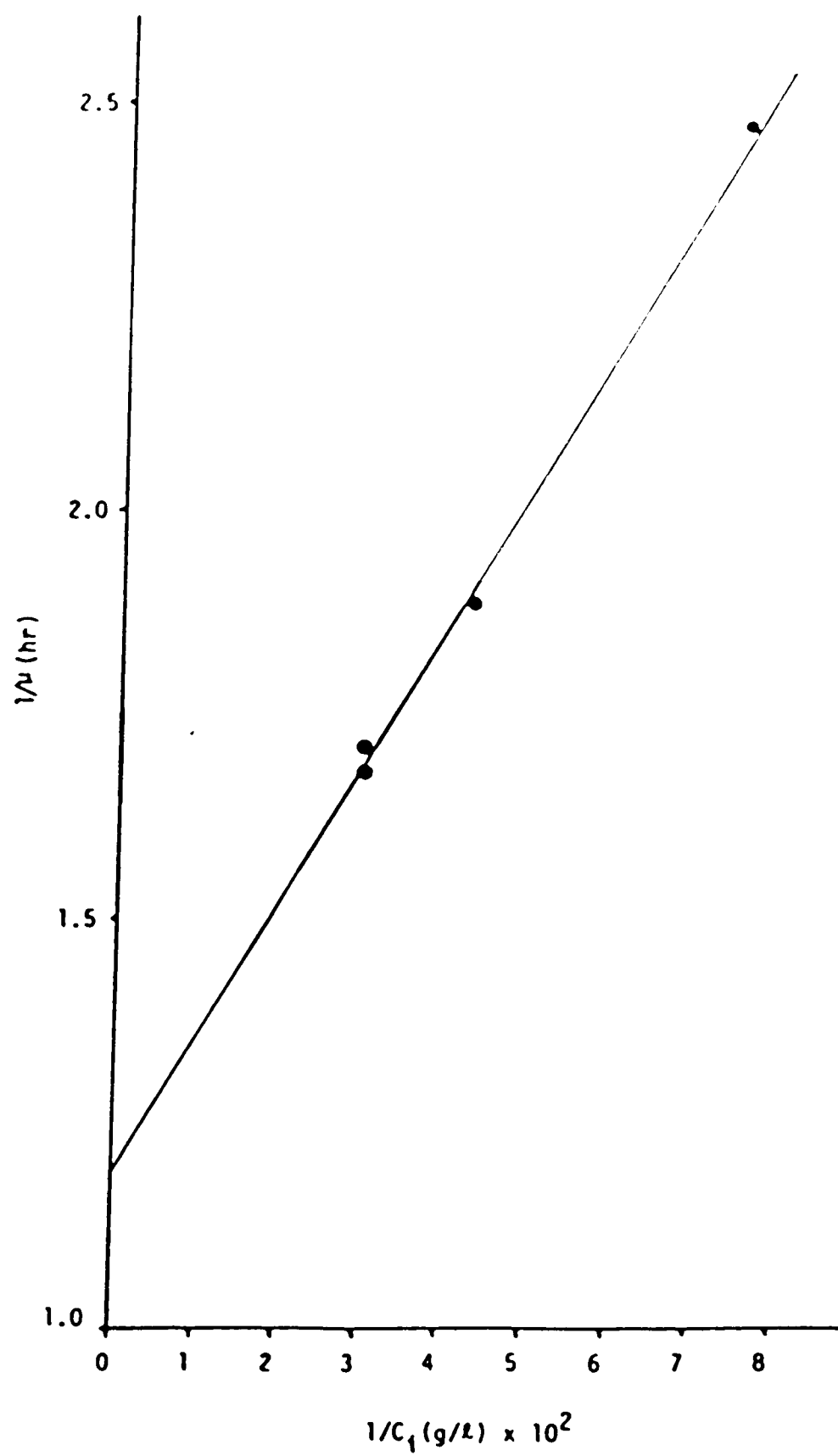


Figure 19. Lineweaver Plot of $1/\mu$ vs. $1/C_i$ at 34°C

Table 10
Sensitivity of Parameter Values

T = 30°C

<u>Monod</u>				
Case 1	μ_{\max}	= 0.819 hr ⁻¹	K_i	= 14.1 g/l
Case 2	μ_{\max}	= 0.816 hr ⁻¹	K_i	= 14.1 g/l
Case 3	μ_{\max}	= 0.817 hr ⁻¹	K_i	= 14.1 g/l
<u>Moser</u>				
Case 1	μ_{\max}	= 0.90 hr ⁻¹	K_i	= 12.3 (g/l) ^{0.879} λ = 0.807
Case 2	μ_{\max}	= 1.083 hr ⁻¹	K_i	= 11.5 (g/l) ^{0.733} λ = 0.733
Case 3	μ_{\max}	= 1.182 hr ⁻¹	K_i	= 11.6 (g/l) ^{0.685} λ = 0.685
<u>Teisser</u>				
Case 1	μ_{\max}	= 0.623 hr ⁻¹	K_i	= 13.2 g/l
Case 2	μ_{\max}	= 0.621 hr ⁻¹	K_i	= 13.3 g/l
Case 3	μ_{\max}	= 0.620 hr ⁻¹	K_i	= 13.3 g/l

T = 34°C

<u>Monod</u>				
Case 1	μ_{\max}	= 0.839 hr ⁻¹	K_1	= 13.9 g/l
Case 2	μ_{\max}	= 0.884 hr ⁻¹	K_1	= 15.5 g/l
Case 3	μ_{\max}	= 0.855 hr ⁻¹	K_1	= 14.5 g/l
<u>Moser</u>				
Case 1	μ_{\max}	= 0.669 hr ⁻¹	K_1	= 46.9 (g/l) ^{1.66} λ = 1.66
Case 2	μ_{\max}	= 0.779 hr ⁻¹	K_1	= 22.2 (g/l) ^{1.23} λ = 1.23
Case 3	μ_{\max}	= 0.715 hr ⁻¹	K_1	= 30.7 (g/l) ^{1.43} λ = 1.43
<u>Teisser</u>				
Case 1	μ_{\max}	= 0.638 hr ⁻¹	K_1	= 13.0 g/l
Case 2	μ_{\max}	= 0.661 hr ⁻¹	K_1	= 14.0 g/l
Case 3	μ_{\max}	= 0.670 hr ⁻¹	K_1	= 13.6 g/l

Case 1: with original experiment without duplicate experiment

Case 2: without original experiment with duplicate experiment

Case 3: with both original and duplicate experiments

Table 10 (continued)

T = 37°C

<u>Monod</u>		
Case 1	$\mu_{\max} = 1.13 \text{ hr}^{-1}$	$K_i = 22.1 \text{ g/l}$
Case 2	$\mu_{\max} = 1.04 \text{ hr}^{-1}$	$K_i = 17.9 \text{ g/l}$
Case 3	$\mu_{\max} = 1.06 \text{ hr}^{-1}$	$K_i = 19.0 \text{ g/l}$
<u>Moser</u>		
Case 1	$\mu_{\max} = 2.72 \text{ hr}^{-1}$	$K_i = 28.1 \quad \lambda = 0.64$
Case 2	$\mu_{\max} = 2.50 \text{ hr}^{-1}$	$K_i = 21.7 \quad \lambda = 0.60$
Case 3	$\mu_{\max} = 2.67 \text{ hr}^{-1}$	$K_i = 24.5 \quad \lambda = 0.61$
<u>Teisser</u>		
Case 1	$\mu_{\max} = 0.798 \text{ hr}^{-1}$	$K_i = 17.8 \text{ g/l}$
Case 2	$\mu_{\max} = 0.760 \text{ hr}^{-1}$	$K_i = 15.5 \text{ g/l}$
Case 3	$\mu_{\max} = 0.766 \text{ hr}^{-1}$	$K_i = 15.9 \text{ g/l}$

0% with the duplicate experiment from the maximum specific growth rate calculated using both experiments. The K_i changed -0.4% without the duplicate point and 0% with the duplicate experiment from the K_i calculated using both experiments. For the Teisser expression, the maximum specific growth rate changed 0.5% and 0.1%. The Moser parameters of maximum specific growth rate changed -23.8% and -8.4%, K_i changed 6.0% and -6.0%, and λ changed 28.3% and 7.0%.

At 34°C and C_i of 33.1 g/l the specific growth rate changed from 0.586 to 0.600 hr⁻¹. For the Monod expression the maximum specific growth rate changed -1.9% and 3.4%, while K_i changed -4.0% and 7.2%. For the Teisser expression the maximum specific growth rate changed -1.7% and 1.8% while K_i changed 3.1% and 3.7%. The Moser parameters of the maximum specific growth rate changed -6.4% and 9.0%, K_i changed 52.7% and -27.9%, and λ changed 15.8% and -13.9%.

At 37°C and C_i of 13.1 g/l, the specific growth rate changed from 0.426 to 0.447 hr⁻¹. For the Monod expression, the maximum specific growth rate changed -6.6% and -9.9% while K_i changed -16.3% and -5.8%. For the Teisser expression, the maximum specific growth rate changed 4.2% and -0.8% while K_i changed -11.9% and -2.5%. The Moser parameters of maximum specific growth rate changed 1.9% and 6.4, K_i changed 14.7% and -11.4%, and λ changed 4.9% and -1.6%.

The parameter values for the Moser expression varied greatly, meaning that the Moser expression is more a curve fit of the data rather than a model of the growth. In calculating the growth parameters for the Monod and Teisser expressions, the K_i is more sensitive to the data than the maximum specific growth rate. This means that the maximum specific growth rate can be determined using only a few points, while K_i needs many points in order to be determined.

An error analysis was performed. Using Equation 15, an error was calculated for each data point. The results of this analysis are shown in Table 11. The average error for the Monod was 0.02% at 30°C, -0.08% at 34°C, and -0.19% at 37°C. For the Teisser expression, it was 0.5% at 30°C, -1.50% at 34°C and -0.72% at 37°C. For the Moser expression, it was 0.15% at 30°C, -0.01% at 34°C, and -0.15% at 37°C. This shows that each expression represents the data quite well.

$$\% \text{ Error} = ((\mu_{\text{exp}} - \mu_{\text{per}}) / \mu_{\text{exp}}) \times 100 \quad (15)$$

Temperature Effects on the Specific Growth Rate

The effect of temperature on the specific growth rate was studied by keeping the glucose concentration and pH constant and varying the temperature. The natural log of the specific growth rate was plotted versus $1/T$, as shown in Figure 20. This

Table 11

Comparison of Predicted and Actual Growth Rates

Monod Expression:

 $T = 30^{\circ}\text{C}$

C_i g/l	μ_p hr ⁻¹	μ_E hr ⁻¹	% Error
13.1	0.393	0.396	0.76
23.1	0.507	0.507	0
23.1	0.507	0.500	-1.38
33.1	0.572	0.576	0.69

Avg. % Error = 0.02

 $T = 34^{\circ}\text{C}$

C_i g/l	μ_p hr ⁻¹	μ_E hr ⁻¹	% Error
13.1	0.406	0.403	-0.74
23.1	0.526	0.532	1.13
33.1	0.594	0.586	-1.54
33.1	0.595	0.600	0.84

Avg. % Error = -0.08

 $T = 37^{\circ}\text{C}$

C_i g/l	μ_p hr ⁻¹	μ_E hr ⁻¹	% Error
13.1	0.433	0.426	-1.64
13.1	0.433	0.447	3.13
23.1	0.582	0.564	-3.19
33.1	0.673	0.682	1.32

Avg. % Error = -0.19

Table 11 (continued)

Teisser Expression:

 $T = 30^{\circ}\text{C}$

C_i g/l	μ_p hr ⁻¹	μ_E hr ⁻¹	% Error
13.1	0.388	0.396	2.02
23.1	0.511	0.507	0.79
23.1	0.511	0.500	-2.20
33.1	0.568	0.576	1.39

Avg. % Error = 0.50

 $T = 34^{\circ}\text{C}$

C_i g/l	μ_p hr ⁻¹	μ_E hr ⁻¹	% Error
13.1	0.414	0.403	-2.73
23.1	0.547	0.532	2.82
33.1	0.611	0.586	-4.27
33.1	0.611	0.600	-1.83

Avg. % Error = -1.50

 $T = 37^{\circ}\text{C}$

C_i g/l	μ_p hr ⁻¹	μ_E hr ⁻¹	% Error
13.1	0.430	0.426	-0.94
13.1	0.430	0.447	3.80
23.1	0.587	0.546	-7.51
33.1	0.670	0.682	1.76

Avg. % Error = -0.72

Table 11 (continued)

Moser Expression:

 $T = 30^{\circ}\text{C}$

C_i g/l	μ_p hr ⁻¹	μ_E hr ⁻¹	% Error
13.1	0.395	0.396	0.25
23.1	0.503	0.507	0.79
23.1	0.503	0.500	-0.60
33.1	0.575	0.576	0.17

Avg. % Error = 0.15

 $T = 34^{\circ}\text{C}$

C_i g/l	μ_p hr ⁻¹	μ_E hr ⁻¹	% Error
13.1	0.403	0.403	0
23.1	0.532	0.532	0
33.1	0.593	0.586	-1.19
33.1	0.593	0.600	1.17

Avg. % Error = -0.01

 $T = 37^{\circ}\text{C}$

C_i g/l	μ_p hr ⁻¹	μ_E hr ⁻¹	% Error
13.1	0.434	0.426	-1.88
13.1	0.434	0.447	2.91
23.1	0.574	0.564	-1.77
33.1	0.678	0.682	0.59

Avg. % Error = -0.15

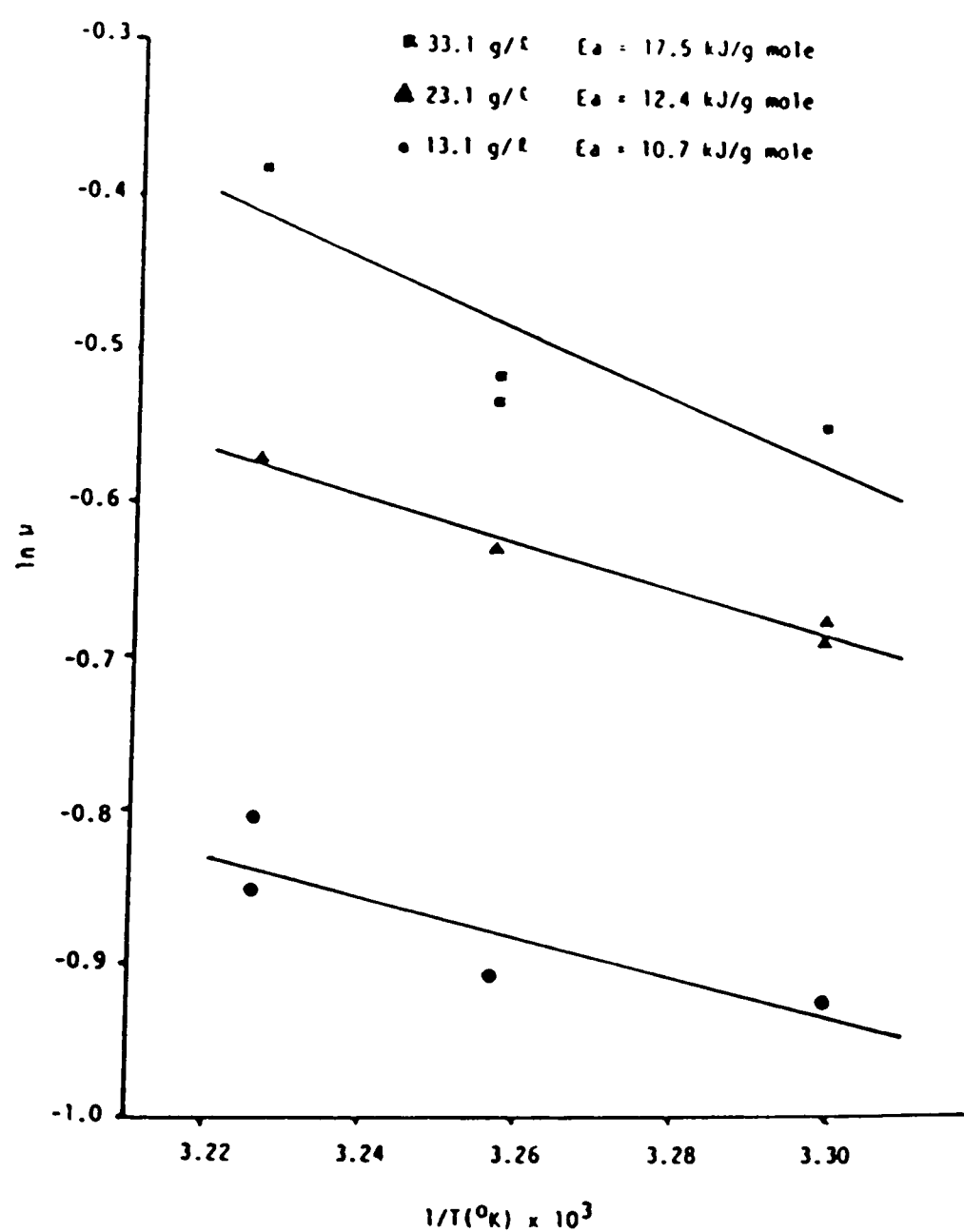


Figure 20. The Natural Log of the Specific Growth Rate vs. $1/T$

resulted in a straight line showing that indeed the Arrhenius expression is true. The activation energy was calculated from the slope of these lines (Equation 12). The activation energy was calculated at each different glucose concentration. An F test analysis was conducted, and, statistically, there is no change in activation energy with glucose concentration. The temperature was raised to 41°C, and the S. cerevisiae died as predicted in the literature (28).

Temperature Effects on the Maximum Specific Growth Rates

Since the specific growth rate followed the Arrhenius expression, it was suggested that the maximum specific growth rate might also follow the Arrhenius expression.

$$\mu_{\max} = \mu_{\max_0} e^{-E_a/RT} \quad (16)$$

This expression for μ_{\max} was substituted in the Monod, Moser, and Teisser expressions and the following modified expressions were derived.

$$\mu = \mu_{\max_0} e^{-E_a/RT} (C_{i0}/(K_i + C_{i0})) \quad (17)$$

$$\mu = \mu_{\max_0} e^{-E_a/RT} (1 + K_i C_{i0}^{-\lambda})^{-1} \quad (18)$$

$$\mu = \mu_{\max_0} e^{-E_a/RT} (1 - e^{-C_{i0}/K_i}) \quad (19)$$

The μ_{\max} calculated previously for each temperature before, could not be used since each expression had a different K_i . The SAS NLIN (Appendix F) was used to calculate a μ_{\max_0} , E_a , and a K_i . An F test analysis was conducted to prove that each expression was valid over a 95% confidence level. The Teisser expression was the best expression based on the residual sum of squares (Table 12 and Figures 21, 22, and 23). This K_i was used in the isothermal expressions to calculate a new μ_{\max} . The $\ln \mu_{\max}$ was then plotted versus $1/T$ and did follow the predicted line (Figures 24, 25, and 26). This means the modified expressions are valid forms to express the effect of temperature on the maximum specific growth rate. The modified expressions were then compared to the experimental data.

Glucose Analysis

The Water's HPLC was used to analyze the glucose concentration. An area under the peak was calculated for the standard glucose concentration. A straight line calibration curve was calculated using a SAS GLM program. Three different glucose standard concentrations were used to prove that the calibration curve would form a straight line. The HPLC could not measure the glucose concentration accurately enough to determine exact glucose concentration, but was used to show

Table 12

Parameter Values for the Modified Monod,
Moser and Teisser Expressions

Modified Monod Expression

$$\mu_{\max_0} = 1510 \text{ hr}^{-1}$$

$$E_a = 18.9 \text{ KJ/g mole}$$

$$K_i = 15.5 \text{ g/l}$$

$$\text{RSOS} = 6.3 \times 10^{-3}$$

Modified Moser Expression

$$\mu_{\max_0} = 1840 \text{ hr}^{-1}$$

$$E_a = 20.2 \text{ KJ/g mole}$$

$$K_i = 149$$

$$\lambda = 2.13$$

$$\text{RSOS} = 5.0 \times 10^{-3}$$

Modified Teisser Expression

$$\mu_{\max_0} = 1350 \text{ hr}^{-1}$$

$$E_a = 19.4 \text{ KJ/g mole}$$

$$K_i = 13.9 \text{ g/l}$$

$$\text{RSOS} = 5.5 \times 10^{-3}$$

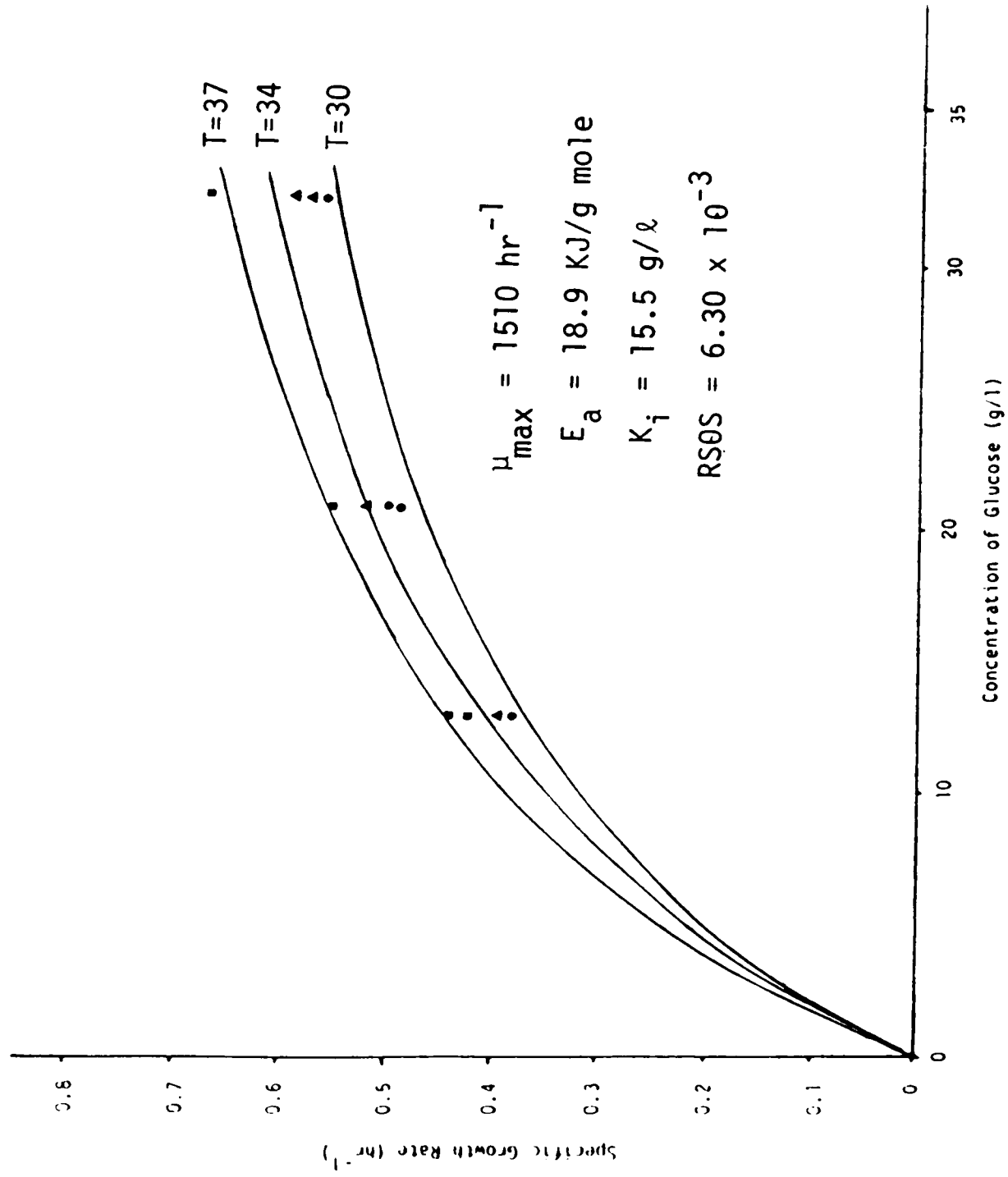


Figure 21. A Plot of the Modified Monod Expression

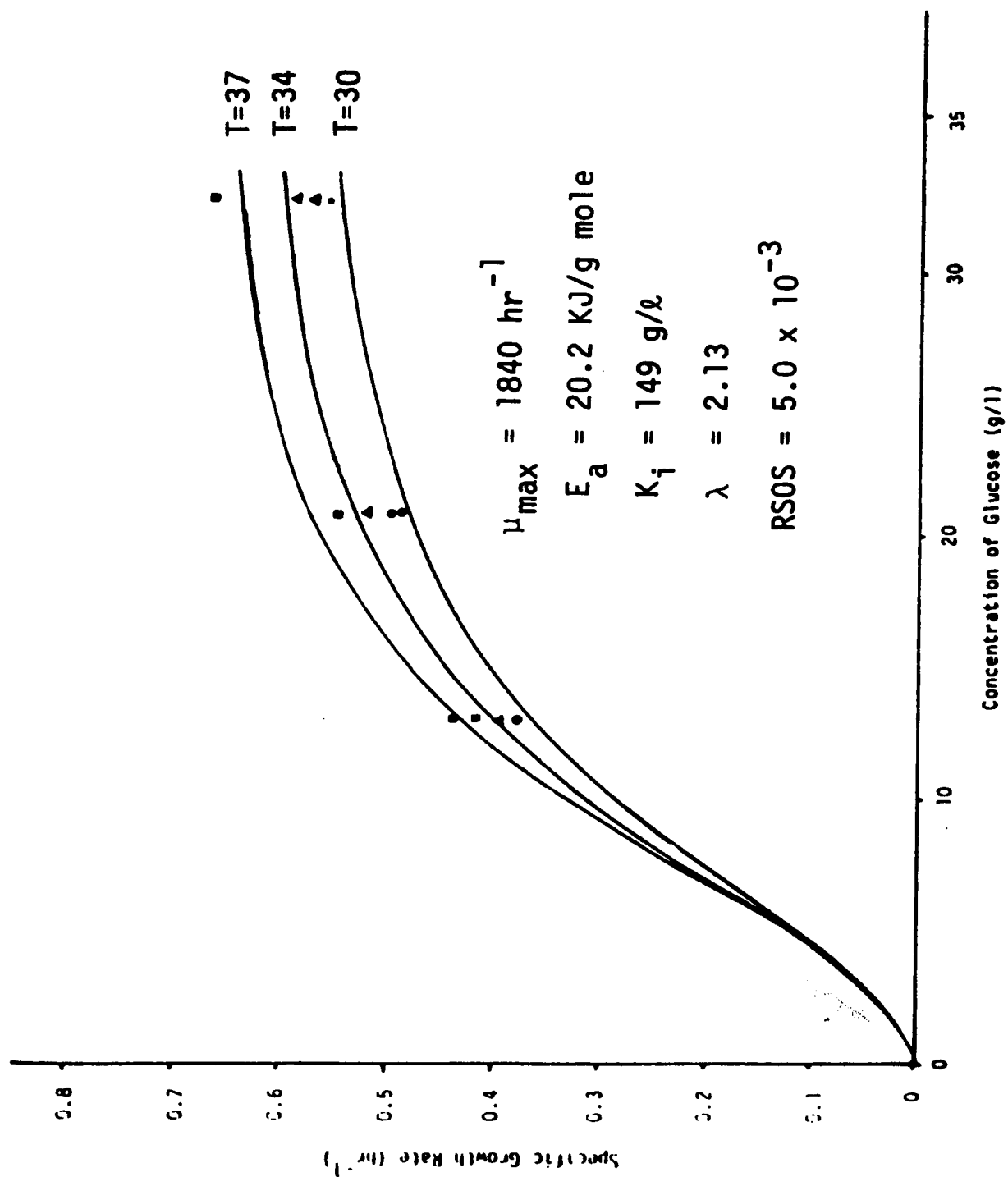


Figure 22. A Plot of the Modified Moser Expression

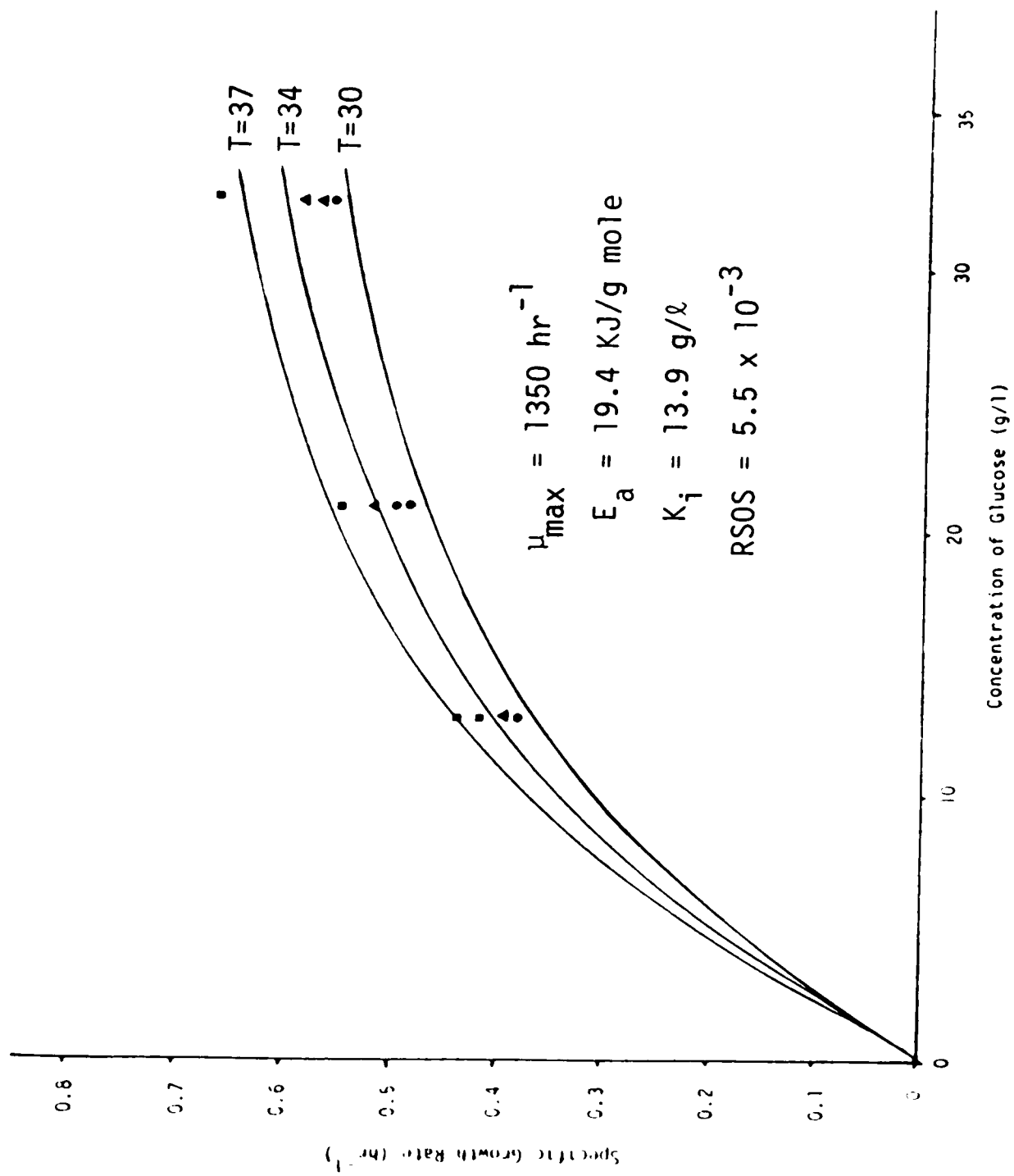


Figure 23. A Plot of the Modified Teisser Expression

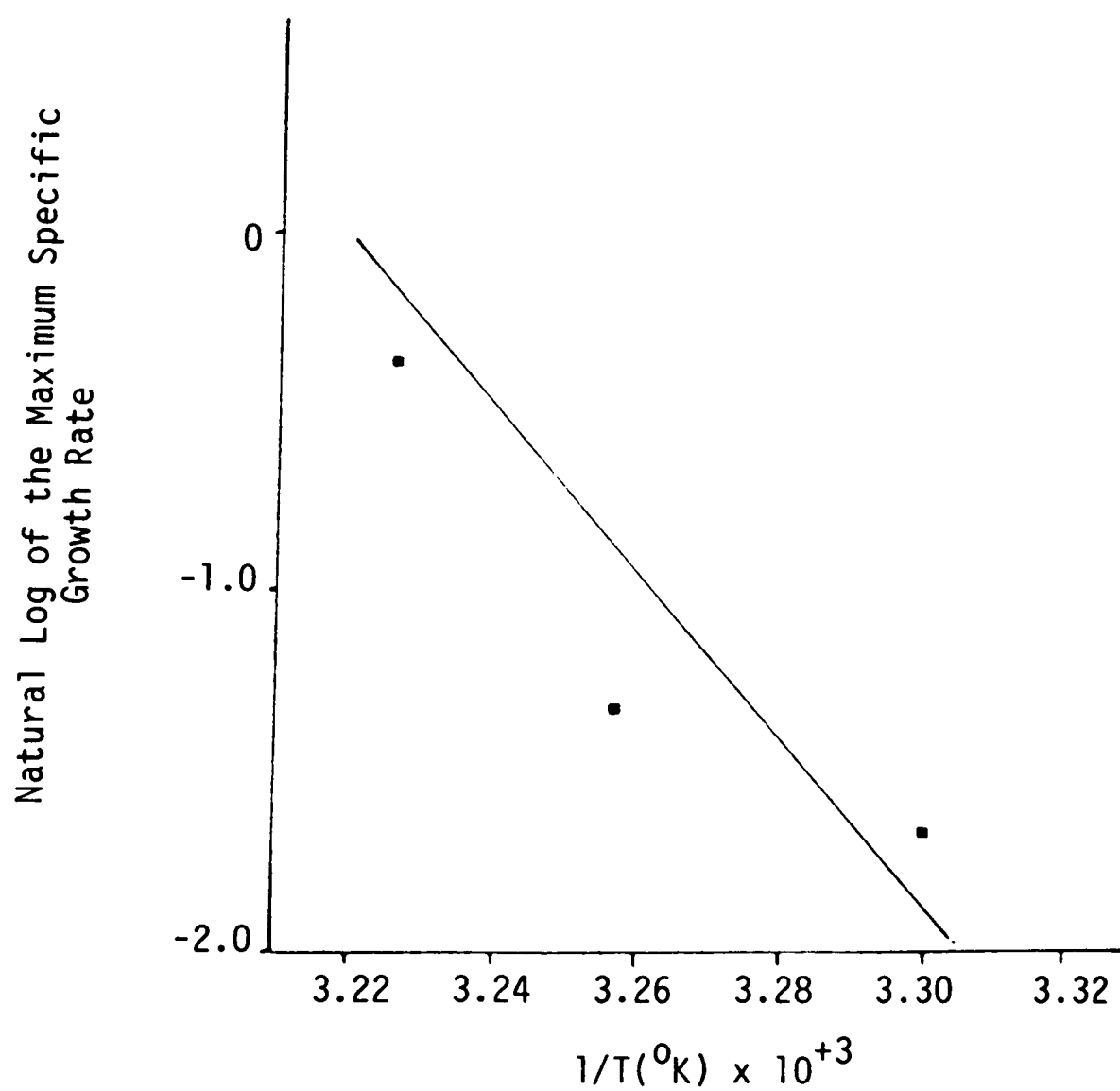


Figure 24. The Natural Log of the Maximum Specific Growth Rate vs. $1/T$ for the Modified Monod Expression

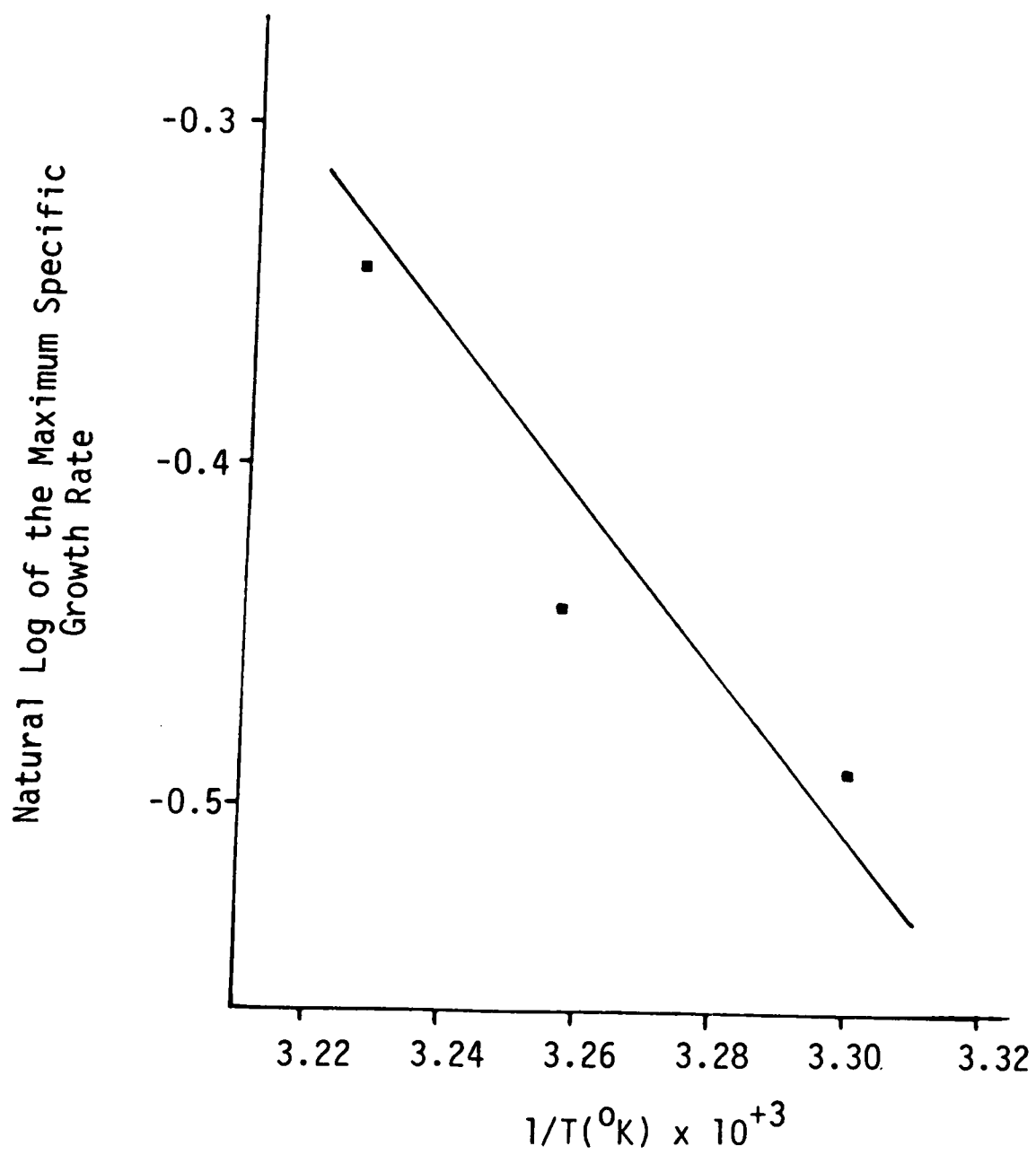


Figure 25. The Natural Log of the Maximum Specific Growth Rate vs. $1/T$ for the Modified Moser Expression

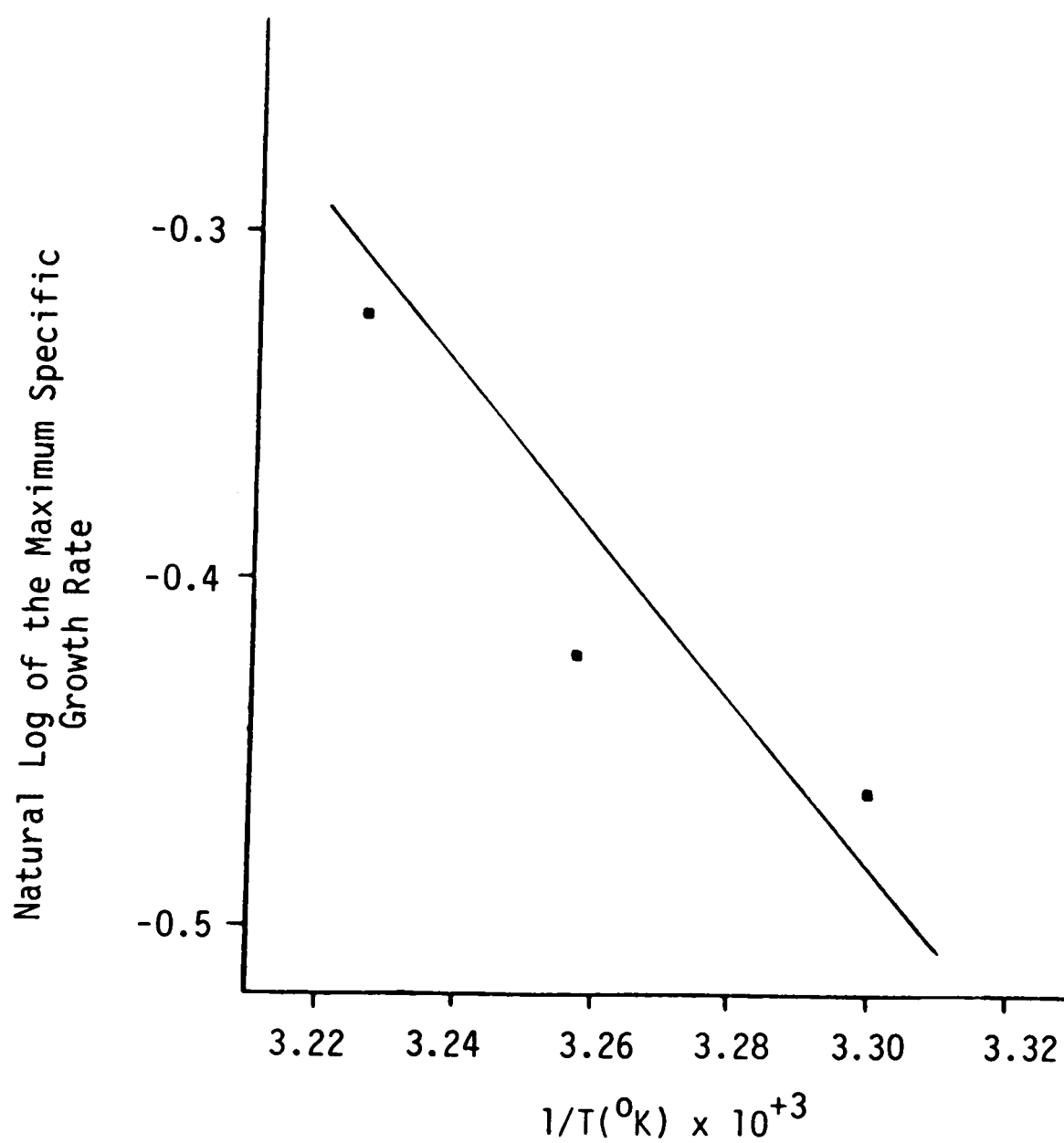


Figure 26. The Natural Log of the Maximum Specific Growth Rate vs. $1/T$ for the Modified Teisser Expression

that the glucose concentration was constant through the 3 to 6 hour mark when the specific growth rates were calculated (Appendix G). This shows that the samples were a consistent representation of the media.

pH Effects

Three experiments were conducted at pH of 4.5, 5.0, and 5.5 at a temperature of 36°C, and a glucose concentration of 23.1 g/l (Figure 27). The pH of 5.0 was found to have the highest specific growth rate. The optimum pH for growth might not be the best pH to ferment glucose to ethanol, because the choice of pH should take into account the pH at which undesirable microorganisms will not live.

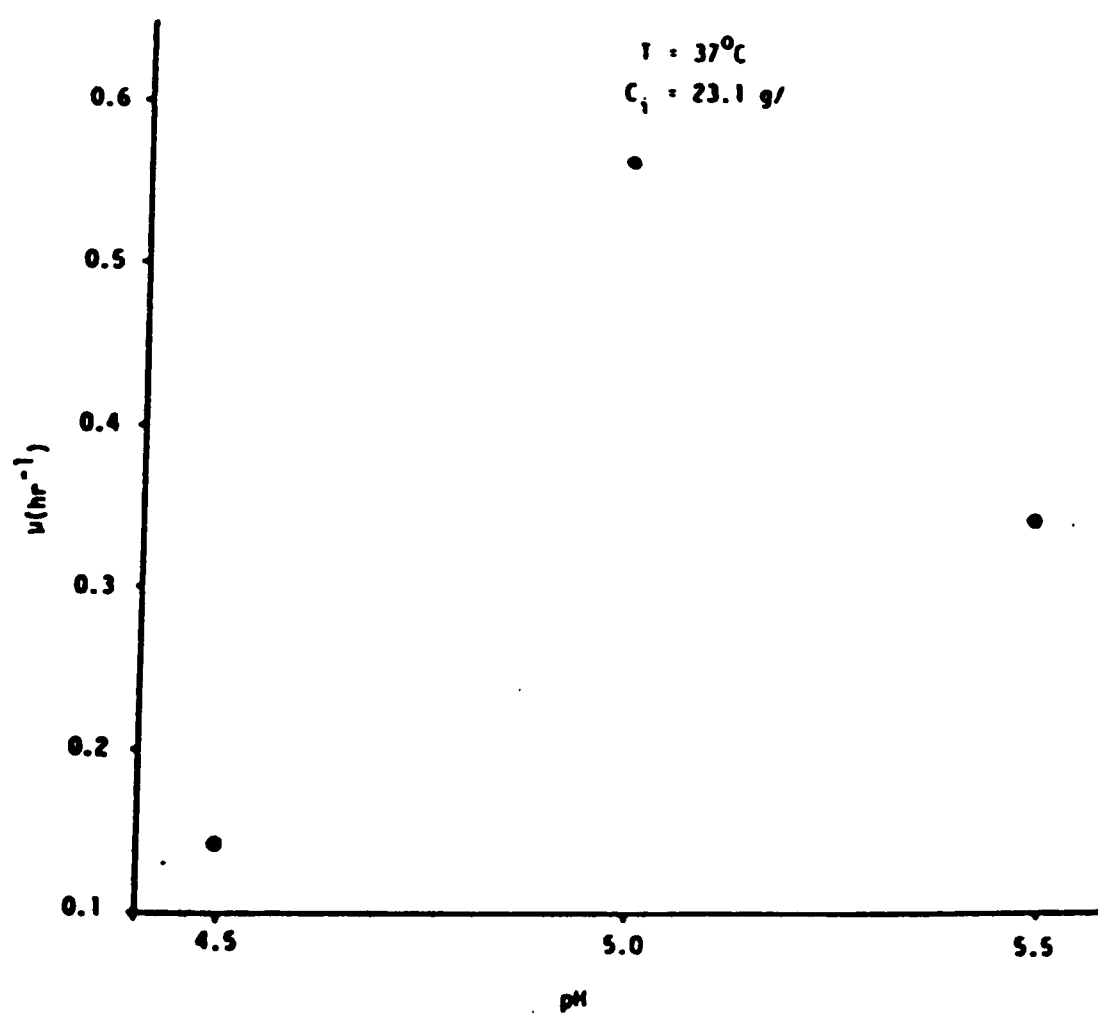


Figure 27. A Plot of the Specific Growth Rate vs. pH

CHAPTER 6

CONCLUSIONS AND RECOMMENDATIONS

Conclusions

As a result of this research, the following conclusions were determined.

1. The Moser expression was determined to be the best model for the range of operating conditions investigated.
2. Glucose ceased to be the growth limiting nutrient between 33.1 and 40.6 g/l.
3. The Arrhenius expression was valid for predicting the temperature dependence of the maximum specific growth rate for the Monod, Moser and Teisser expressions.

Recommendations

The author recommends that the following items be considered for further research on this topic.

1. The cell mass, instead of cell number, should be correlated with optical density because of the inherent errors in the plating technique.
2. The fermenter should be operated at aerobic or anaerobic conditions instead of static aerobic where both conditions occur.

LIST OF REFERENCES

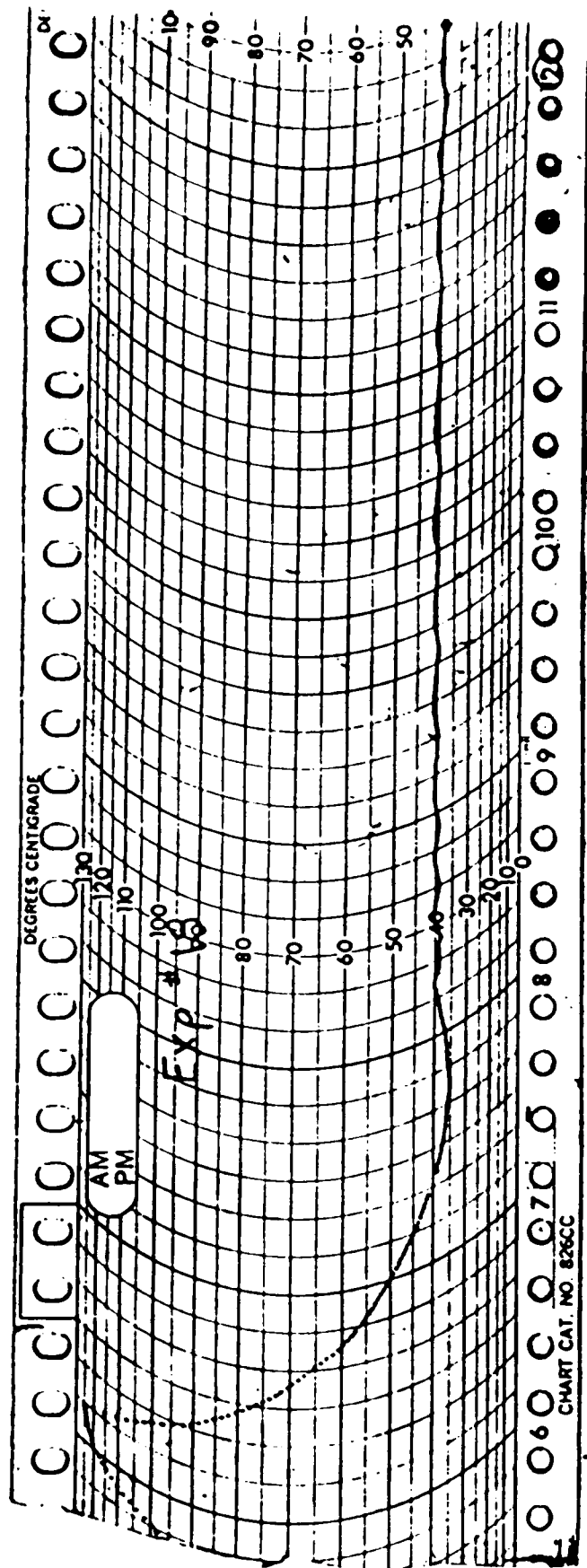
1. Aiba, S., A. E. Humphrey and N. F. Millis, Biochemical Engineering, Academic Press, New York (1965).
2. Aiba, S., M. Shoda and M. Nagatani, "Kinetics of Product Inhibition in Alcohol Fermentation," Biotechnology and Bioengineering, 10, 845-864 (1968).
3. Atkinson, B., Biochemical Reactors, Pion Limited, London (1974).
4. Bach, H. P., W. Woehrer and M. Roehr, "Continuous Determination of Ethanol During Aerobic Cultivation of Yeasts," Biotechnology and Bioengineering, 20: 799-807 (1978).
5. Bailey, J. E. and D. F. Ollis, Biochemical Engineering Fundamentals, McGraw-Hill, St. Louis (1977).
6. Barford, J. P. and R. J. Hall, "Estimation of the Length of Cell Cycle Phase from Asynchronous Cultures of *S. cerevisiae*," Experimental Cell Research, 102: 276 (1976).
7. Barford, J. P. and R. J. Hall, "A Mathematical Model for the Aerobic Growth of *Saccharomyces cerevisiae* with Saturated Respiratory Capacity," Biotechnology and Bioengineering, 23, 1735-1762 (1981).
8. Bijkerk, A. H. and R. J. Hall, "A Mechanistic Model of the Aerobic Growth of *Saccharomyces cerevisiae*," Biotechnology and Bioengineering, 19, 267-296 (1977).
9. Carter, B. L. and M. H. Jagadish, "The Relationship Between Cell Size and Cell Division in the Yeast *S. cerevisiae*," Experimental Cell Research, 112: 15-22 (1978).
10. Chemapec, Inc., Chemapec P.E.C. Glass Fermenter Type GF0014 Operating Manual, Chemapec, Inc., Mannedorf, Switzerland (1969).
11. Clements, L. D., S. R. Beck and P. E. Fletcher, Fuel Grade Ethanol from Cotton Gin Residues, Center of Energy Research, Lubbock, TX (1982).
12. Cook, A. H., The Chemistry and Biology of Yeasts, Academic Press, Inc., New York (1958).

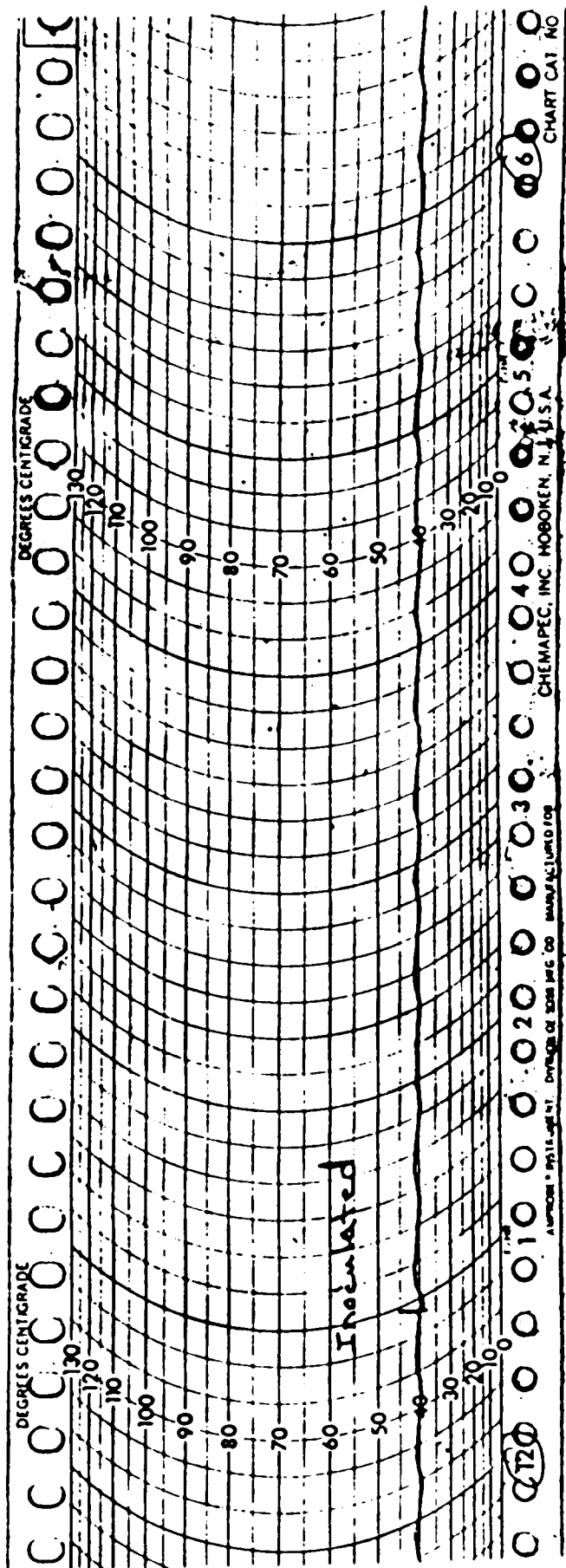
13. Daniel, D. W., "Kinetic Analysis of Cellulose Hydrolysis in Cotton Gin Trash," M.S. Thesis, Texas Tech University (1983).
14. Gencer, M. A. and R. Mutharasan, "Ethanol Fermentation in a Yeast Immobilizer Tubular Fermentor," Biotechnology and Bioengineering, 25: 2243 (1983).
15. Ghose, T. K. and R. D. Tyagi, "Rapid Ethanol Fermentation of Cellulose Hydrolysate I. Batch Versus Continuous Systems," Biotechnology and Bioengineering, 21: 1387-1400 (1979).
- 28
16. Heintz, C. E., Department of Biological Sciences, Texas Tech University, Lubbock, TX, personal communication.
17. Leung, A. T. and E. Montoya, "Minigrator, An Innovative Low-Cost Computing Integrator," Autolab Technical Bulletin: 29 112-74, Spectra-Physics, Santa Clara, CA (1974).
18. Levenberger, H. G., "Cultivation of Saccharomyces cerevisiae in Continuous Culture," Archiv Fuer Mikrobiologie, 79: 176-186 (1971).
19. Lievense, J. C., and H. C. Lim, "The Growth and Dynamics of S. cerevisiae," Annual Reports on Fermentation Processes, 5: 211-262 (1982).
20. Maxon, W. D. and M. J. Johnson, "Aeration Studies on Propagation of Baker's Yeast," Industrial and Engineering Chemistry, 45: 2554-2560 (1953).
21. Monod, J., "The Growth of Bacterial Cultures," Annual Review of Microbiology, 3: 371-394 (1949).
22. Moser, H., The Dynamics of Bacterial Population Maintained in the Chemostat, Carnegie Institute, Washington, DC 34. (1958).
23. Novak, M., "Alcoholic Fermentation: On the Inhibitory Effect of Ethanol," Biotechnology and Bioengineering, 23: 201-211 (1981).
24. Peringer, P., H. Blachere, G. Corrien and A. G. Love, "A Generalized Mathematical Model for the Growth Kinetics of Saccharomyces cerevisiae with Experimental Determination of Parameters," Biotechnology and Bioengineering, 6, 431-454 (1974).

25. Ray, A. A., SAS User's Guide: Statistics, 1982 edition, SAS Institute, Inc., Cary, NC (1982).
26. Rizzuti, L., et al., "Kinetic Parameter Determination in Monocultures and Monosubstrate Biological Reactors," Canadian Journal of Chemical Engineering, 60: 608-612 (1982).
27. Rose, A. H. and J. S. Harrison, The Yeast, Volume 2, Academic Press, New York (1971).
28. Sa-Correia, I. and N. Von Uder, "Temperature Profiles of Ethanol Tolerance Effects of Ethanol on the Minimum and Maximum Temperatures for Growth of Yeast *Saccharomyces cerevisiae* and *Kluyveromyces fragilis*," Biotechnology and Bioengineering, 25: 1665-1667 (1983).
29. Sigma Chemical Company, "The Quantitative Ultraviolet Enzymatic Determination of Ethyl Alcohol (Ethanol) in Blood, Serum, Plasma or Urine at 340 nm," Sigma Technical Bulletin No. 332-UV, Sigma Chemical Company, St. Louis (1982).
30. Smith, A. L., Microbiology Laboratory Manual and Workbook, 5th edition, C. V. Mosby Company, St. Louis (1981).
31. Society of American Bacteriologist, Manual of Microbiological Methods, McGraw-Hill, New York (1957).
32. Sullivan, H. L., "The Effects of Paraquat and Arsenic Acid on the Growth of Distiller's Yeast," M.S. Thesis, Texas Tech University (1982).
33. Venkataramani, E. S., Department of Chemical Engineering, Texas Tech University, Lubbock, TX, personal communication.
34. Waters' Associates, Sample Clarification Kit: Instruction Manual, Waters' Associates, Millford, MA (1977).
35. Woehrer, W. and W. Roehr, "Regulatory Aspects of Baker's Yeast Metabolism in Aerobic Fed-Batch Cultures," Biotechnology and Bioengineering, 23: 567-581 (1981).
36. Yoon, H., G. Klinzing and H. W. Blanch, "Competition for Mixed Substrates by Microbiological Populations," Biotechnology and Bioengineering, 19, 1193-1210 (1977).

APPENDIX A

TYPICAL TEMPERATURE PROFILE






```

*
*
* General
*
// JOB ,,CLAS
// EXEC SAS
DATA A;
  INPUT X Y @@;
  DSDS;
  0
0.016 130000
0.019 500000
0.114 1100000
;
PROC PRINT;
PROC GLM;
  MODEL Y=X;
  OUTPUT OUT=
PROC PLOT
  PLOT Y*X;
//

```

APPENDIX B

GENERAL LEAST SQUARES PROGRAM

```
*  
*  
* General Least Squares Program  
*  
*  
// JOB , ,CLASS=A,MSGLEVEL=(2,0)  
// EXEC SAS  
DATA A;  
    INPUT X Y @@;  
    CARDS;  
0      0  
0.036  130000  
0.079  500000  
0.114  1100000  
;  
    PROC PRINT;  
    PROC GLM;  
        MODEL Y=X;  
    OUTPUT OUT=NEW P=YHAT R=RESID;  
    PROC PLOT DATA=NEW;  
    PLOT Y*X='*' YHAT*X='.'/OVERLAY;  
//
```

APPENDIX C

SPECIFIC GROWTH RATE CURVES

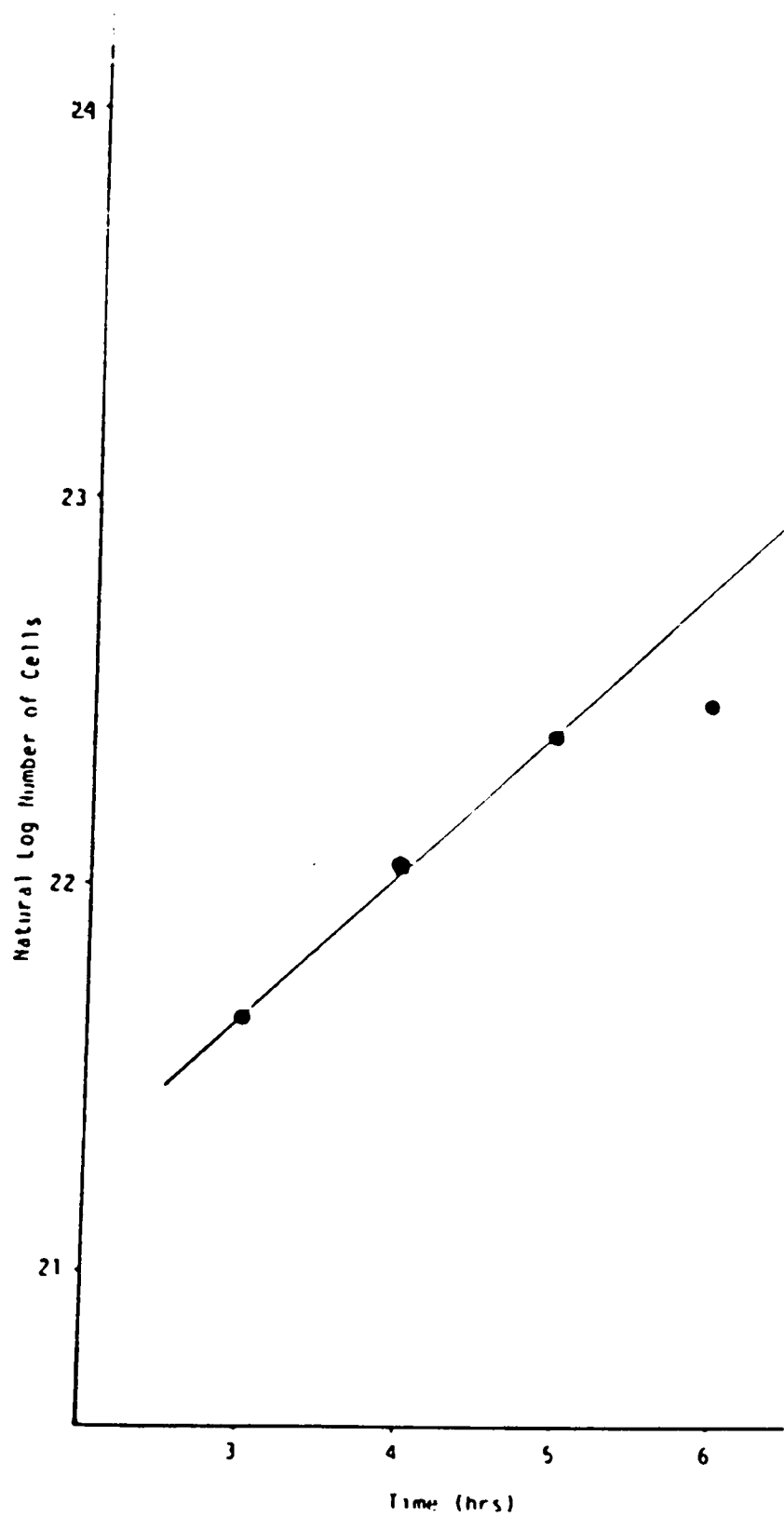


Figure C.1. Natural Log of the Number of Cells Versus Time for $T = 30^{\circ}\text{C}$, $C_i = 23.1 \text{ g/l}$, $\text{pH} = 4.5$ and $\mu = 0.373 \text{ hr}^{-1}$

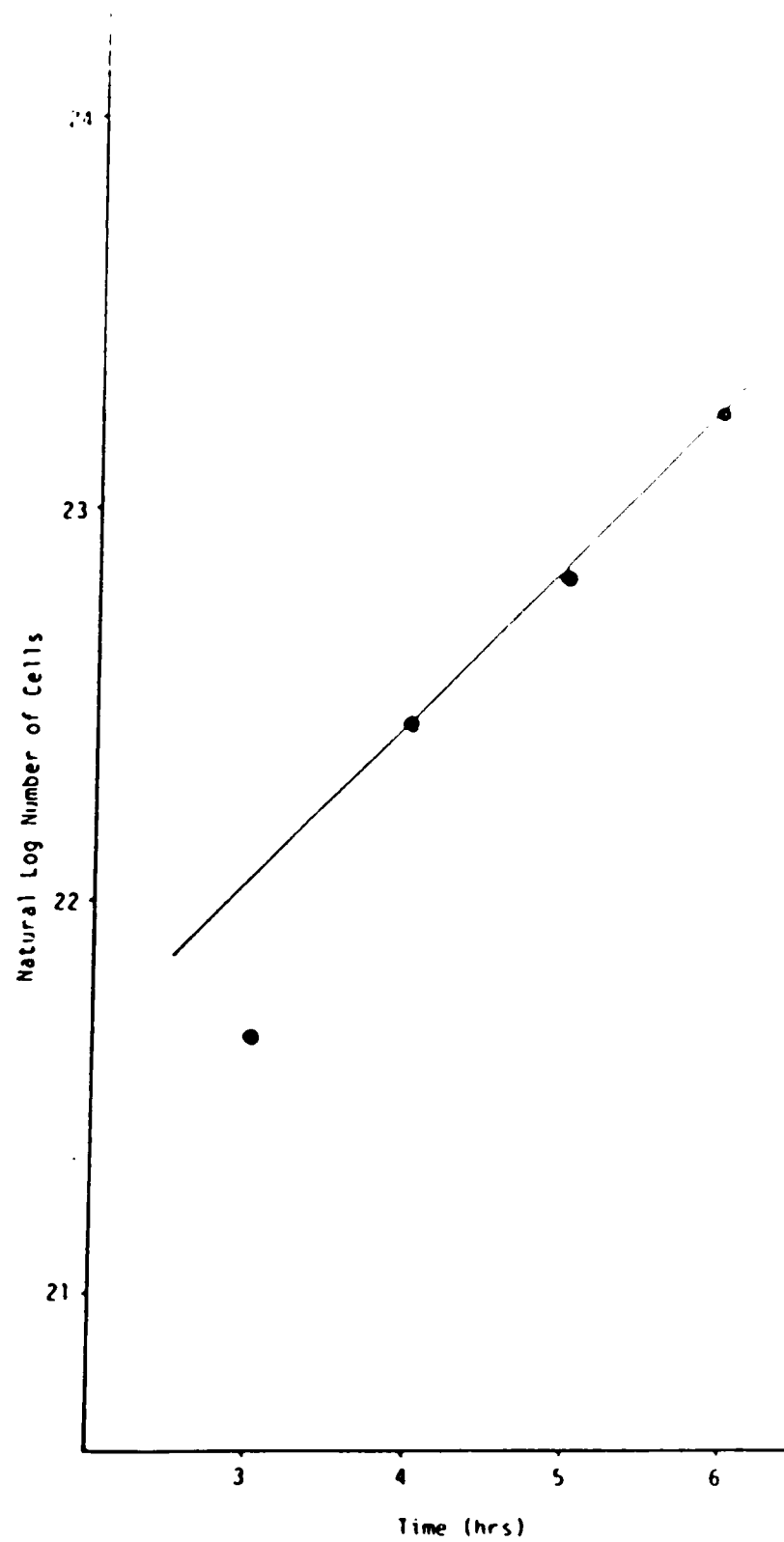


Figure C.2. Natural Log of the Number of Cells Versus Time for $T = 30^{\circ}\text{C}$, $C_i = 13.1 \text{ g/l}$, $\text{pH} = 5.0$ and $\mu = 0.396 \text{ hr}^{-1}$

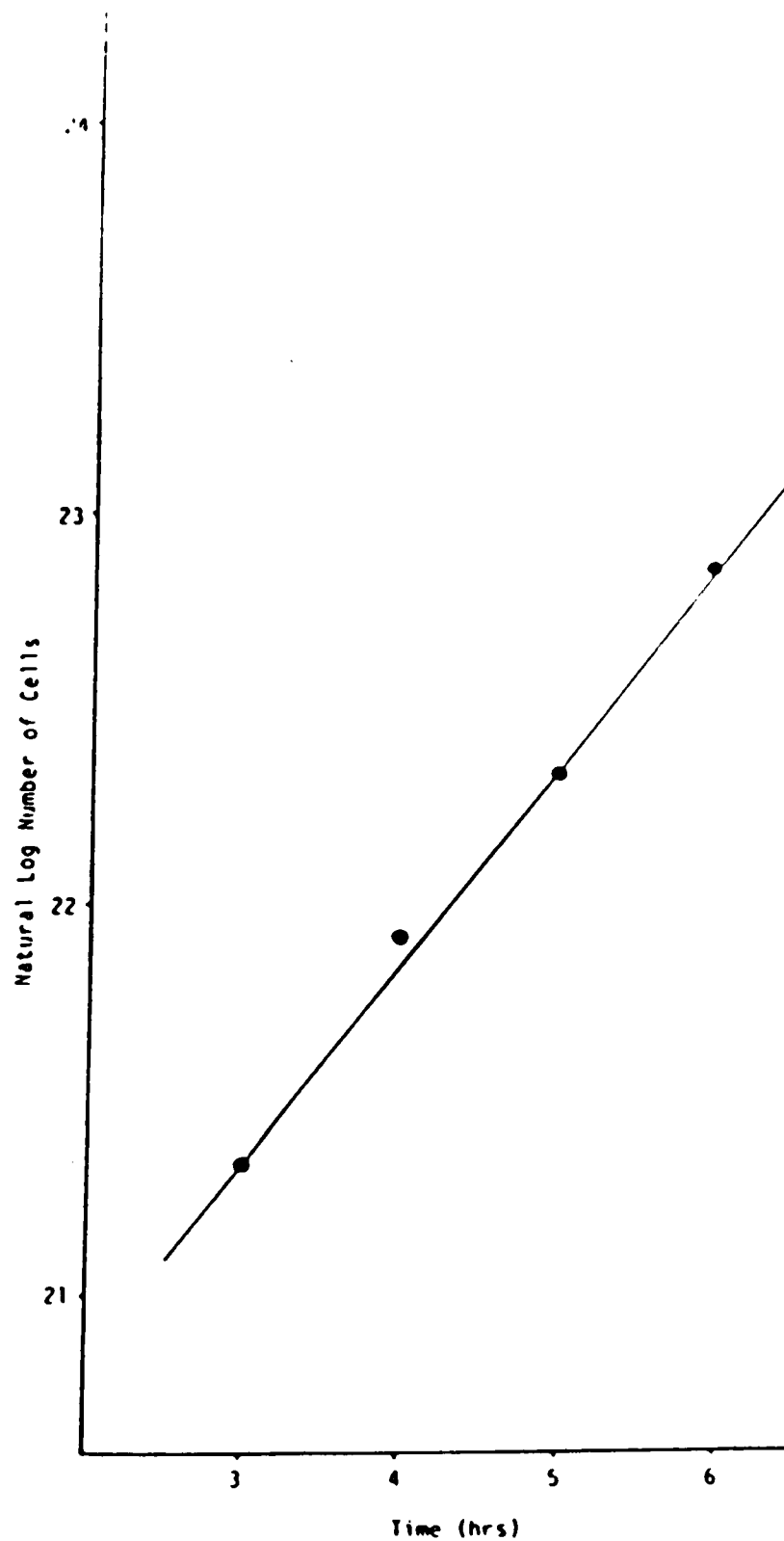


Figure C.3. Natural Log of the Number of Cells Versus Time for $T = 30^{\circ}\text{C}$, $C_i = 23.1 \text{ g/l}$, $\text{pH} = 5.0$ and $\mu = 0.507 \text{ hr}^{-1}$

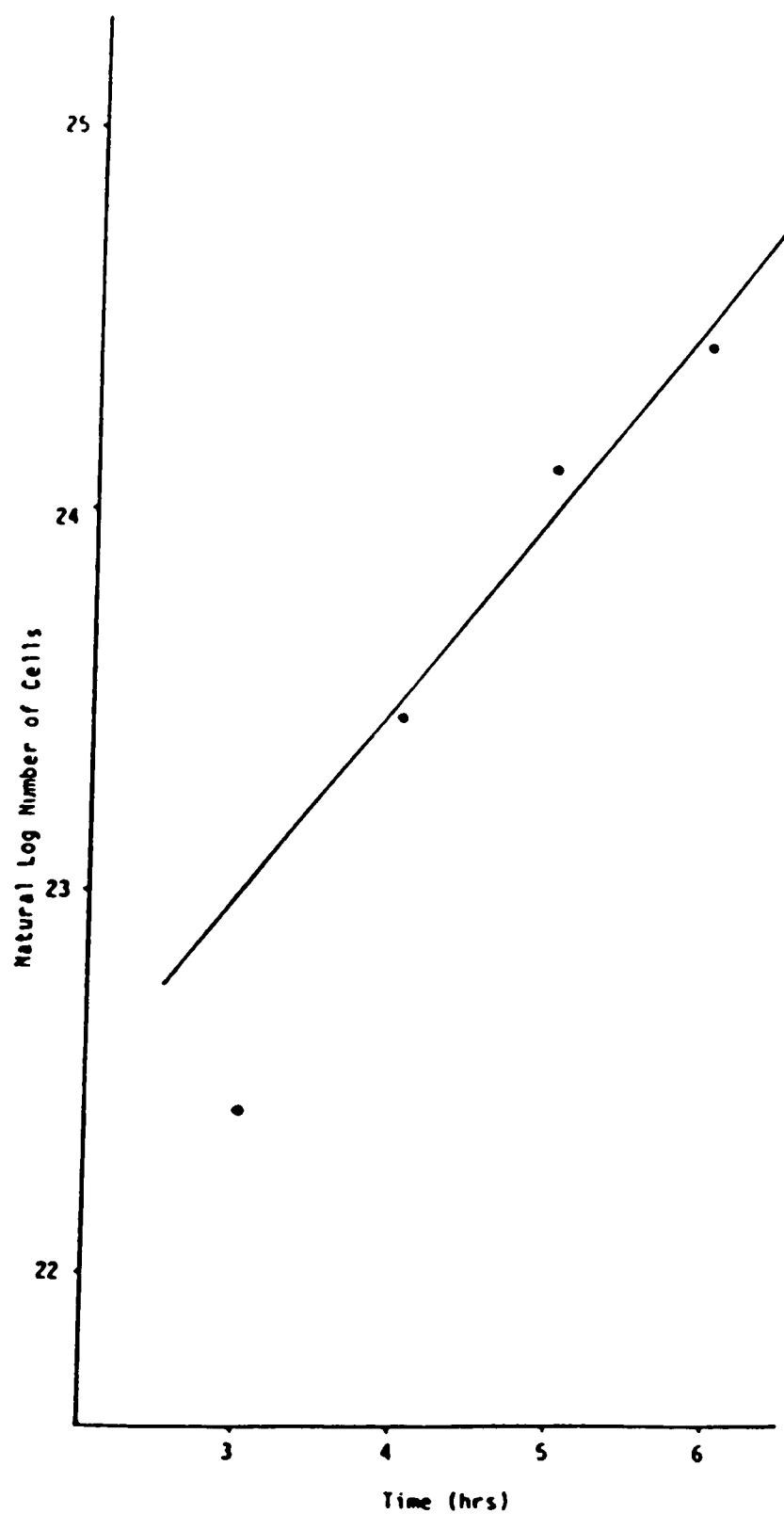


Figure C.4. Natural Log of the Number of Cells Versus Time for $T = 30^{\circ}\text{C}$, $C_i = 23.1 \text{ g/l}$, $\text{pH} = 5.0$ and $\mu = 0.500 \text{ hr}^{-1}$

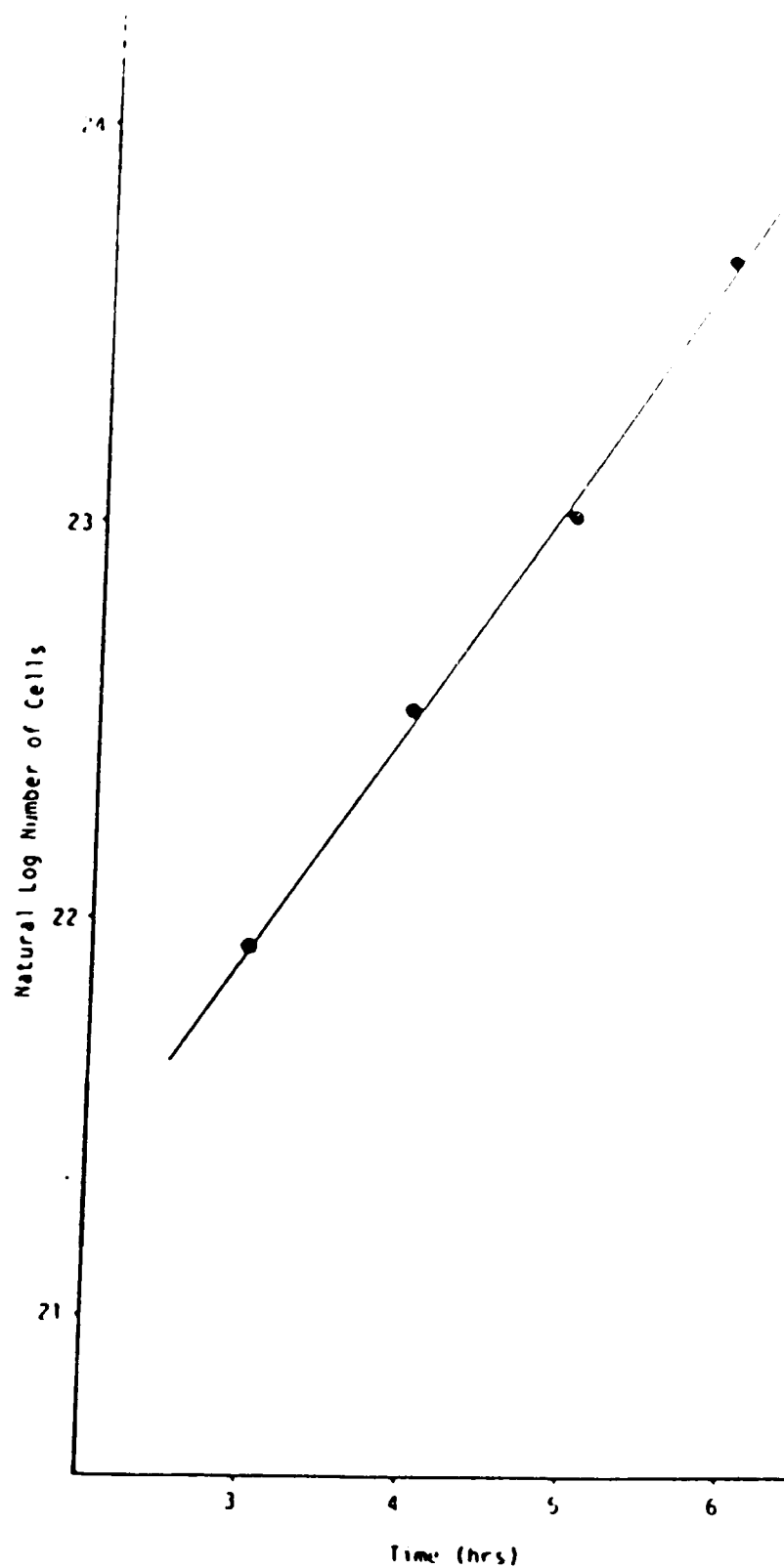


Figure C.5. Natural Log of the Number of Cells Versus Time for $T = 30^{\circ}\text{C}$, $C_i = 33.1 \text{ g/l}$, $\text{pH} = 5.0$ and $\mu = 0.576 \text{ hr}^{-1}$

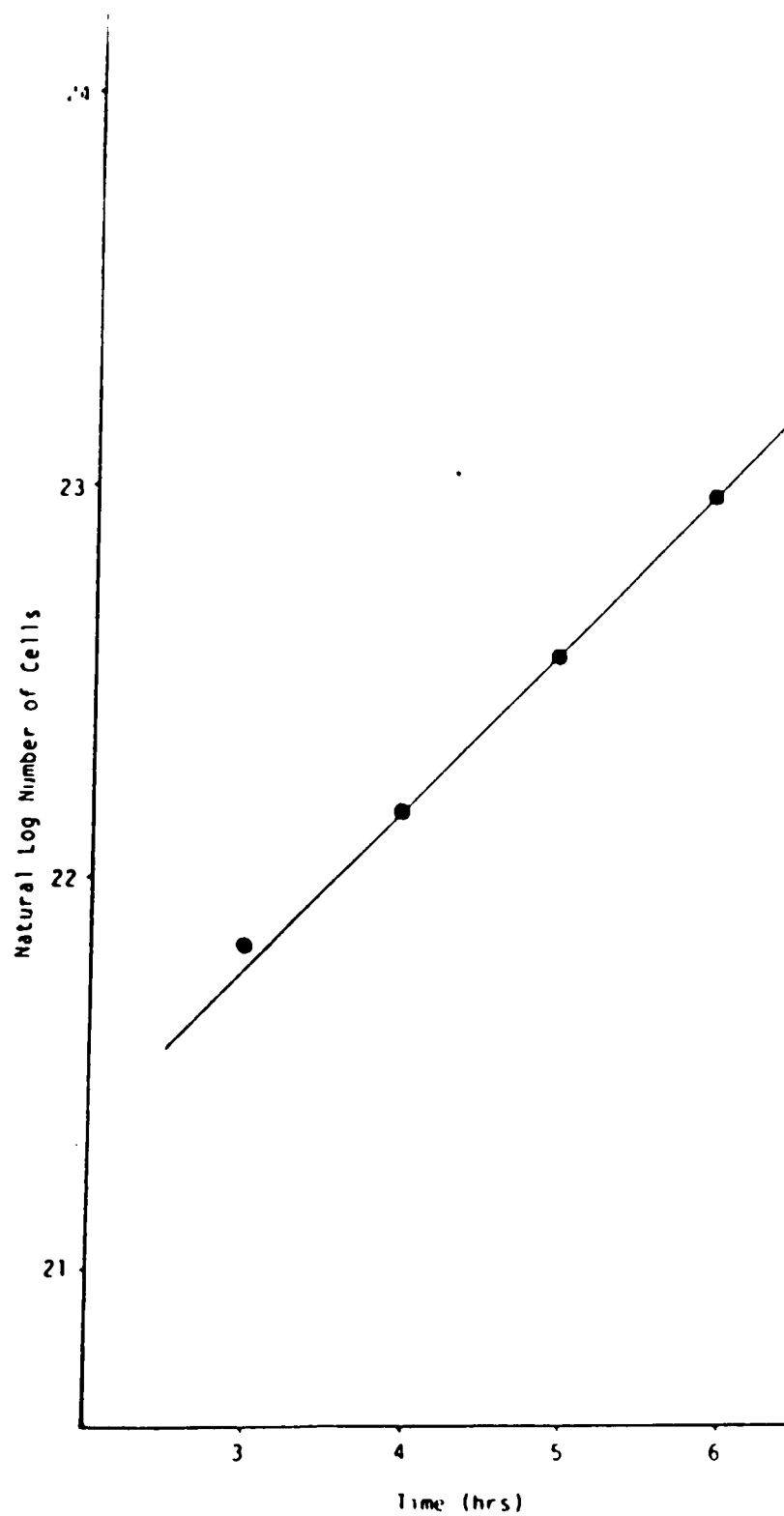


Figure C.6. Natural Log of the Number of Cells Versus Time for $T = 34^{\circ}\text{C}$, $C_i = 13.1 \text{ g/l}$, $\text{pH} = 5.0$ and $\mu = 0.403 \text{ hr}^{-1}$

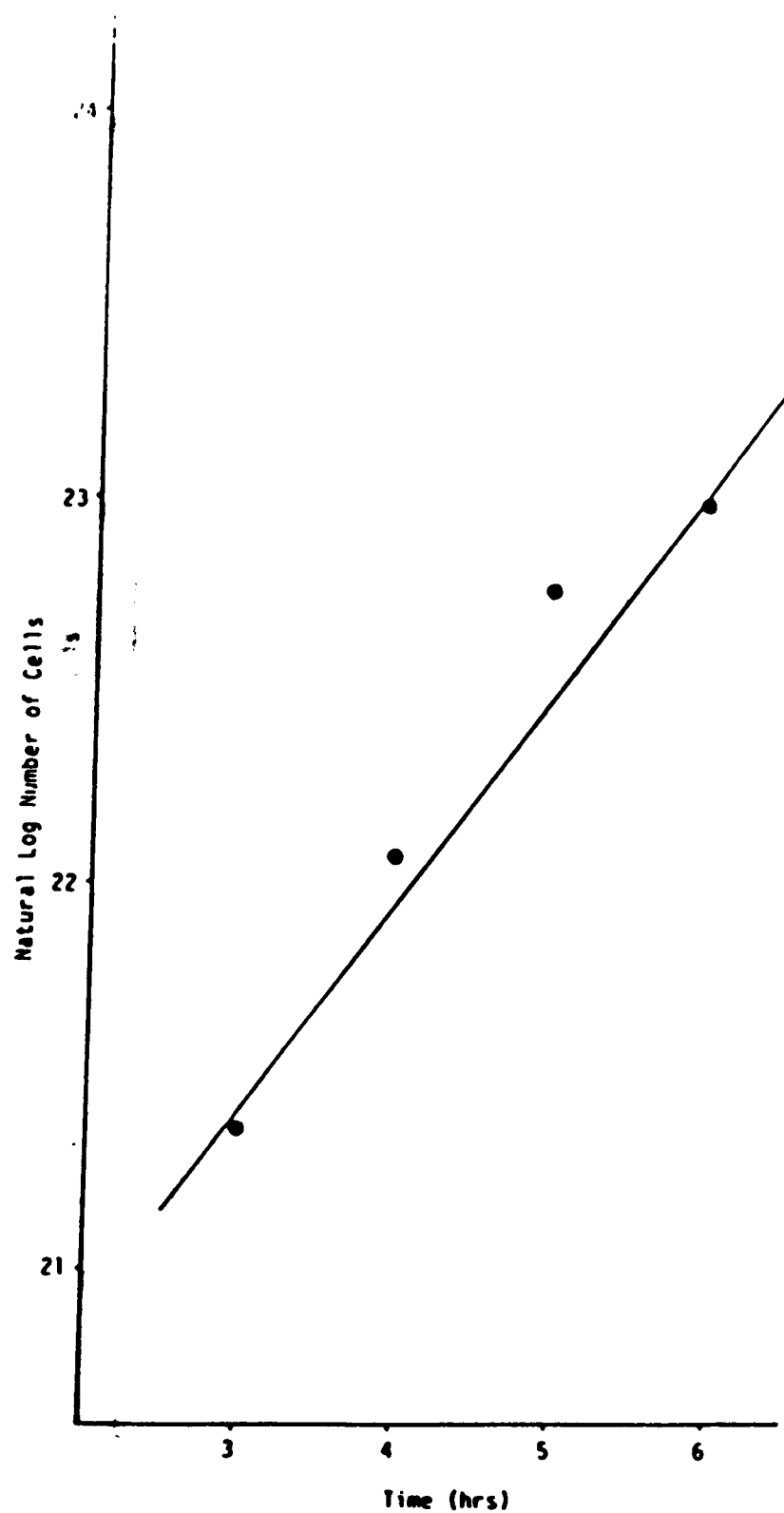


Figure C.7. Natural Log of the Number of Cells Versus Time for $T = 37^{\circ}\text{C}$, $C_i = 23.1 \text{ g/l}$, $\text{pH} = 5.0$ and $\mu = 0.532 \text{ hr}^{-1}$

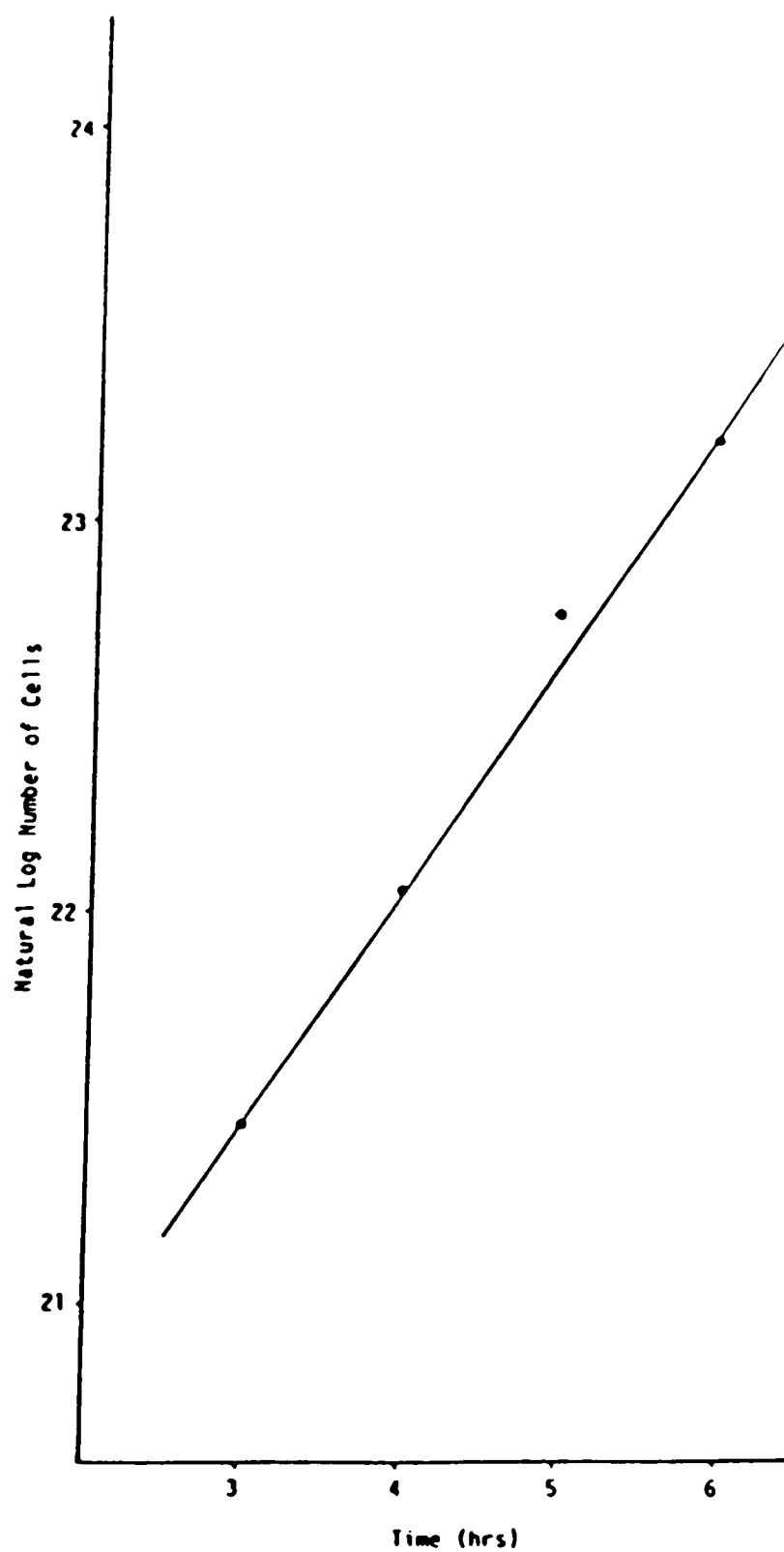


Figure C.8. Natural Log of the Number of Cells Versus Time for $T = 34^{\circ}\text{C}$, $C_i = 33.1 \text{ g/l}$, $\text{pH} = 5.0$ and $\mu = 0.586 \text{ hr}^{-1}$

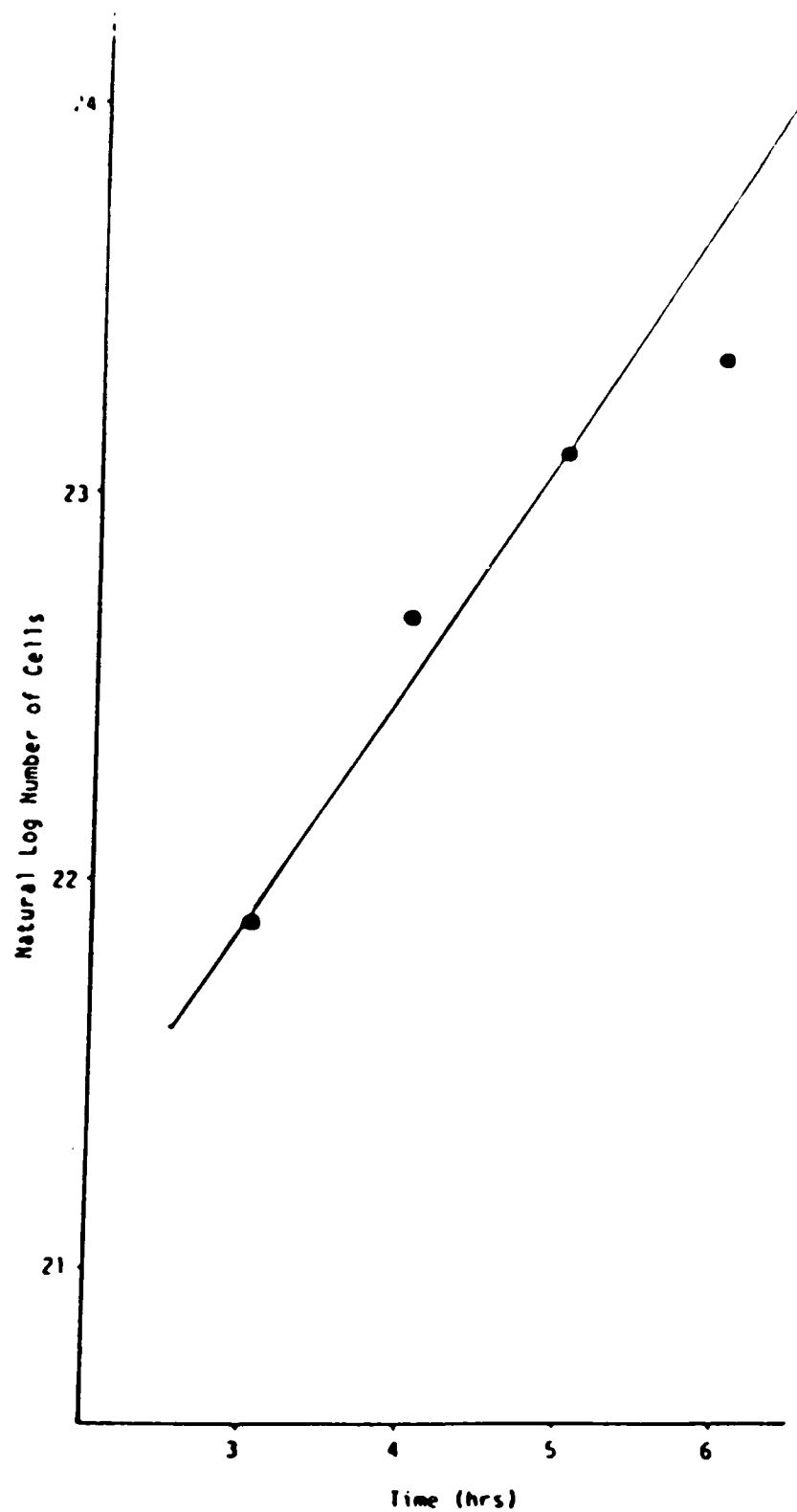


Figure C.9. Natural Log of the Number of Cells Versus Time for $T = 34^{\circ}\text{C}$, $C_i = 33.1 \text{ g/l}$, $\text{pH} = 5.0$ and $\mu = 0.600 \text{ hr}^{-1}$

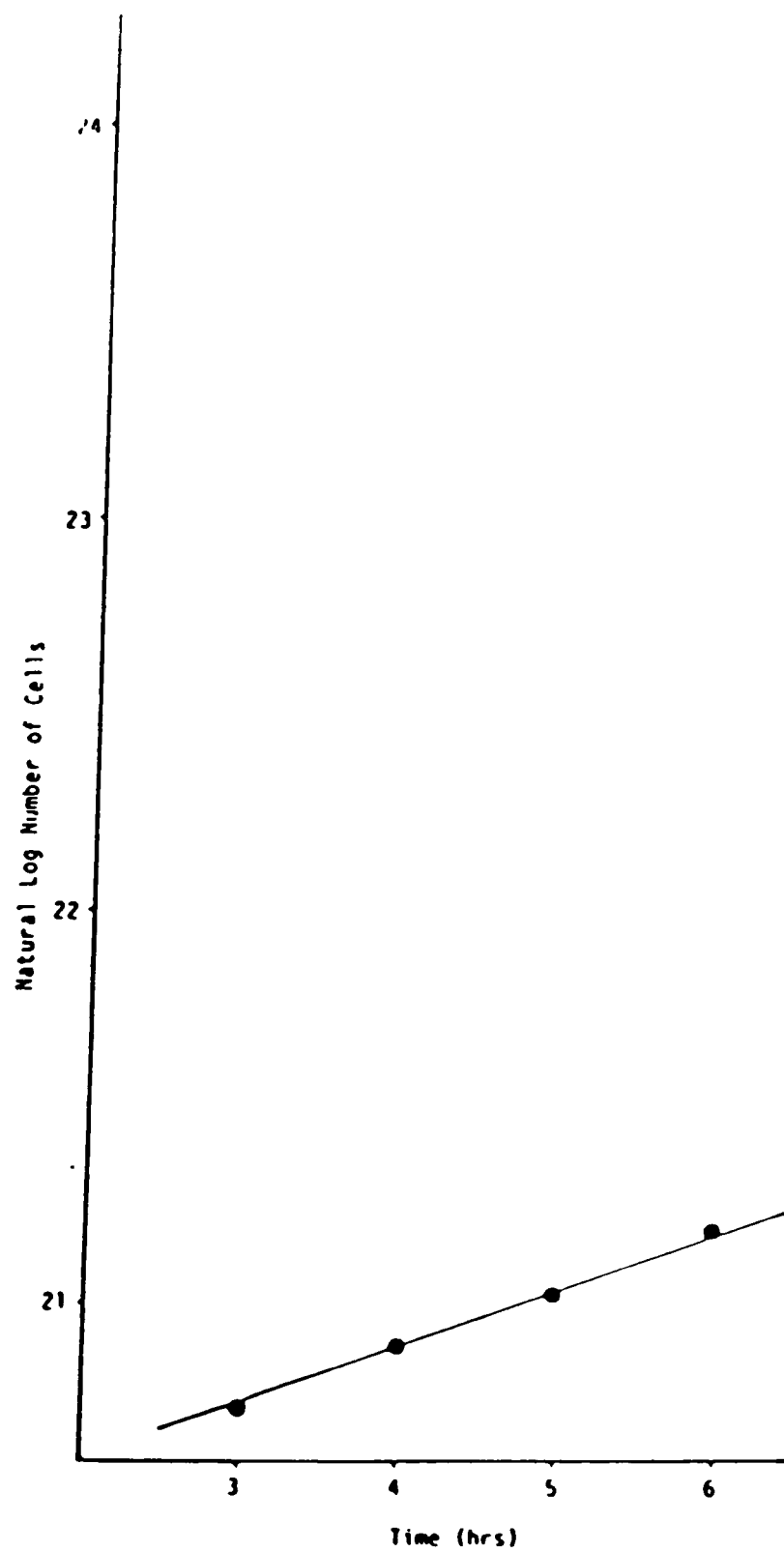


Figure C.10. Natural Log of the Number of Cells Versus Time for $T = 37^{\circ}\text{C}$, $C_i = 23.1 \text{ g/l}$, $\text{pH} = 4.5$ and $\mu = 0.143 \text{ hr}^{-1}$

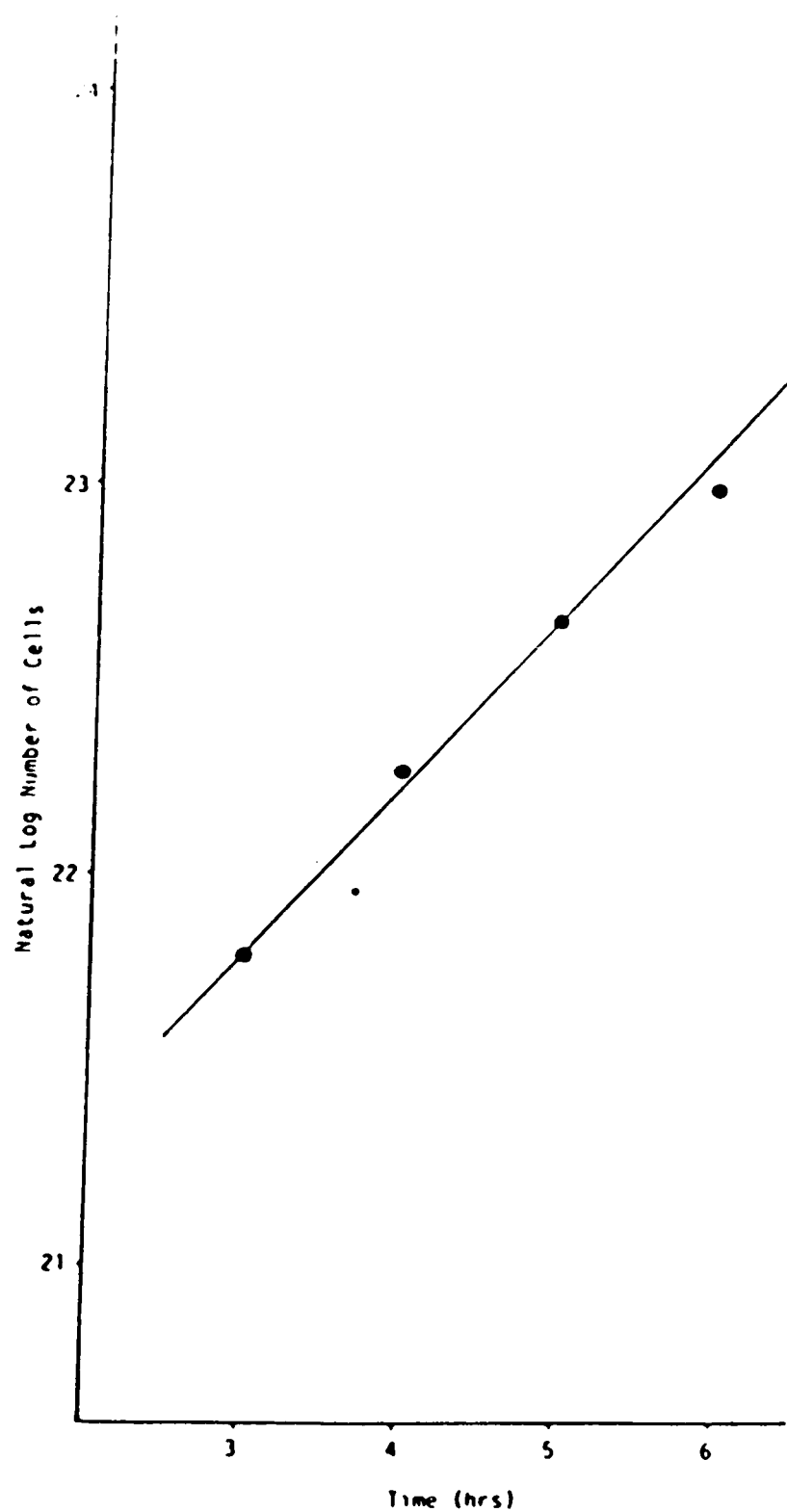


Figure C.11. Natural Log of the Number of Cells Versus Time for $T = 37^{\circ}\text{C}$, $C_i = 13.1 \text{ g/l}$, $\text{pH} = 5.0$ and $\mu = 0.426 \text{ hr}^{-1}$

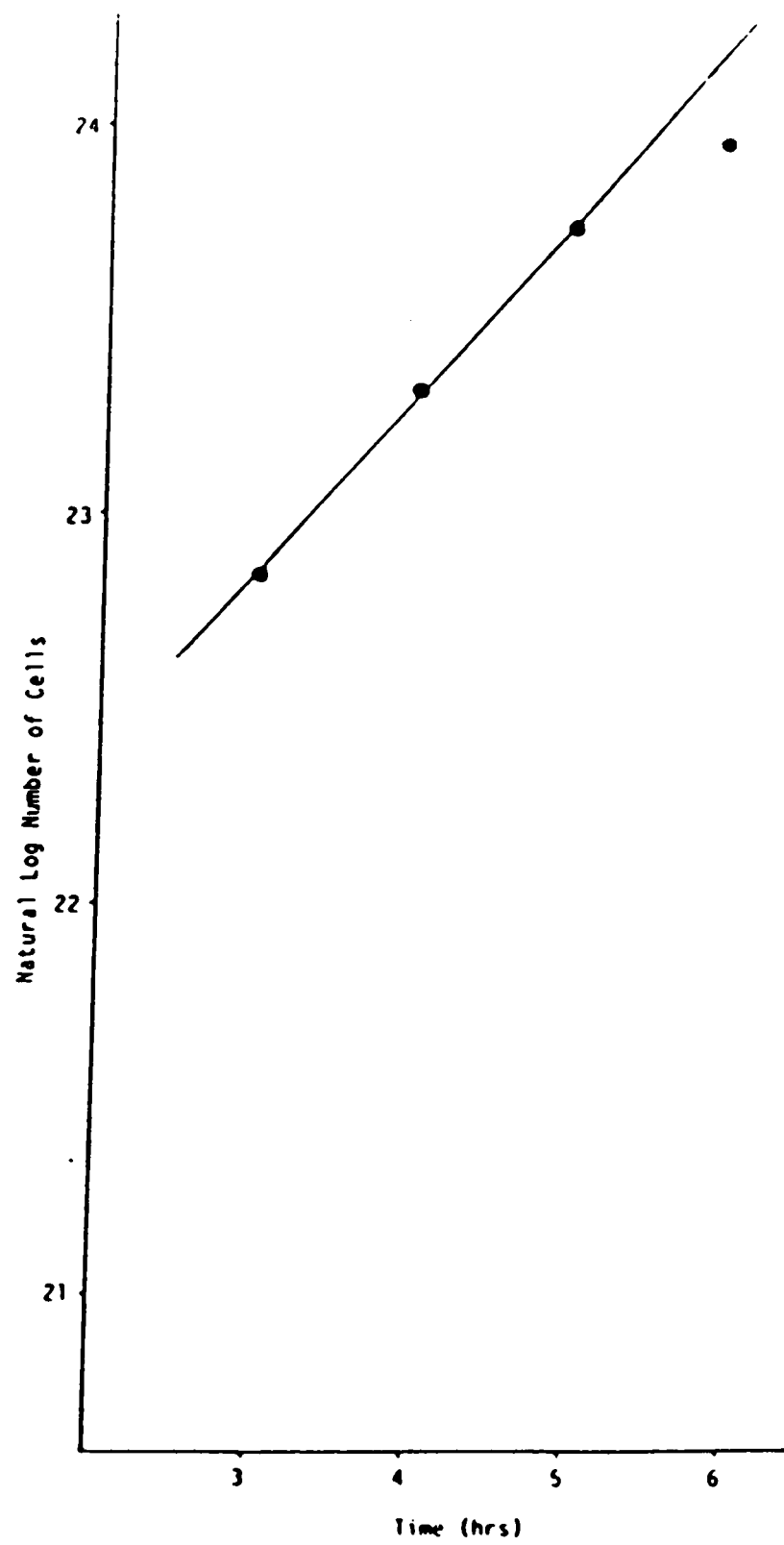


Figure C.12. Natural Log of the Number of Cells Versus Time for $T = 37^{\circ}\text{C}$, $C_i = 13.1 \text{ g/l}$, $\text{pH} = 5.0$ and $\mu = 0.447 \text{ hr}^{-1}$

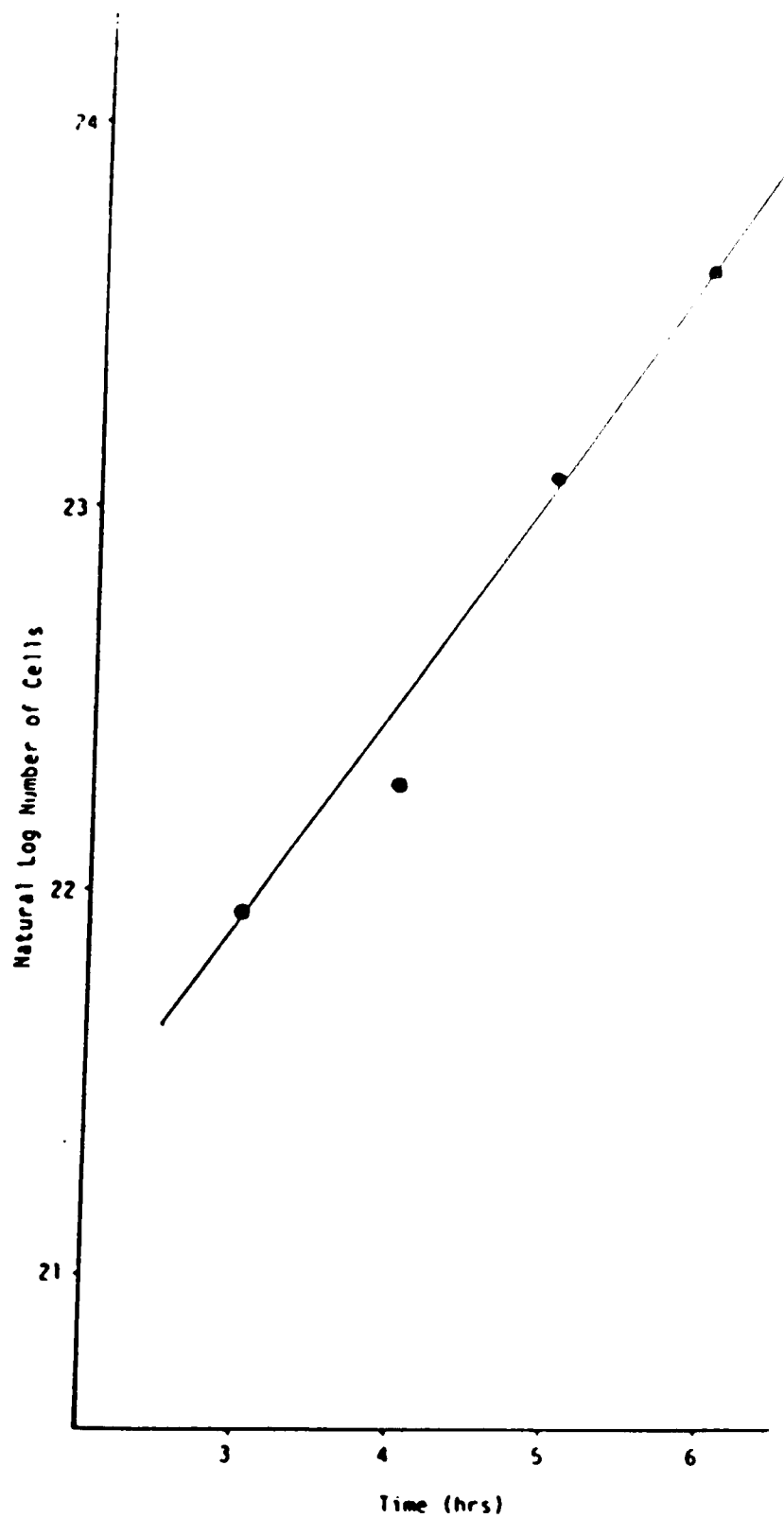


Figure C.13. Natural Log of the Number of Cells Versus Time for $T = 37^{\circ}\text{C}$, $C_i = 23.1 \text{ g/l}$, $\text{pH} = 5.0$ and $\mu = 0.564 \text{ hr}^{-1}$

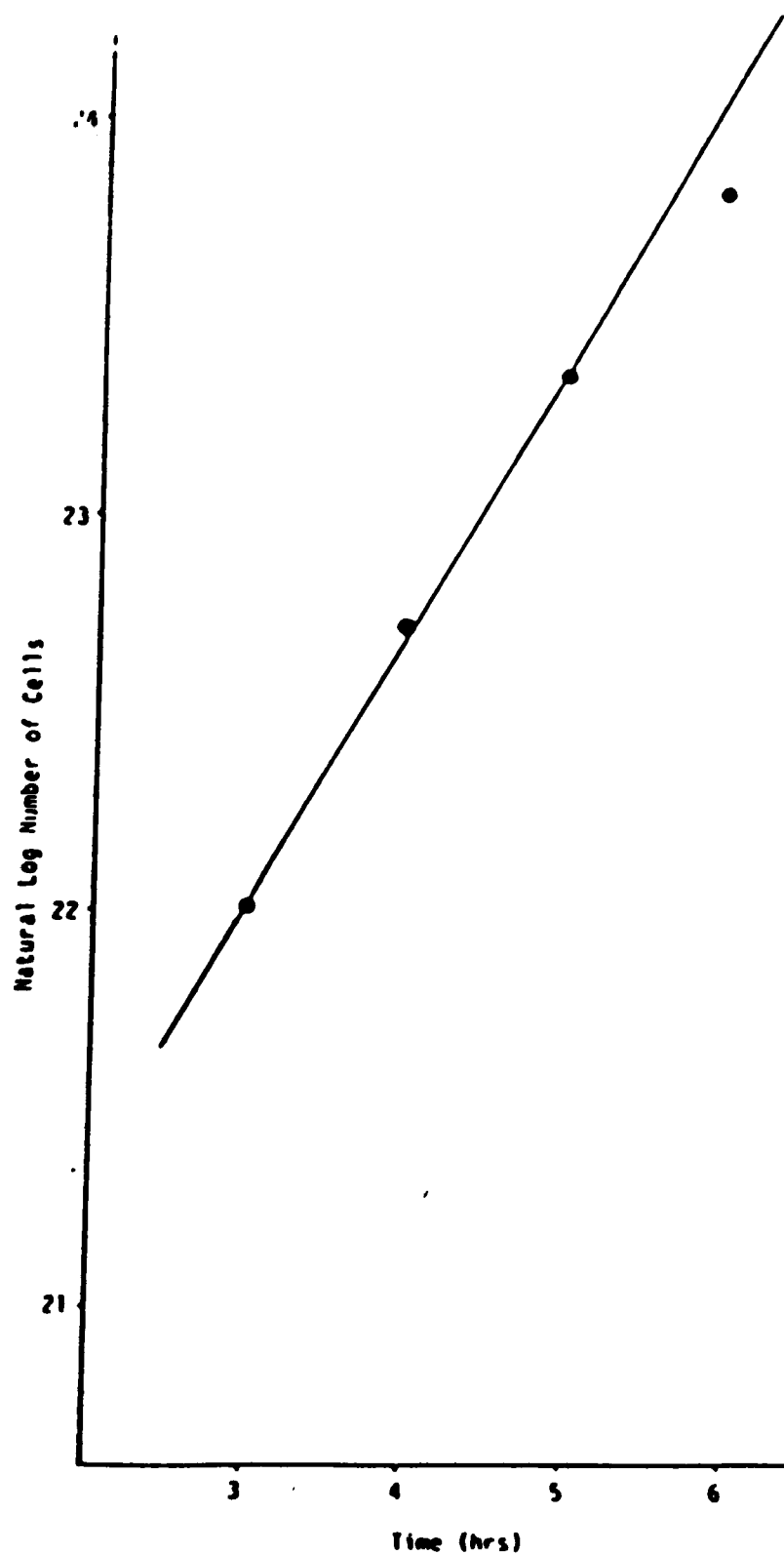


Figure C.14. Natural Log of the Number of Cells Versus Time for $T = 37^{\circ}\text{C}$, $C_i = 33.1 \text{ g/l}$, $\text{pH} = 5.0$ and $\mu = 0.682 \text{ hr}^{-1}$

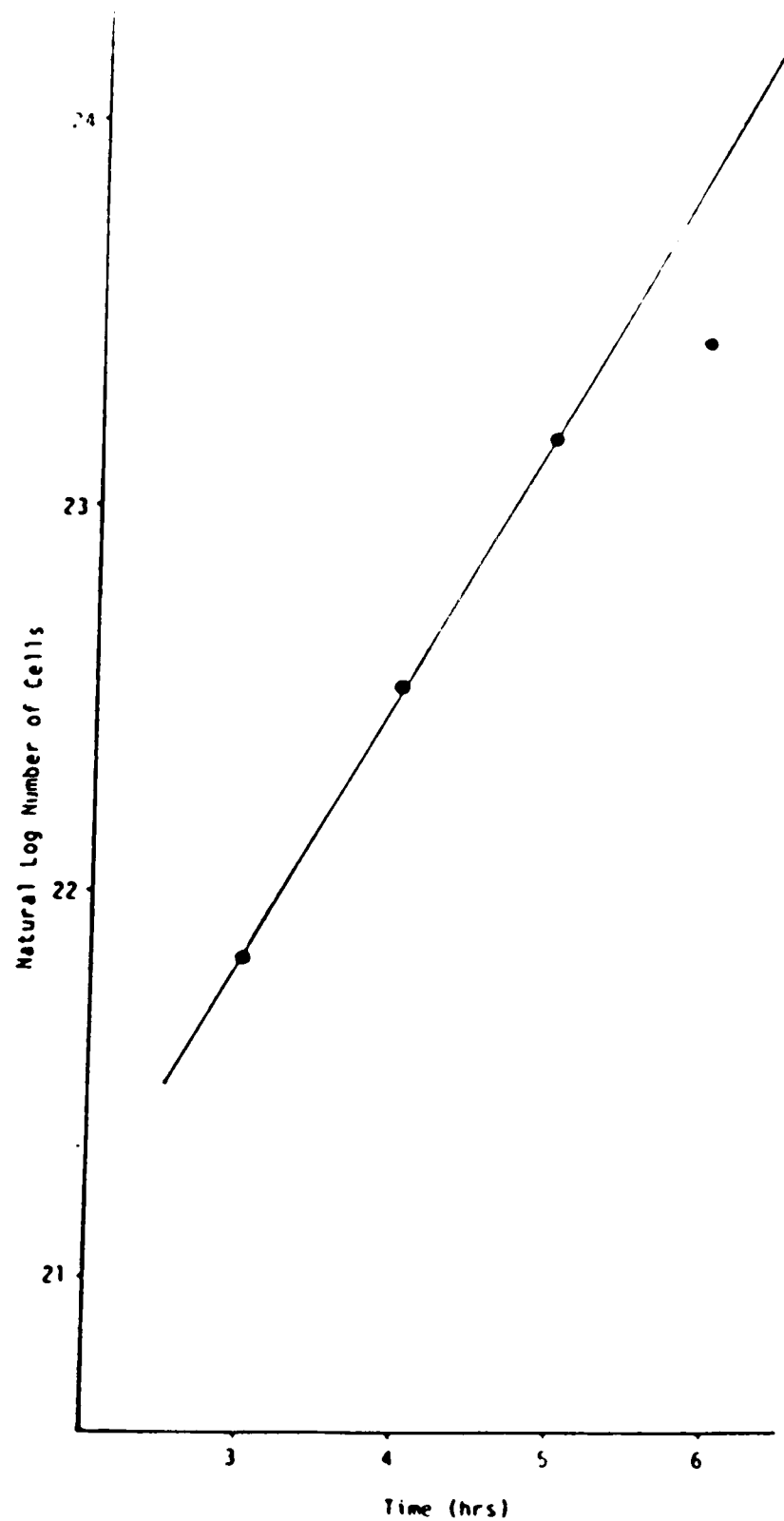


Figure C.15. Natural Log of the Number of Cells Versus Time for $T = 37^{\circ}\text{C}$, $C_i = 40.6 \text{ g/l}$, $\text{pH} = 5.0$ and $\mu = 0.684 \text{ hr}^{-1}$

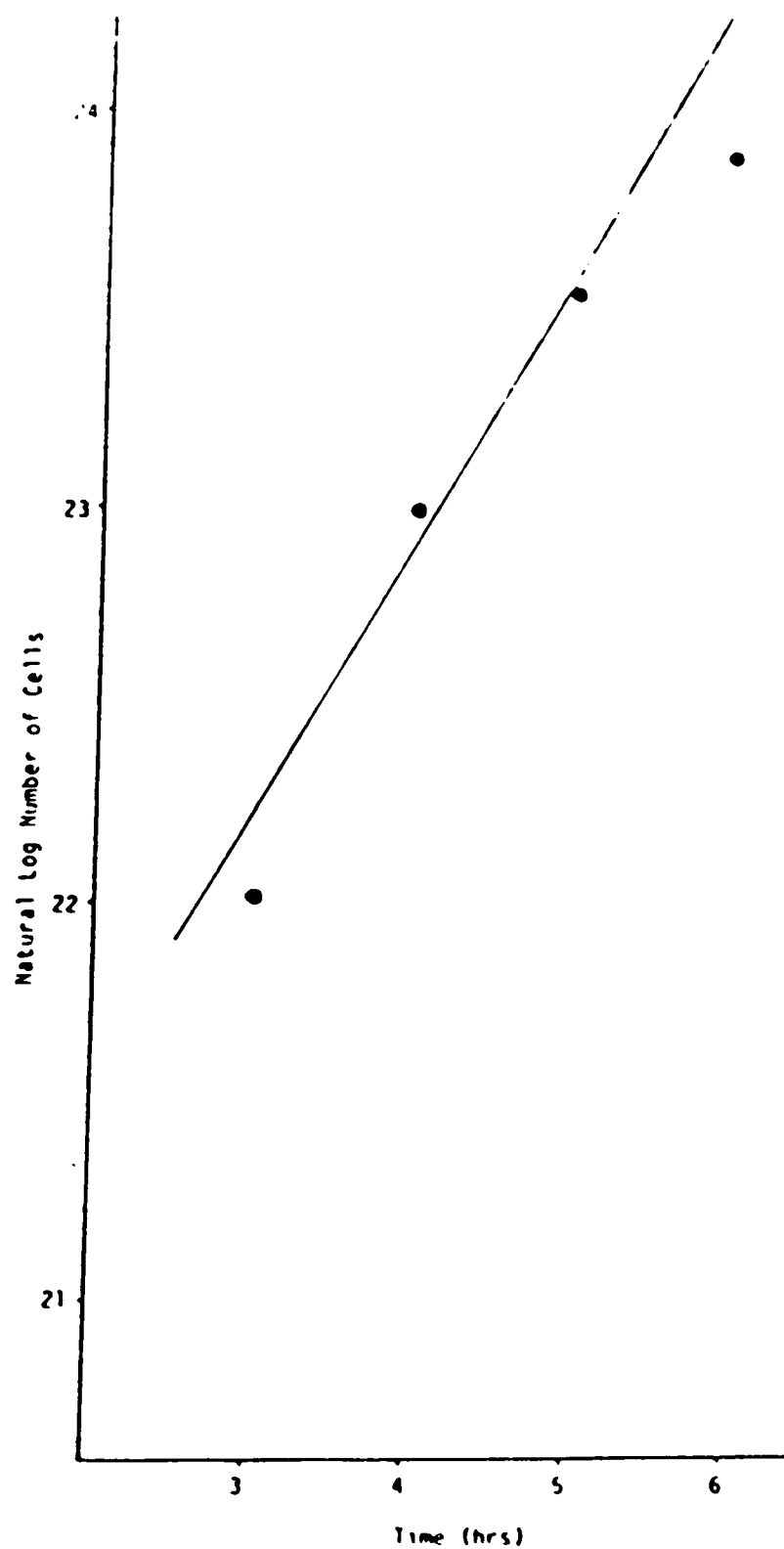


Figure C.16. Natural Log of the Number of Cells Versus Time for $T = 37^{\circ}\text{C}$, $C_i = 60.6 \text{ g/l}$, $\text{pH} = 5.0$ and $\mu = 0.677 \text{ hr}^{-1}$

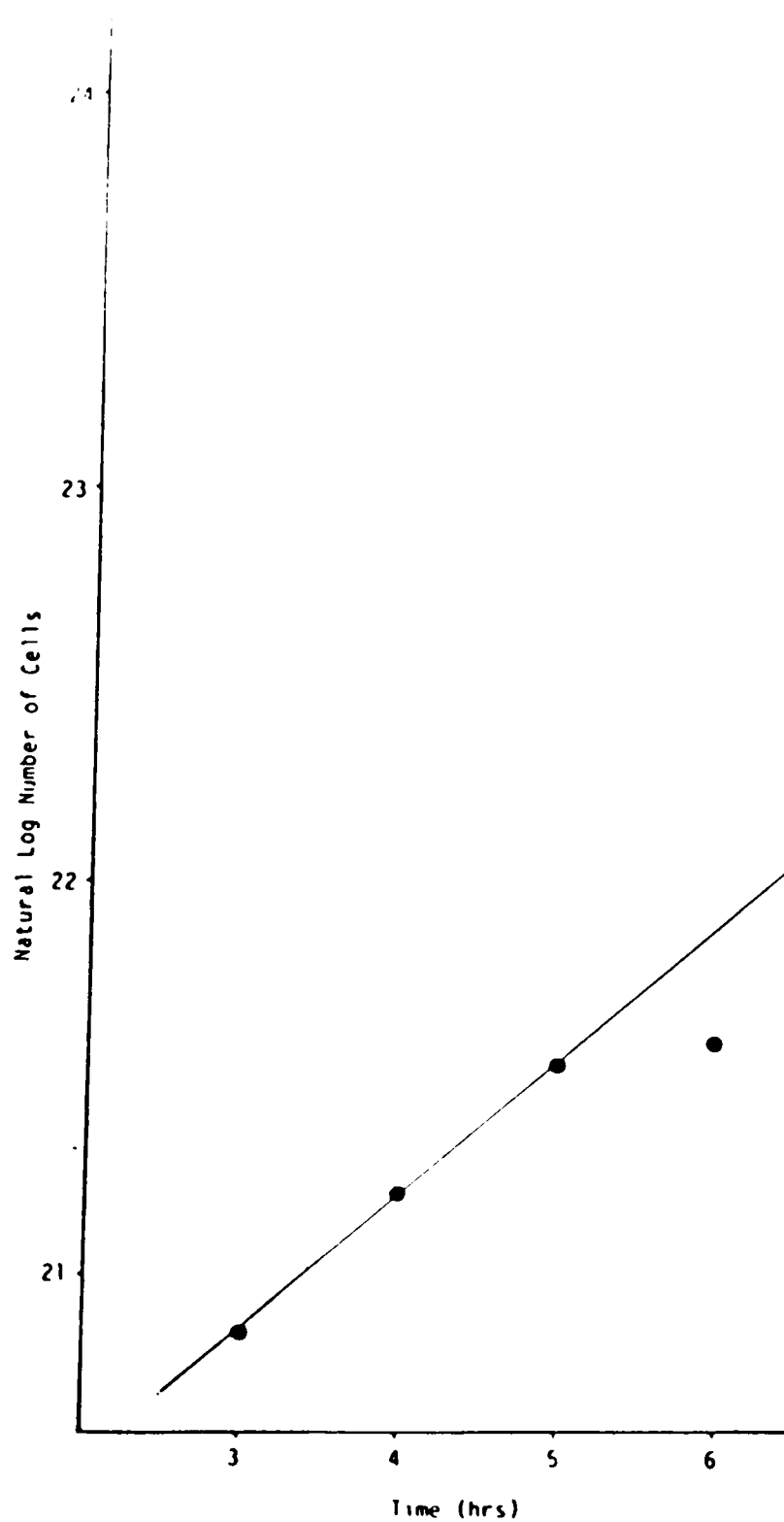


Figure C.17. Natural Log of the Number of Cells Versus Time for $T = 37^{\circ}\text{C}$, $C_i = 23.1 \text{ g/l}$, $\text{pH} = 5.5$ and $\mu = 0.341 \text{ hr}^{-1}$

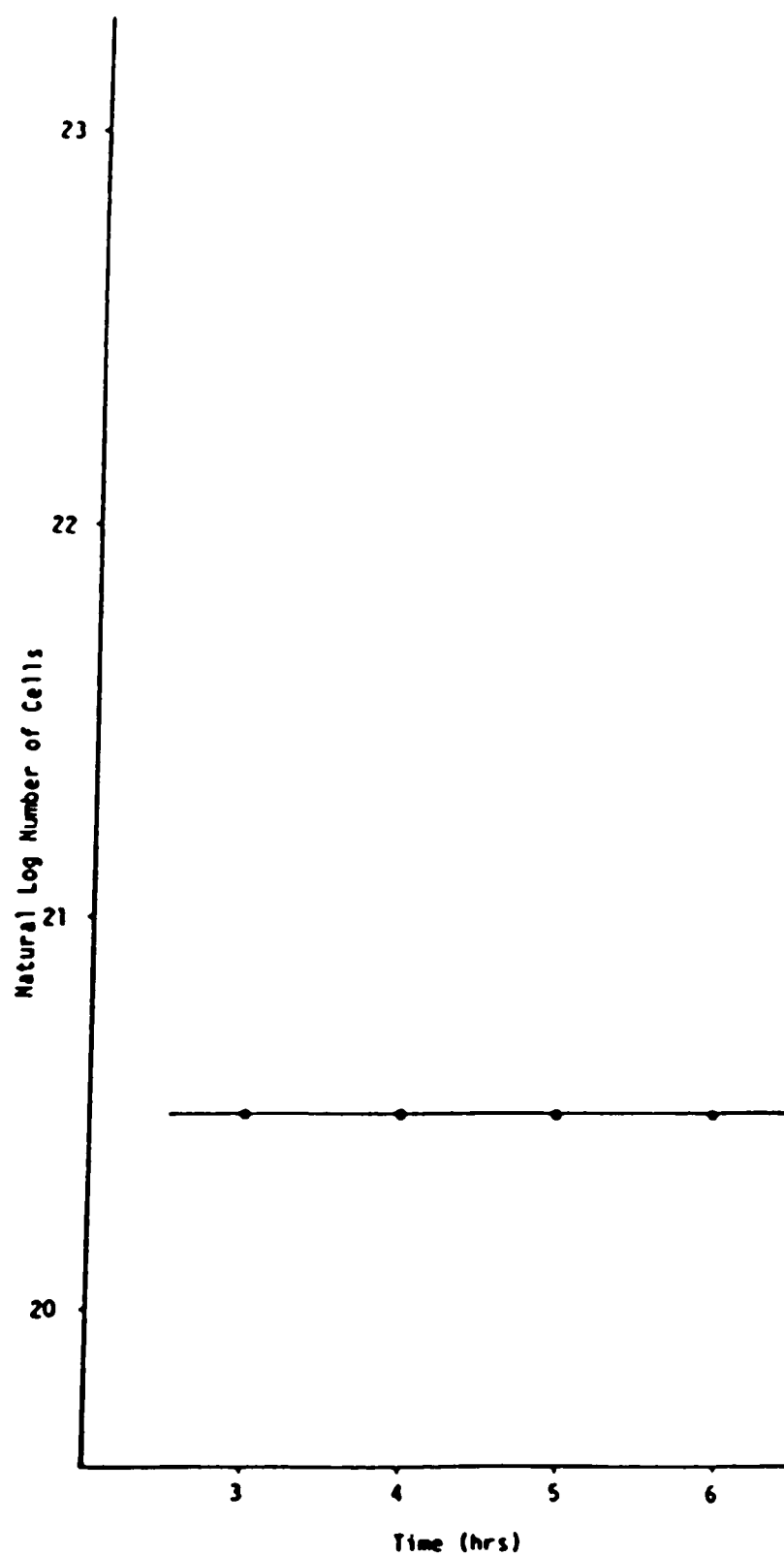


Figure C.18. Natural Log of the Number of Cells Versus Time for $T = 41^{\circ}\text{C}$, $C_i = 23.1 \text{ g/l}$, $\text{pH} = 5.0$ and $\mu = 0.0 \text{ hr}^{-1}$

[illegible]

APPENDIX D

NLIN PROGRAMS FOR THE MONOD, MOSER
AND TEISSER EXPRESSIONS

```

*
*
* NLIN Program for the Monod Expression
*
* X is the glucose concentration
* Y is the specific growth rate
*
*
// JOB , , CLASS=A, MSGLEVEL=(2,0)
// EXEC SAS
DATA A;
  INPUT X Y @@;
  CARDS;
0 0
13.1 .172
23.1 .220
23.1 .217
33.1 .250
;
PROC PRINT;
PROC NLIN BEST=5;
  PARMS YMAX=0.4 XKS=0.7;
  DUM=XKS+X;
  MODEL Y=YMAX*X/DUM;
  DER.YMAX=X/DUM;
  DER.XKS=-YMAX*X/(DUM**2);
  OUTPUT OUT=NEW PREDICTED=YP;
PROC PLOT DATA=NEW;
PLOT Y*X='*' YP='.'/OVERLAY;
//

```

```

*
*
* NLIN Program for the Moser Expression
*
* X is the glucose concentration
* Y is the specific growth rate
*
*
// JOB , ,CLASS=A,MSGLEVEL=(2,0)
// EXEC SAS
  DATA A;
    INPUT X Y @@;
    CARDS;
0.01 0
13.1 .172
23.1 .220
23.1 .217
33.1 .250
;
  PROC PRINT;
  PROC NLIN BEST=5;
    PARMS YMAX=0.4 XKS=0.7;
    R=1.98717;
    DUM1=1;
    DUM2=1/(X**XL);
    DUM3=1+(XKS*DUM2);
    MODEL Y=YMAX*DUM1/DUM3;
    DER.YMAX=DUM1/DUM3;
    DER.XKS=-YMAX*DUM1*XKS*DUM2*LOG(X)/(DUM3**2);
  OUTPUT OUT=NEW PREDICTED=YP;
  PROC PLOT DATA=NEW;
  PLOT Y*X='*' YP='.'/OVERLAY;
//

```



```

*
*
* NLIN Program for the Teisser Expression
*
* X is the glucose concentration
* Y is the specific growth rate
*
*
// JOB , ,CLASS=A,MSGLEVEL=(2,0)
// EXEC SAS
DATA A;
  INPUT X Y @@;
  CARDS;
0 0
13.1 .172
23.1 .220
23.1 .217
33.1 .250
;
PROC PRINT;
PROC NLIN BEST=5;
  PARMS YMAX=0.4 XKS=0.7;
  R=1.98717;
  DUM2=1/EXP(X/XKS);
  MODEL Y=YMAX*(1-DUM2);
  DER.YMAX=1-DUM2;
  DER.XKS=-YMAX*DUM2*X/(XKS**2);
  OUTPUT OUT=NEW PREDICTED=YP;
PROC PLOT DATA=NEW;
PLOT Y*X='*' YP='.'/OVERLAY;
//

```

APPENDIX E

VIALE CELL CONCENTRATION PROFILE

Inverting:

Starting with the Monod expression:

$$\mu = (\mu_{\max} C_i / K_s + C_i) \quad (\text{E.1})$$

Inverting:

$$1/\mu = [(K_s / \mu_{\max} C_i) + (C_i / \mu_{\max} C_i)] \quad (\text{E.2})$$

Rewriting:

$$1/\mu = [K_s / \mu_{\max} (1/C_i) + 1/\mu_{\max}] \quad (\text{E.3})$$

APPENDIX F

NLIN PROGRAMS FOR THE ARRHENIUS EXPRESSION
IN THE MONOD, MOSER AND TEISSER EXPRESSIONS

```

*
*
* NLIN Program for the Modified Moser Expression
*
* X is the glucose concentration
* Y is the specific growth rate
* T is absolute temperature
*
*
// JOB , ,CLASS=A,MSGLEVEL=(2,0)
// EXEC SAS
DATA A;
  INPUT X Y T @@@;
  CARDS;
0.01 0 303
13.1 .396 303
23.1 .507 303
23.1 .500 303
33.1 .576 303
0 0 307
13.1 .403 307
23.1 .532 307
33.1 .586 307
33.1 .600 307
0 0 310
13.1 .426 310
13.1 .447 310
23.1 .640 310
33.1 .682 310
40.6 .684 310
60.6 .677 310
;
PROC PRINT;
PROC NLIN BEST=17;
  PARMS YMAX=0.855 XKS=14.5 XL=1 EA=2000.0;
  R=1.98717;
  DUM1=EXP(EA/(R*T));
  DUM2=1/(X**XL);
  DUM3=1+(XKS*DUM2);
  MODEL Y=YMAX*DUM1/DUM3;
  DER.YMAX=DUM1/DUM3;
  DER.XKS=-YMAX*DUM2*DUM1/(DUM3**2);
  DER.EA=-YMAX*DUM1/(DUM3*R*T);
  DER.XL=YMAX*DUM1*XKS*DUM2*LOG(X)/(DUM3**2);
  OUTPUT OUT=NEW PREDICTED=YP;
PROC PLOT DATA=NEW;
PLOT Y*X='*' YP*X='.'/OVERLAY;
//

```

```

*
*
* NLIN Program for the Modified Teisser Expression
*
* X is the glucose concentration
* Y is the specific growth rate
* T is absolute temperature
*
*
// JOB , ,CLASS=A,MSGLEVEL=(2,0)
// EXEC SAS
  DATA A;
    INPUT X Y T @@@;
    CARDS;
0 0 303
13.1 .396 303
23.1 .507 303
23.1 .500 303
33.1 .576 303
0 0 307
13.1 .403 307
23.1 .532 307
33.1 .586 307
33.1 .600 307
0 0 310
13.1 .426 310
13.1 .447 310
23.1 .640 310
33.1 .682 310
40.6 .684 310
60.6 .677 310
;
  PROC PRINT;
  PROC NLIN BEST=17;
    PARMS YMAX=0.4 XKS=9.0 EA=1000.0;
    R=1.98717;
    DUM1=EXP(EA/(R*T));
    DUM2=1/EXP(X/XKS);
    MODEL Y=YMAX*DUM1*(1-DUM2);
    DER.YMAX=DUM1*(1-DUM2);
    DER.XKS=-YMAX*DUM1*DUM2*X/(XKS**2);
    DER.EA=-YMAX*DUM1*(1-DUM2)/(R*T);
  OUTPUT OUT=NEW PREDICTED=YP;
  PROC PLOT DATA=NEW;
  PLOT Y*X='*' YP*X='.'/OVERLAY;
//

```

```

*
*
* NLIN Program for the Modified Monod Expression
*
* X is the glucose concentration
* Y is the specific growth rate
* T is absolute temperature
*
*
// JOB , ,CLASS=A,MSGLEVEL=(2,0)
// EXEC SAS
DATA A;
  INPUT X Y T @@@;
  CARDS;
0 0 303
13.1 .396 303
23.1 .507 303
23.1 .500 303
33.1 .576 303
0 0 307
13.1 .403 307
23.1 .532 307
33.1 .586 307
33.1 .600 307
0 0 310
13.1 .426 310
13.1 .447 310
23.1 .640 310
33.1 .682 310
40.6 .684 310
60.6 .677 310
;
PROC PRINT;
PROC NLIN BEST=17;
  PARMS YMAX=0.4 XK0=9.0 EA=1000.0;
  R=1.98717;
  DUM1=EXP(EA/(R*T));
  DUM2=XK0+X;
  MODEL Y=YMAX*X/(DUM2*DUM1);
  DER.YMAX=X/(DUM2*DUM1);
  DER.XK0=-YMAX*X/((DUM2**2)*DUM1);
  DER.EA=-YMAX*X/(DUM1*R*T*DUM2);
  OUTPUT OUT=NEW PREDICTED=YP;
PROC PLOT DATA=NEW;
PLOT Y*X='*' YP*X='.'/OVERLAY;
//

```

APPENDIX G

GLUCOSE CONCENTRATION PROFILE

Wt. % Glucose

2.00

Figure G.1. Weight
 C_1

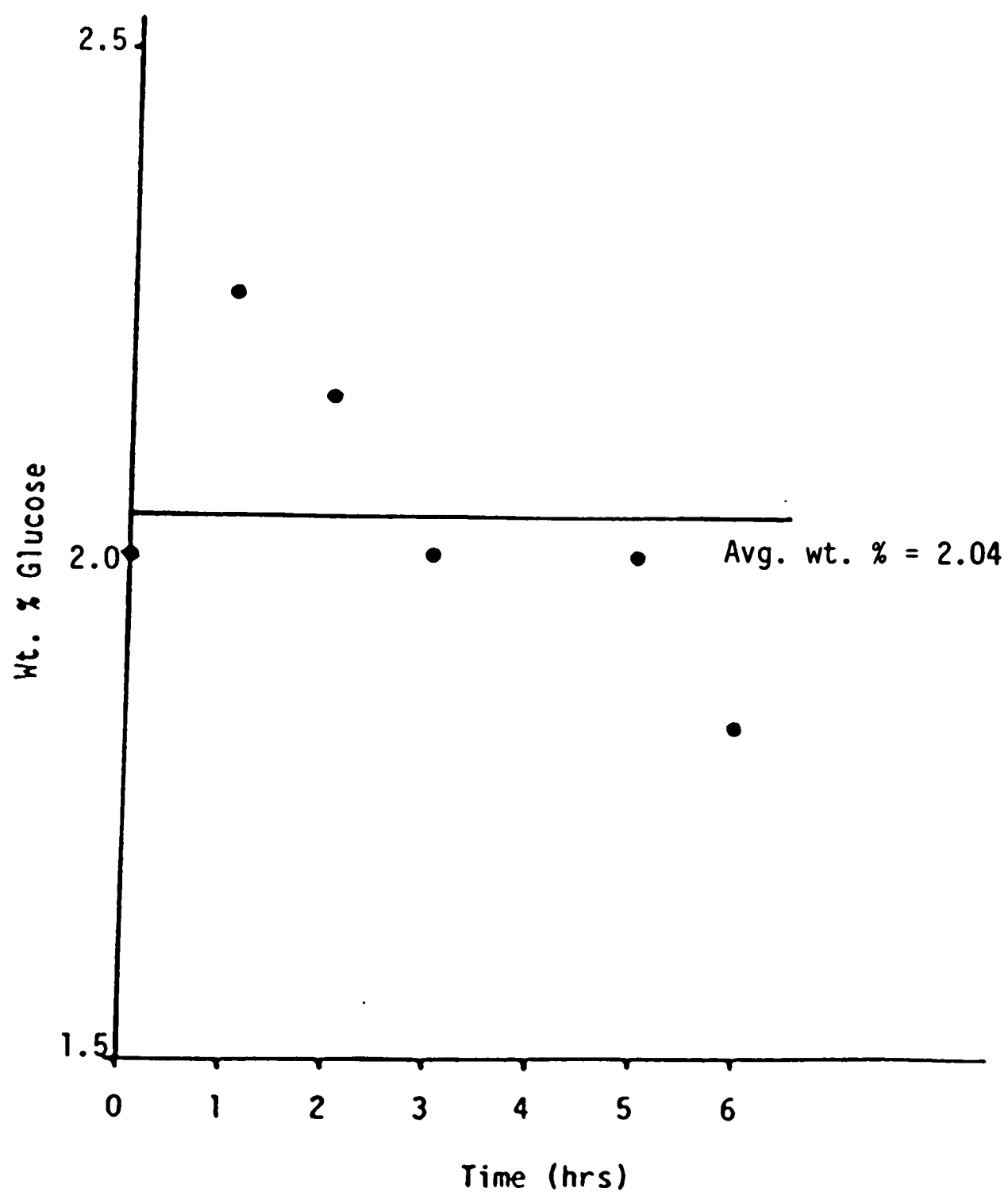


Figure G.1. Weight Percent Glucose versus Time for $T = 30^{\circ}\text{C}$, $C_i = 23.1 \text{ g/l}$, $\text{pH} = 4.5$ and $\mu = 0.373 \text{ hr}^{-1}$

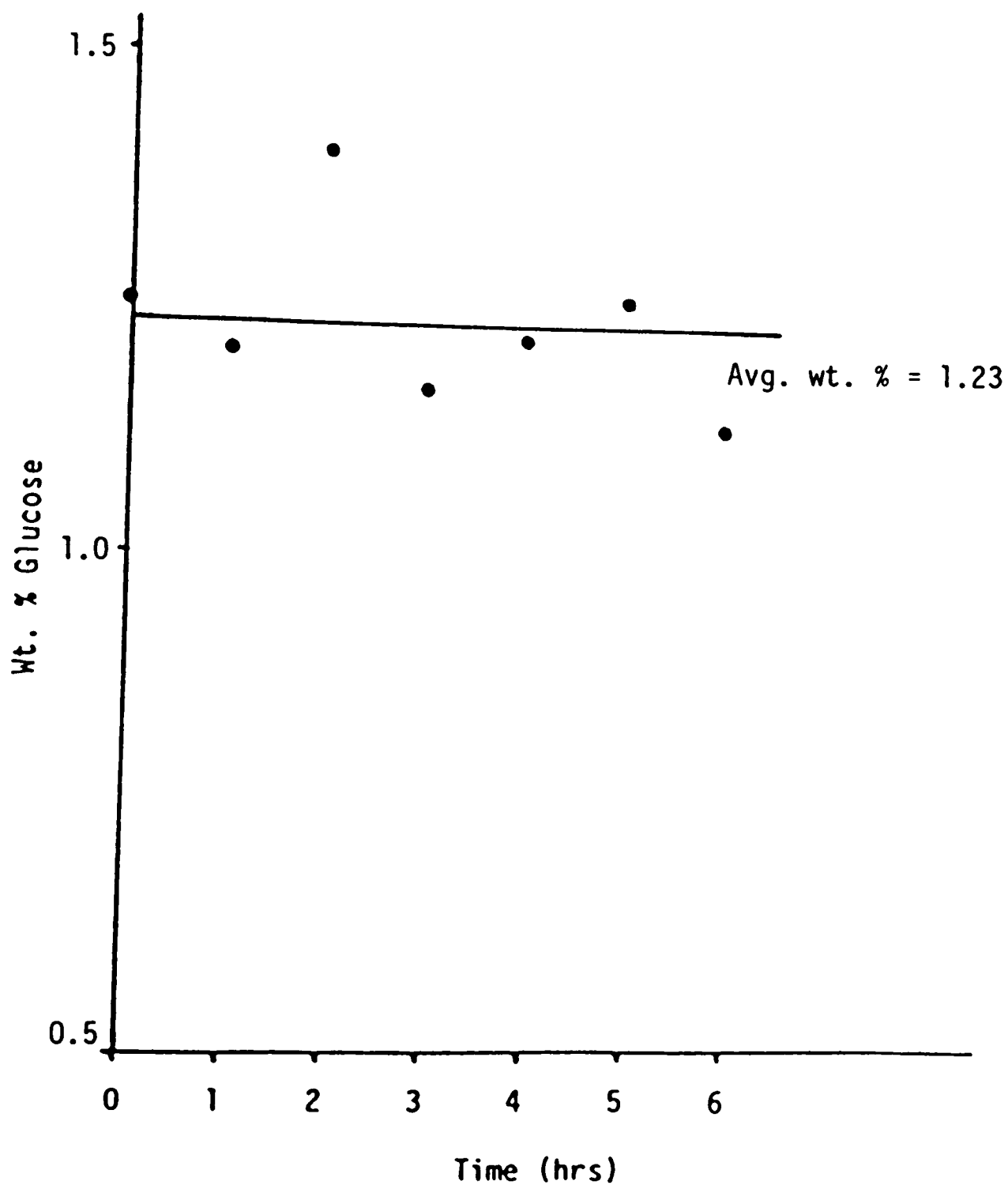


Figure G.2. Weight Percent Glucose versus Time for $T = 30^{\circ}\text{C}$, $C_i = 13.1 \text{ g/l}$, $\text{pH} = 5.0$ and $\mu = 0.396 \text{ hr}^{-1}$

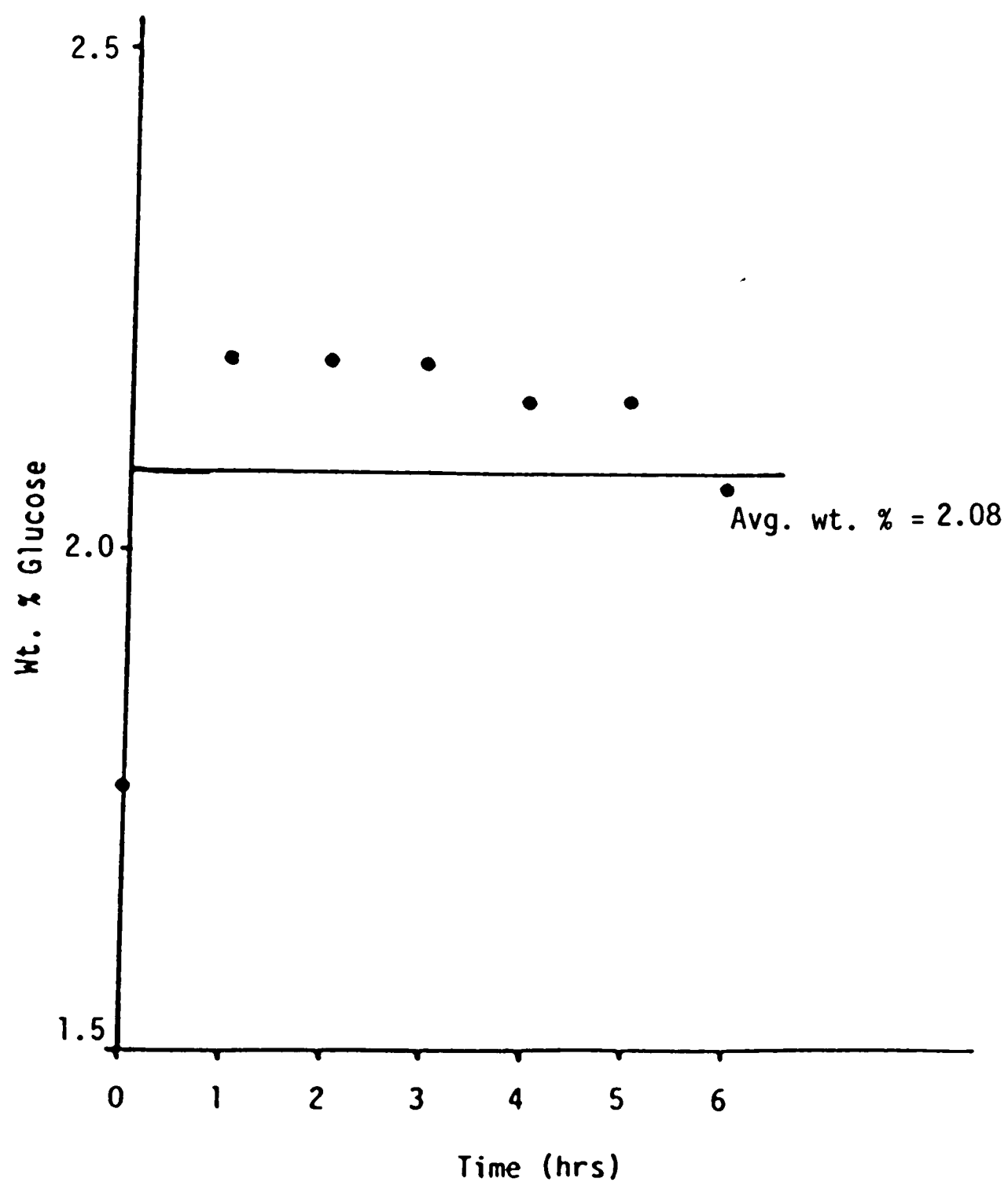


Figure G.3. Weight Percent Glucose versus Time for $T = 30^{\circ}\text{C}$, $C_i = 23.1 \text{ g/l}$, $\text{pH} = 5.0$ and $\mu = 0.507 \text{ hr}^{-1}$

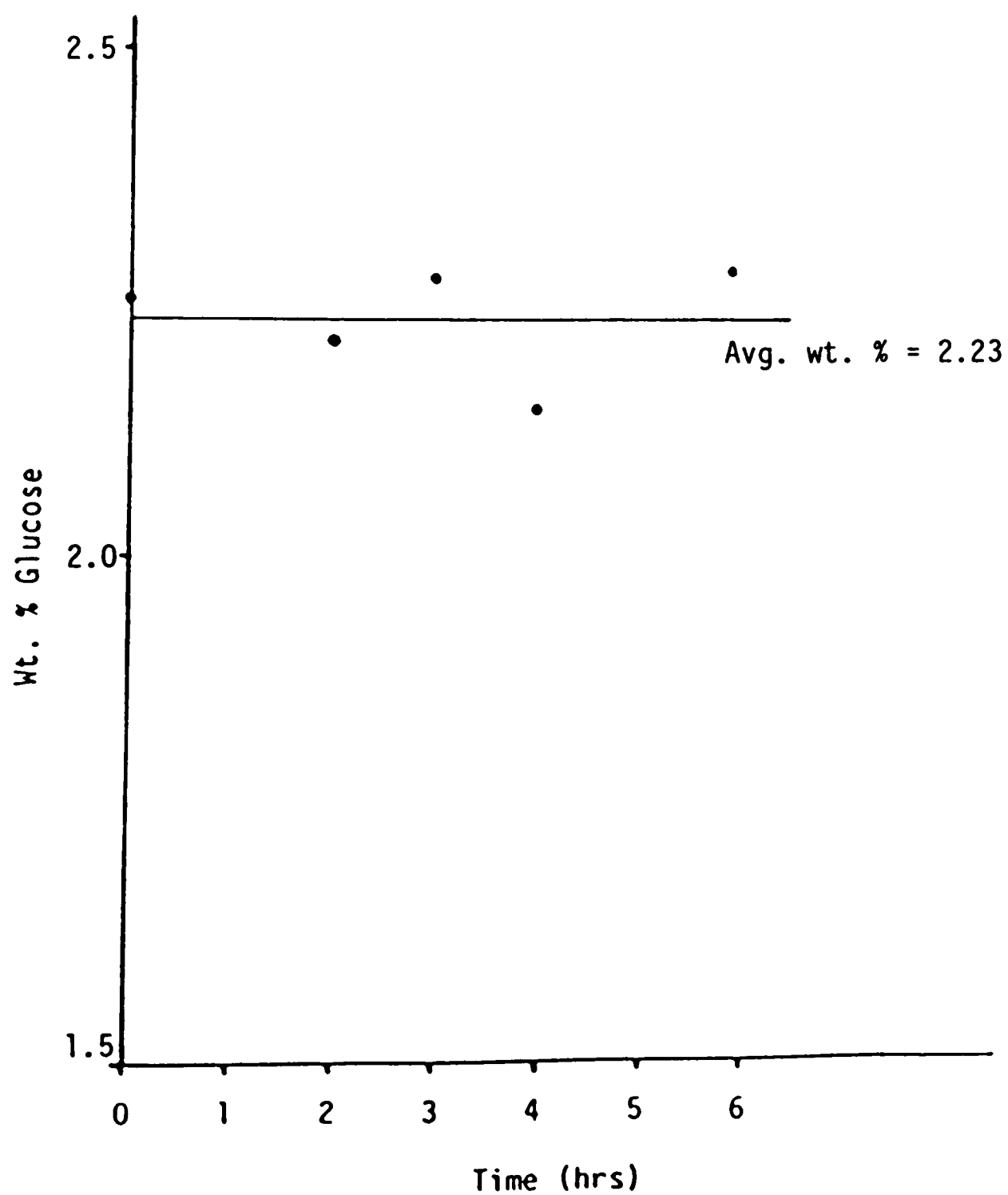


Figure G.4. Weight Percent Glucose versus Time for $T = 30^{\circ}\text{C}$, $C_i = 23.1 \text{ g/l}$, $\text{pH} = 5.0$ and $\mu = 0.500 \text{ hr}^{-1}$

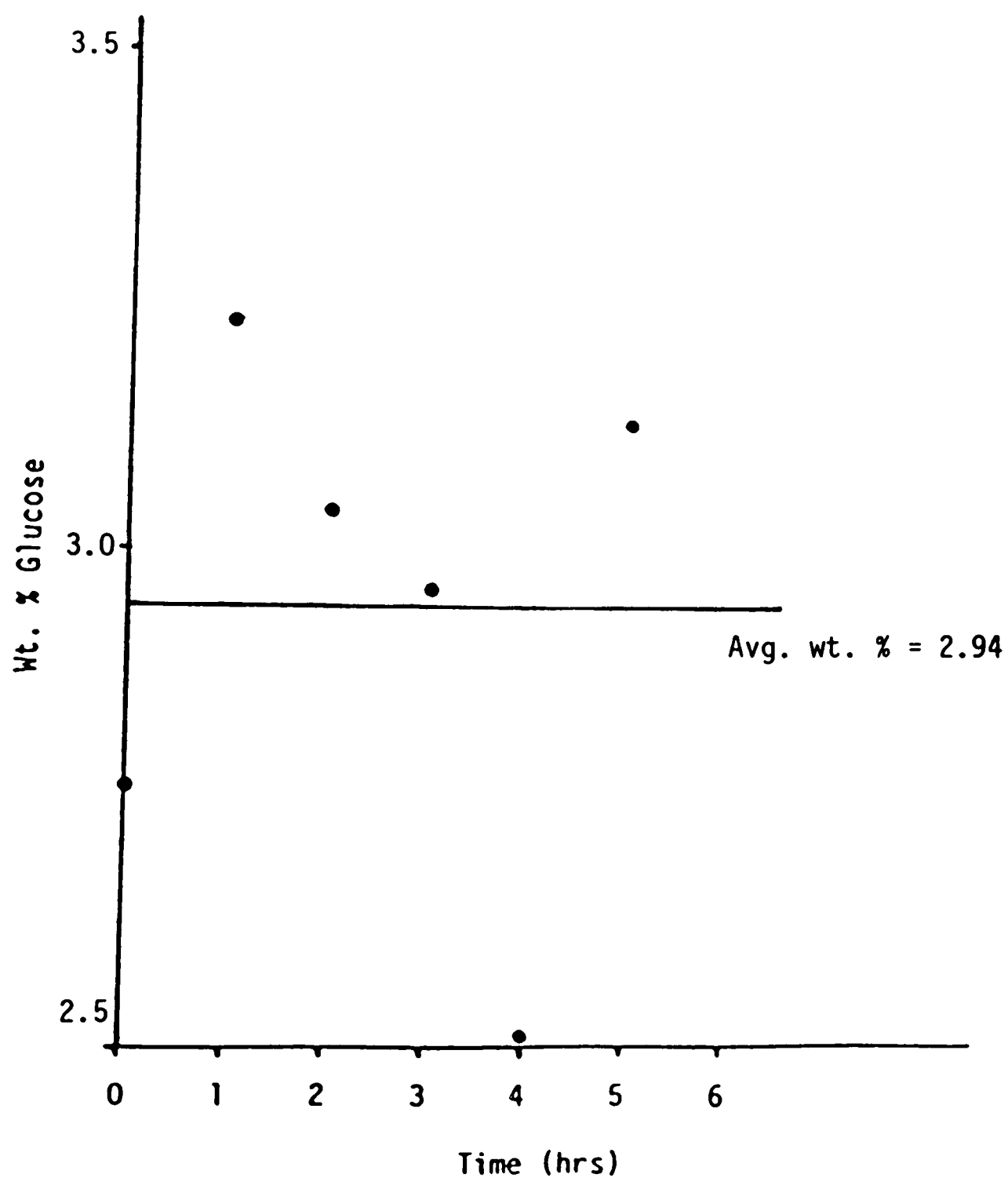


Figure G.5. Weight Percent Glucose versus Time for $T = 30^{\circ}\text{C}$, $C_i = 33.1 \text{ g/l}$, $\text{pH} = 5.0$ and $\mu = 0.576 \text{ hr}^{-1}$

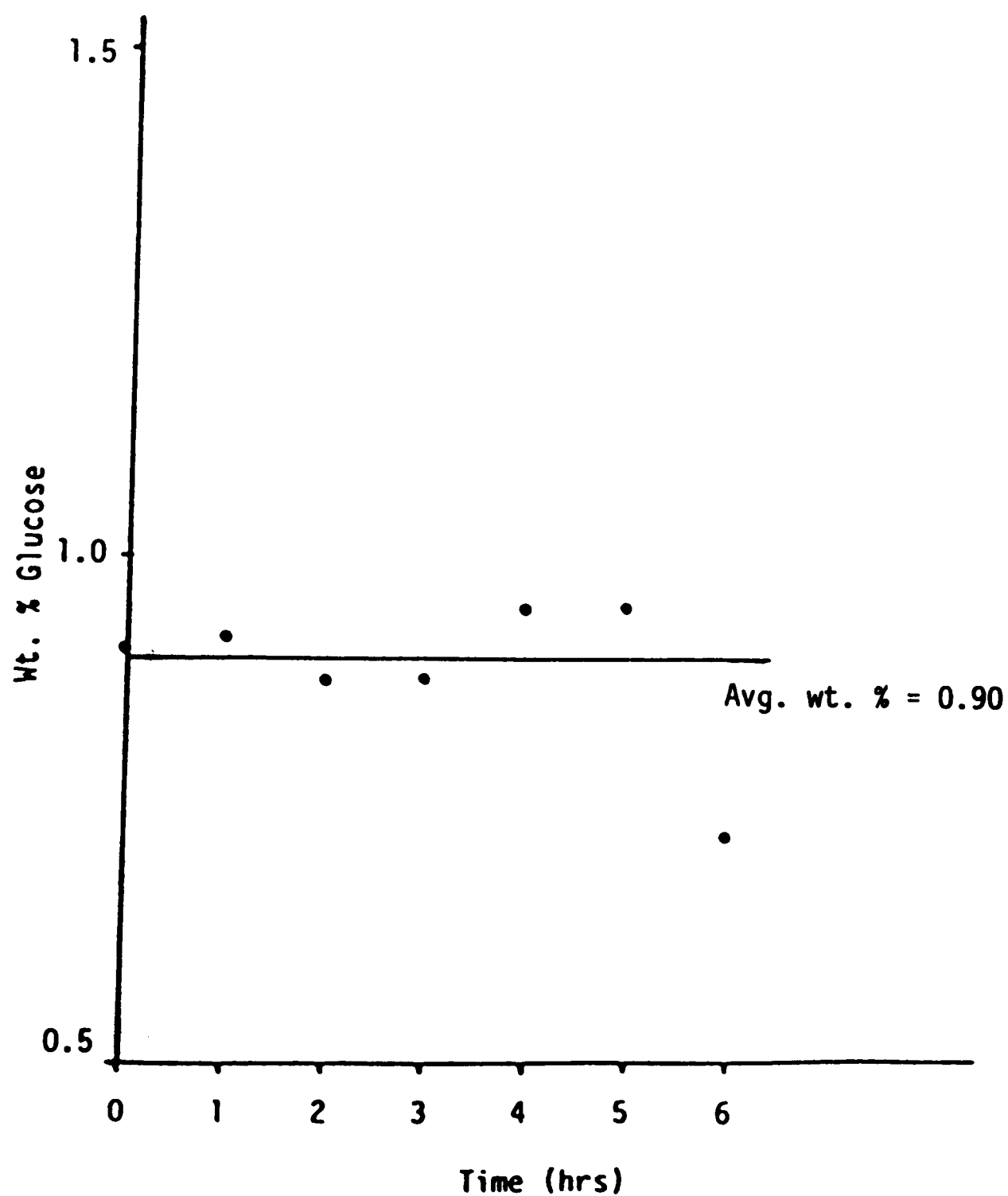


Figure G.6. Weight Percent Glucose versus Time for $T = 34^{\circ}\text{C}$, $C_i = 13.1 \text{ g/l}$, $\text{pH} = 5.0$ and $\mu = 0.403 \text{ hr}^{-1}$

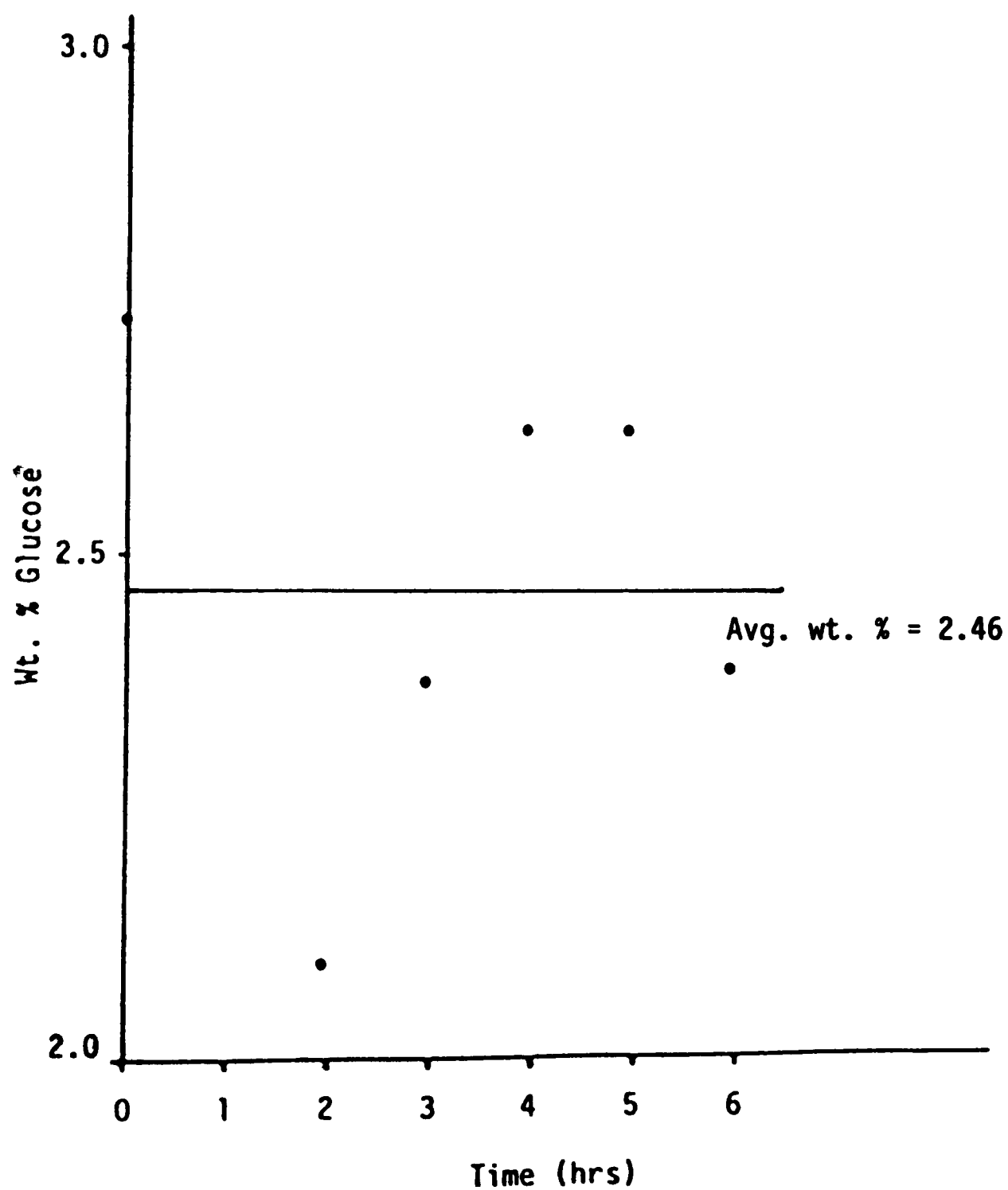


Figure G.7. Weight Percent Glucose versus Time for $T = 34^{\circ}\text{C}$, $C_i = 23.1 \text{ g/l}$, $\text{pH} = 5.0$ and $\mu = 0.532 \text{ hr}^{-1}$

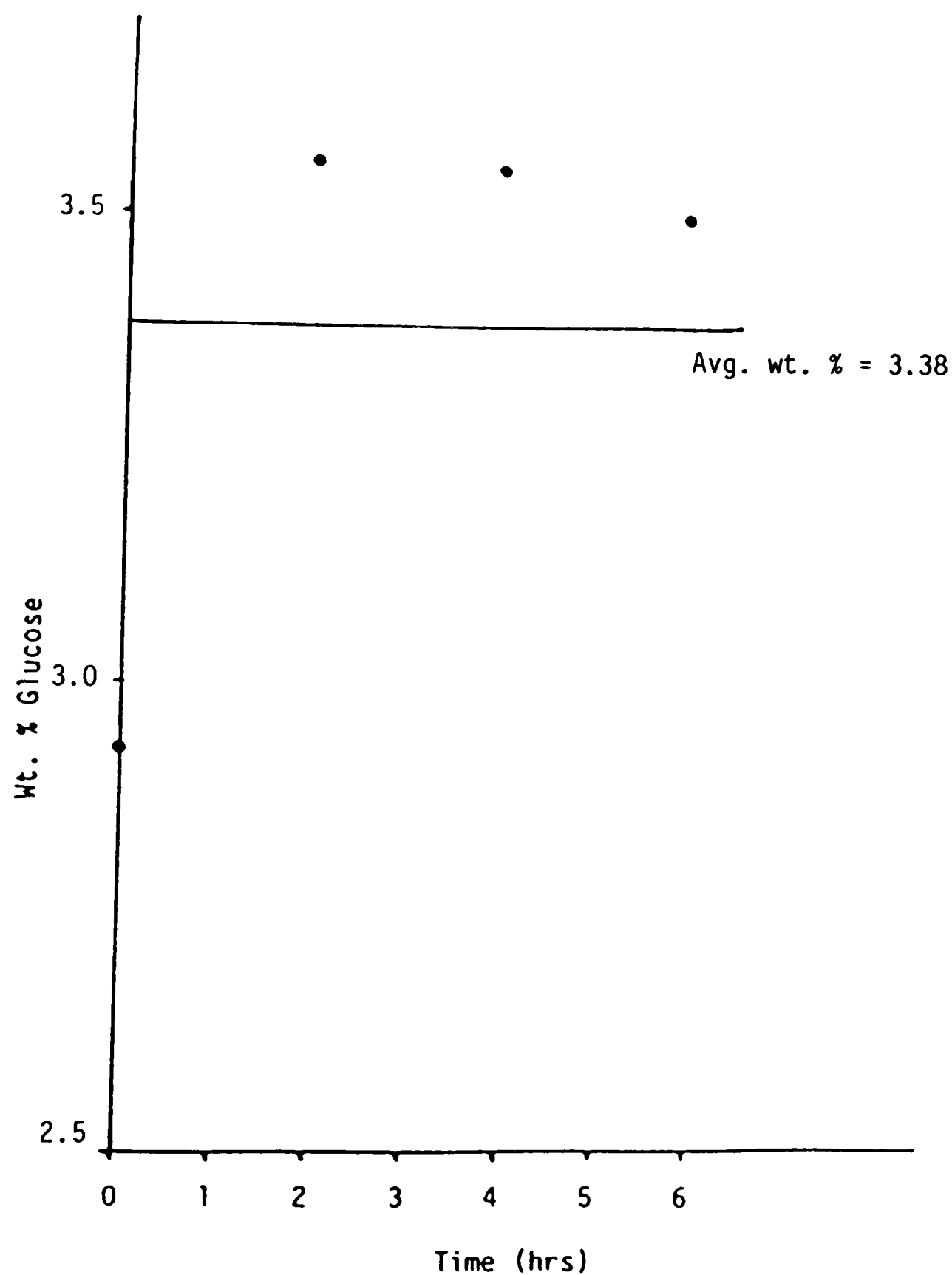


Figure G.8. Weight Percent Glucose versus Time for $T = 34^{\circ}\text{C}$, $C_i = 33.1 \text{ g/l}$, $\text{pH} = 5.0$ and $\mu = 0.586 \text{ hr}^{-1}$

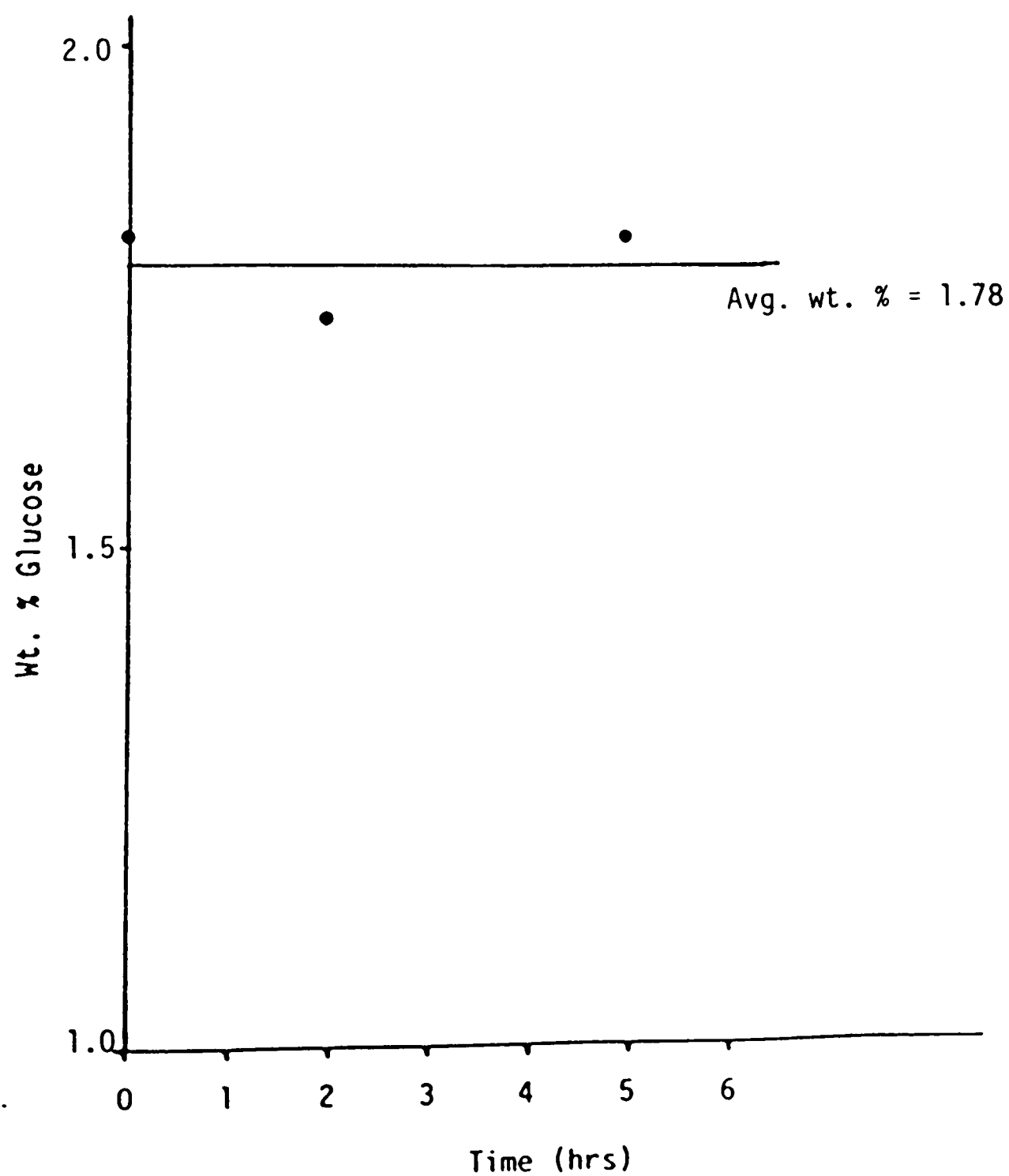


Figure G.9. Weight Percent Glucose versus Time for $T = 34^{\circ}\text{C}$, $C_i = 33.1 \text{ g/l}$, $\text{pH} = 5.0$ and $\mu = 0.600 \text{ hr}^{-1}$

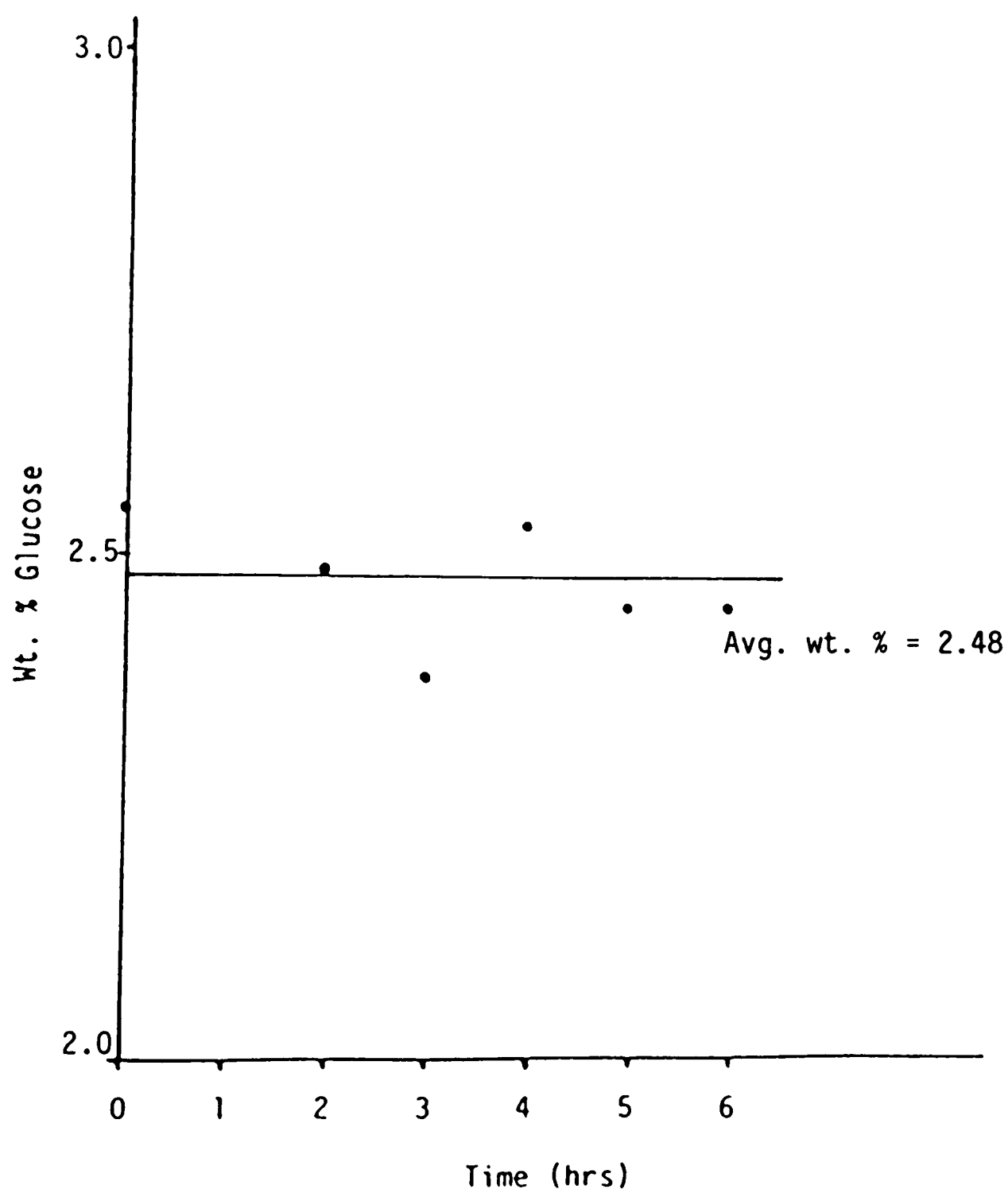


Figure G.10. Weight Percent Glucose versus Time for $T = 37^{\circ}\text{C}$, $C_i = 23.1 \text{ g/l}$, $\text{pH} = 4.5$ and $\mu = 0.143 \text{ hr}^{-1}$

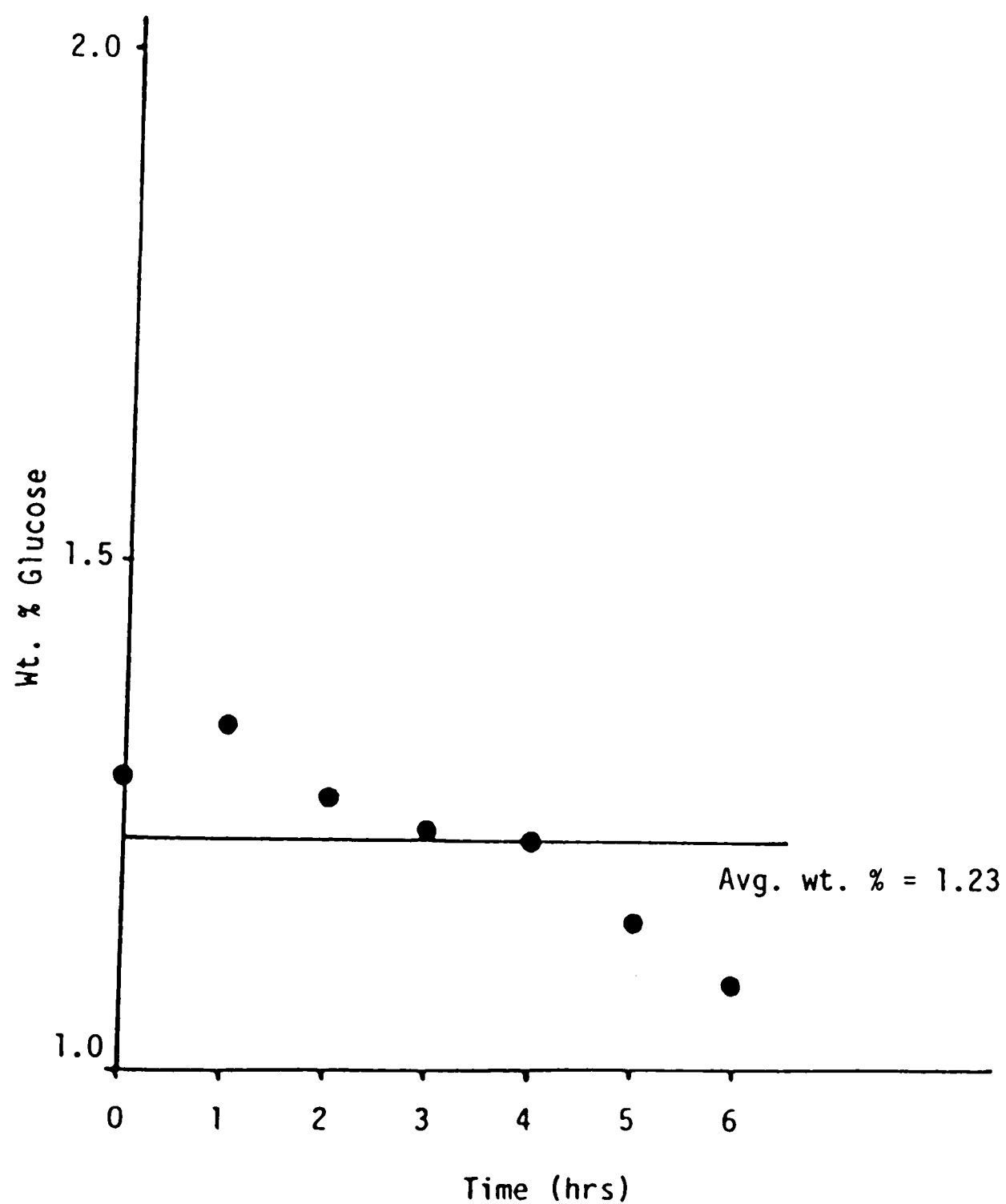


Figure G.11. Weight Percent Glucose versus Time for $T = 37^{\circ}\text{C}$, $C_i = 13.1 \text{ g/l}$, $\text{pH} = 5.0$ and $\mu = 0.426 \text{ hr}^{-1}$

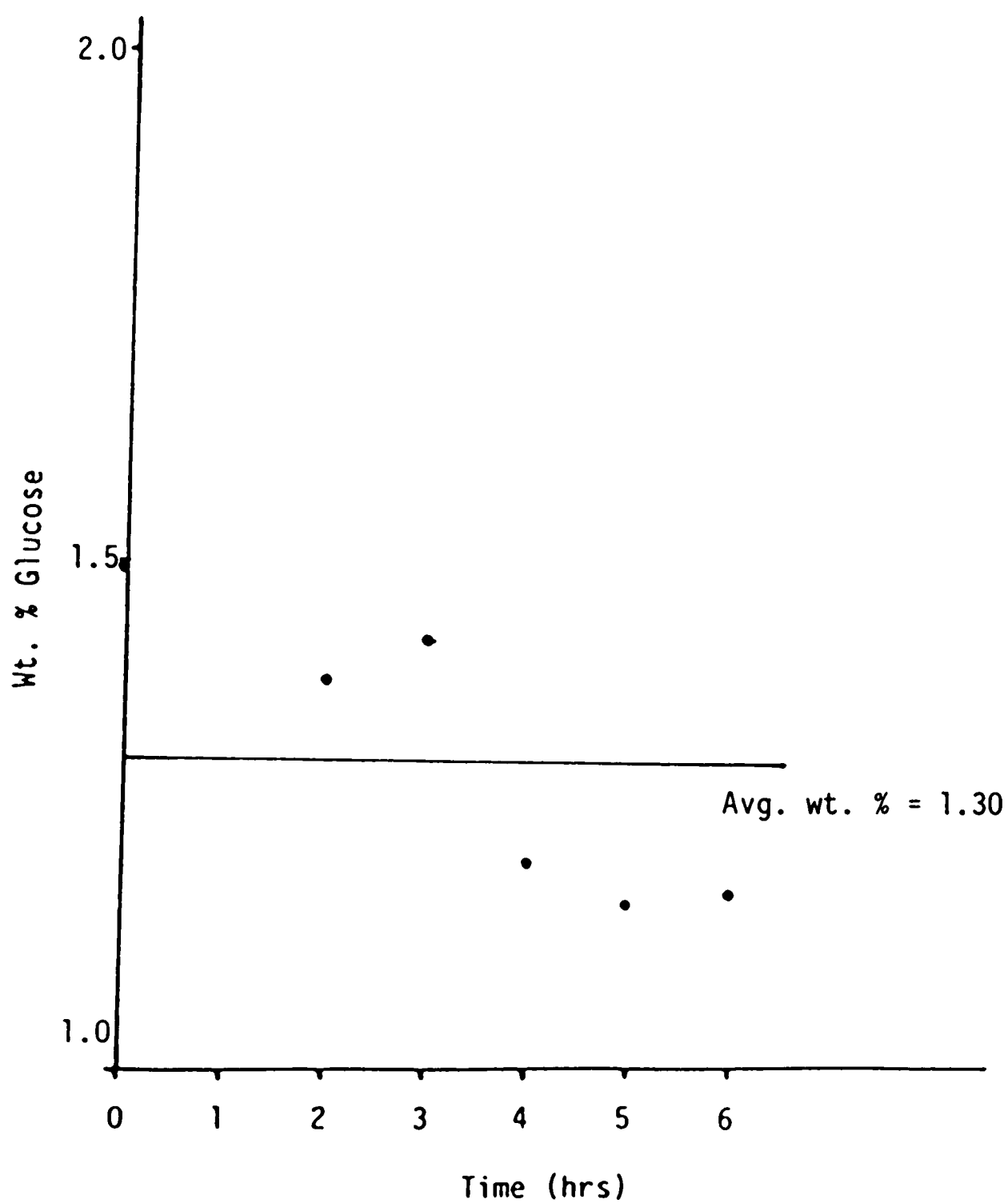


Figure G.12. Weight Percent Glucose versus Time for $T = 37^{\circ}\text{C}$, $C_i = 13.1 \text{ g/l}$, $\text{pH} = 5.0$ and $\mu = 0.447 \text{ hr}^{-1}$

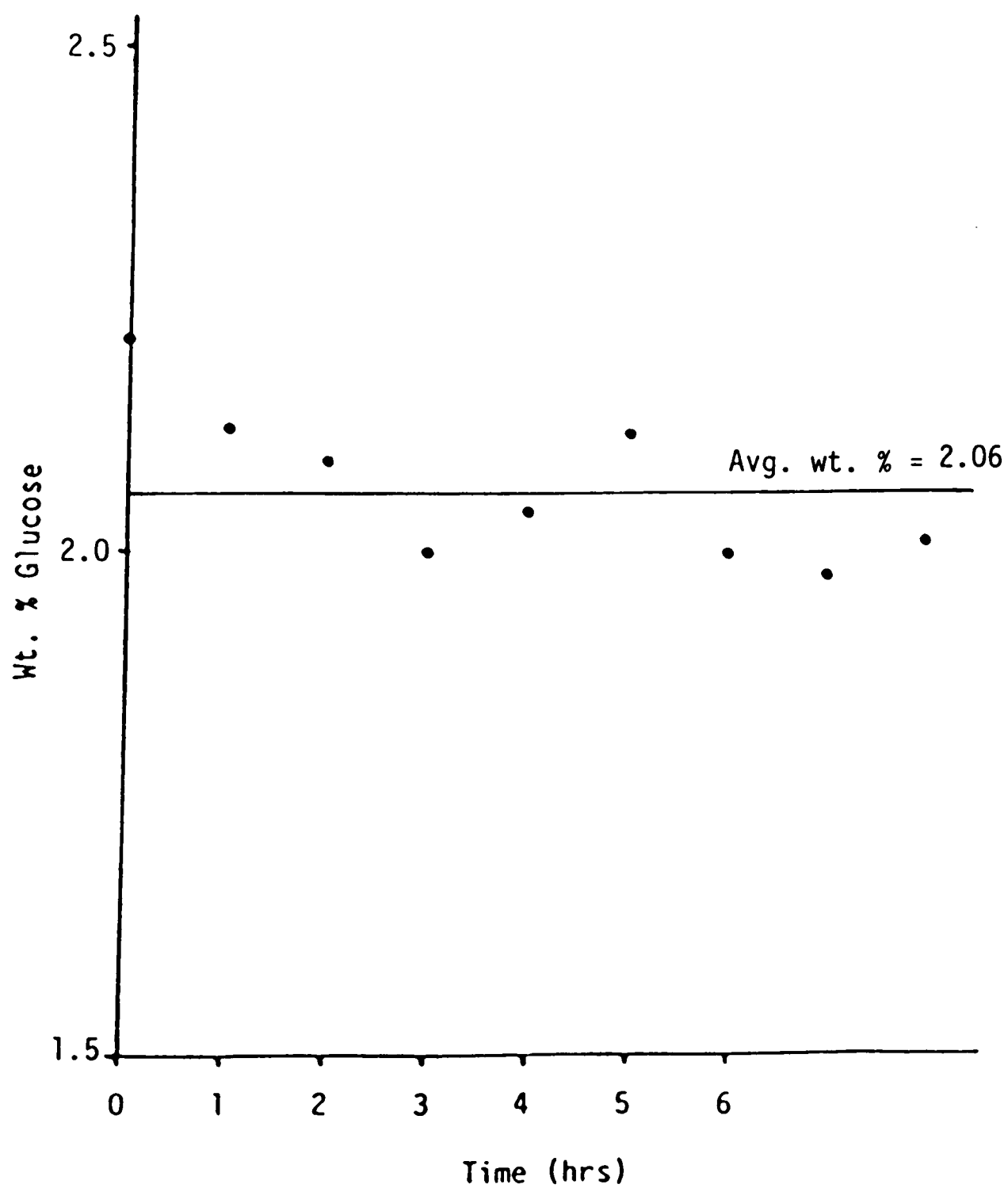


Figure G.13. Weight Percent Glucose versus Time for $T = 37^{\circ}\text{C}$, $C_i = 23.1 \text{ g/l}$, $\text{pH} = 5.0$ and $\mu = 0.564 \text{ hr}^{-1}$

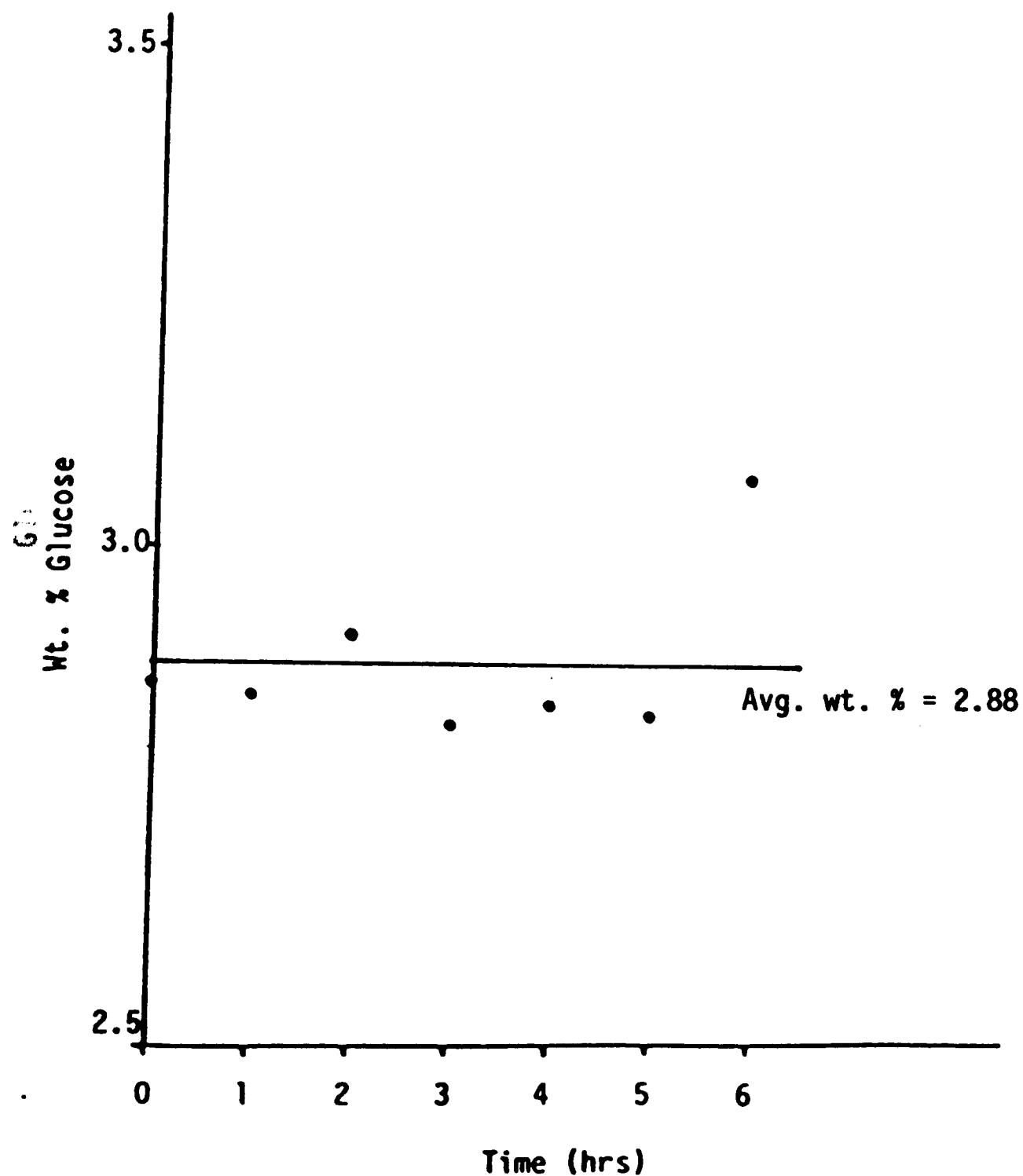


Figure G.14. Weight Percent Glucose versus Time for $T = 37^{\circ}\text{C}$, $C_i = 33.1 \text{ g/l}$, $\text{pH} = 5.0$ and $\mu = 0.682 \text{ hr}^{-1}$

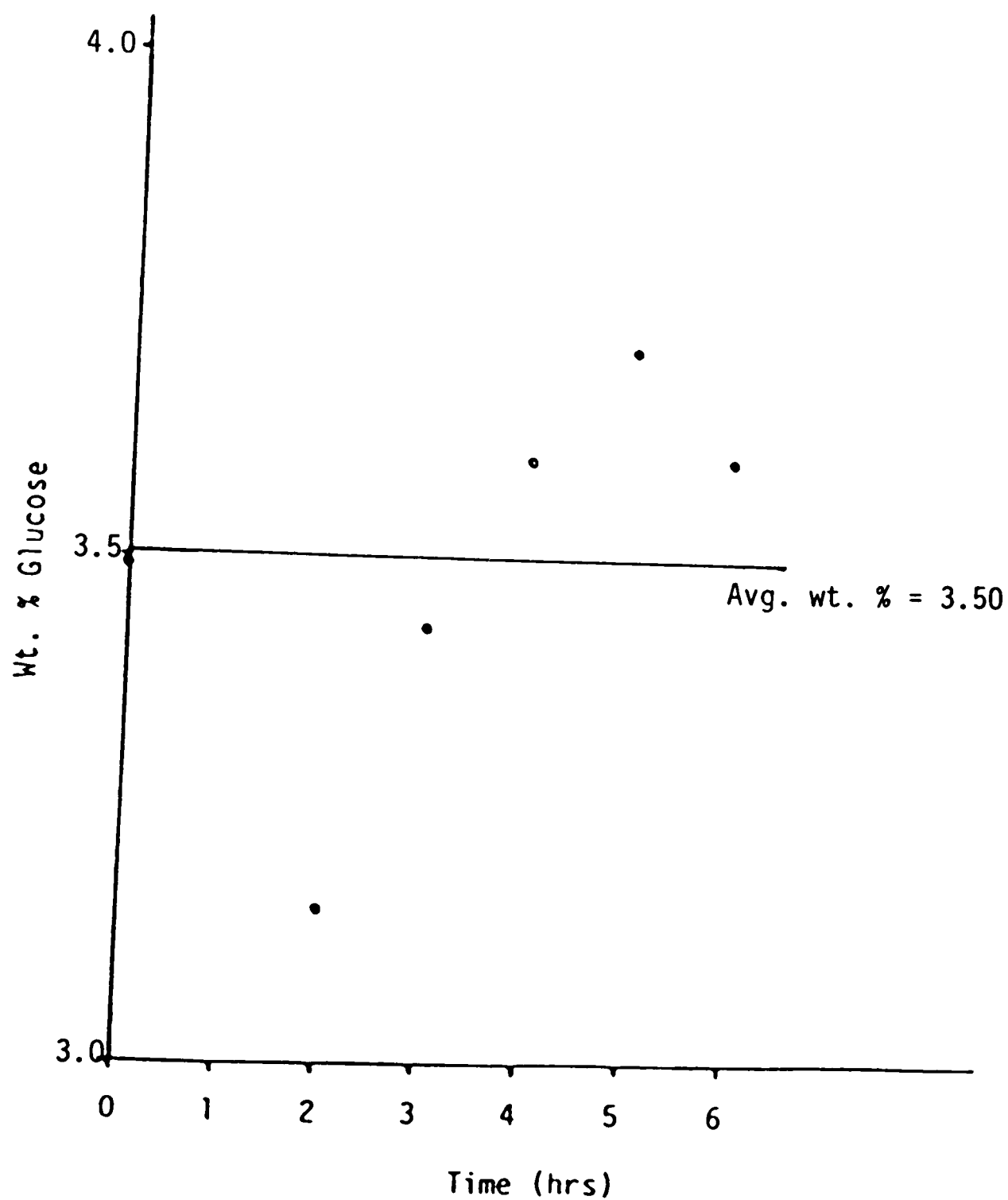


Figure G.15. Weight Percent Glucose versus Time for $T = 37^{\circ}\text{C}$, $C_i = 40.6 \text{ g/l}$, $\text{pH} = 5.0$ and $\mu = 0.684 \text{ hr}^{-1}$

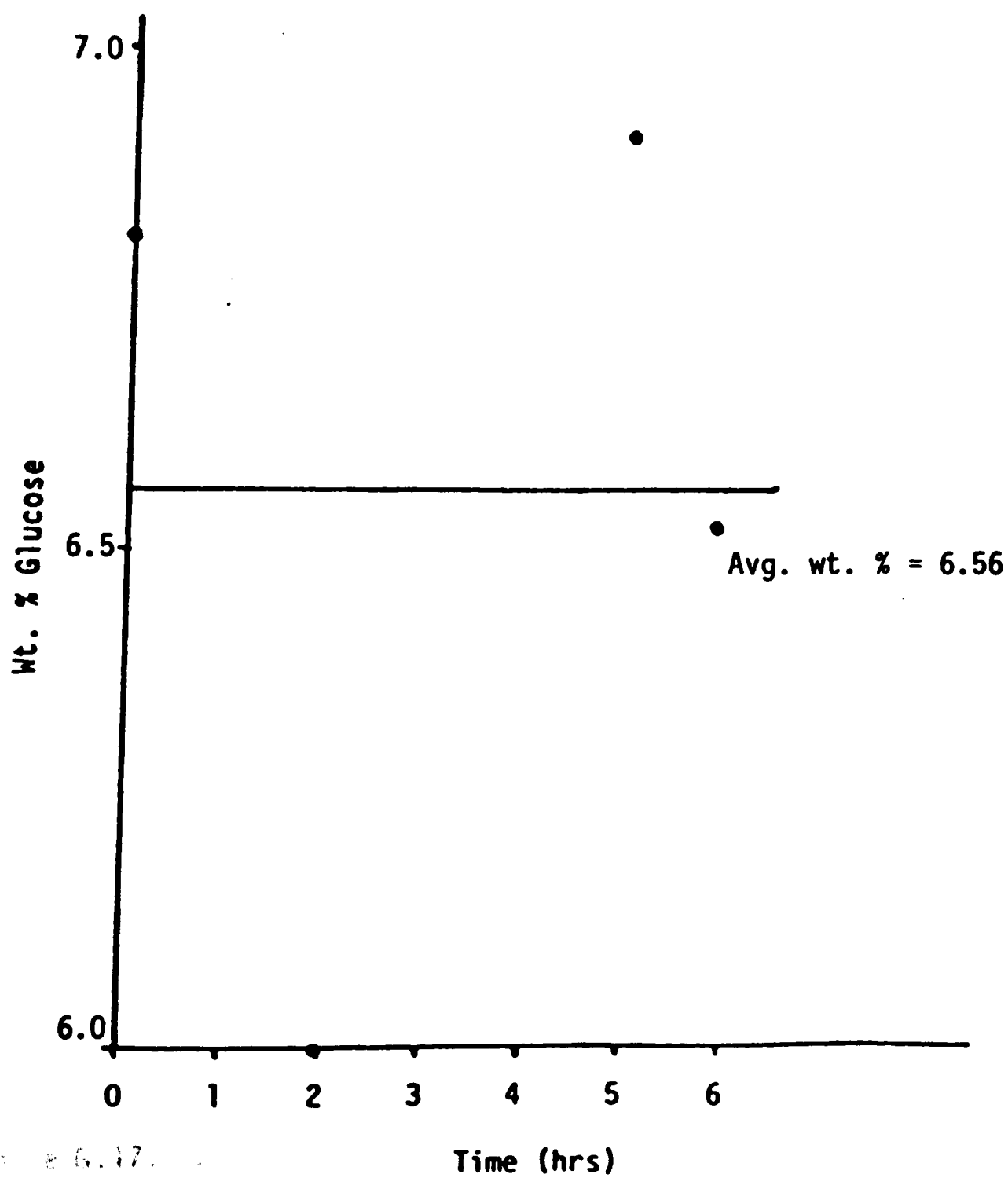


Figure G.16. Weight Percent Glucose versus Time for $T = 37^{\circ}\text{C}$, $C_i = 60.6 \text{ g/l}$, $\text{pH} = 5.0$ and $\mu = 0.677 \text{ hr}^{-1}$

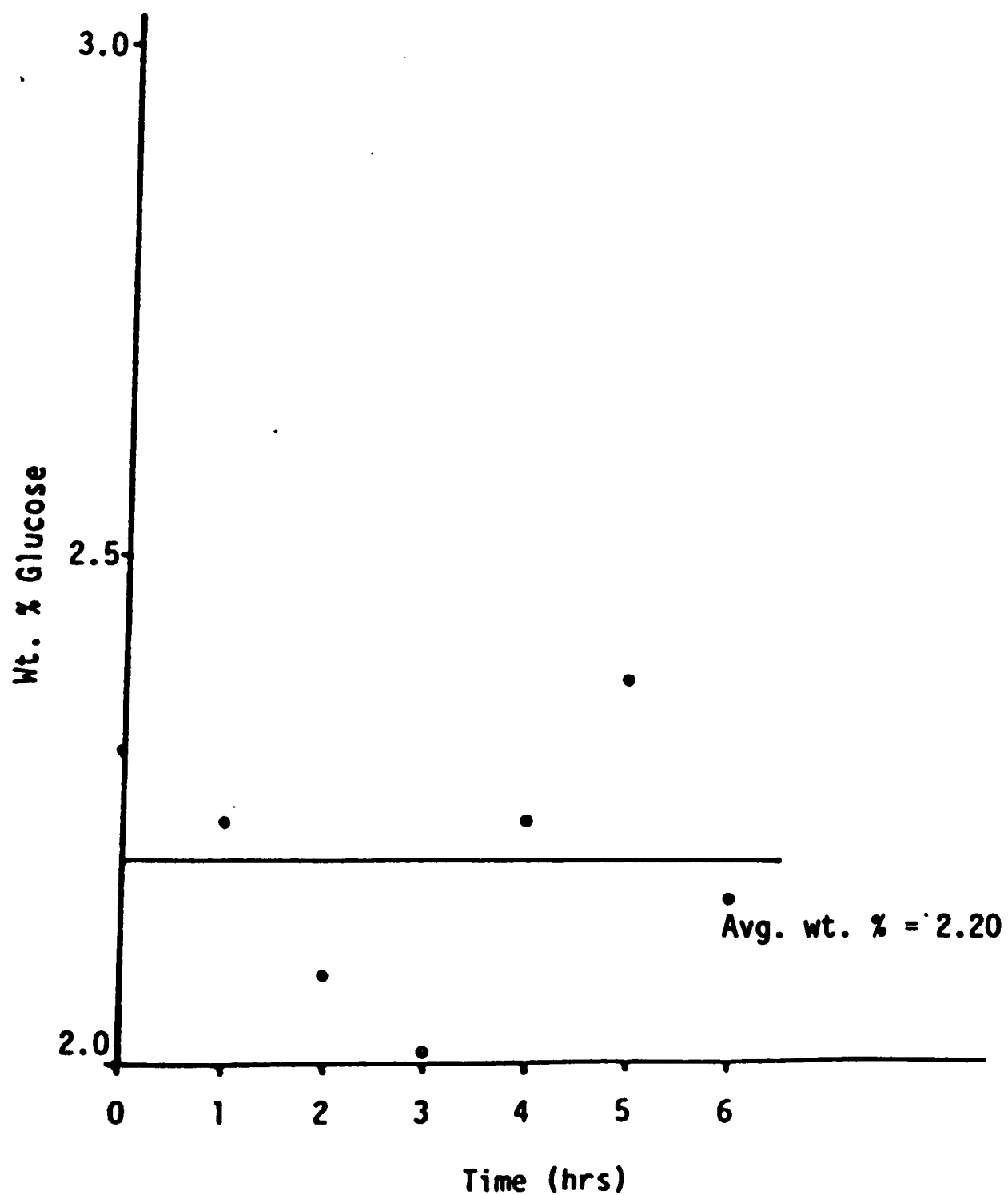


Figure G.17. Weight Percent Glucose versus Time for $T = 37^{\circ}\text{C}$, $C_i = 23.1 \text{ g/l}$, $\text{pH} = 5.5$ and $\mu = 0.341 \text{ hr}^{-1}$

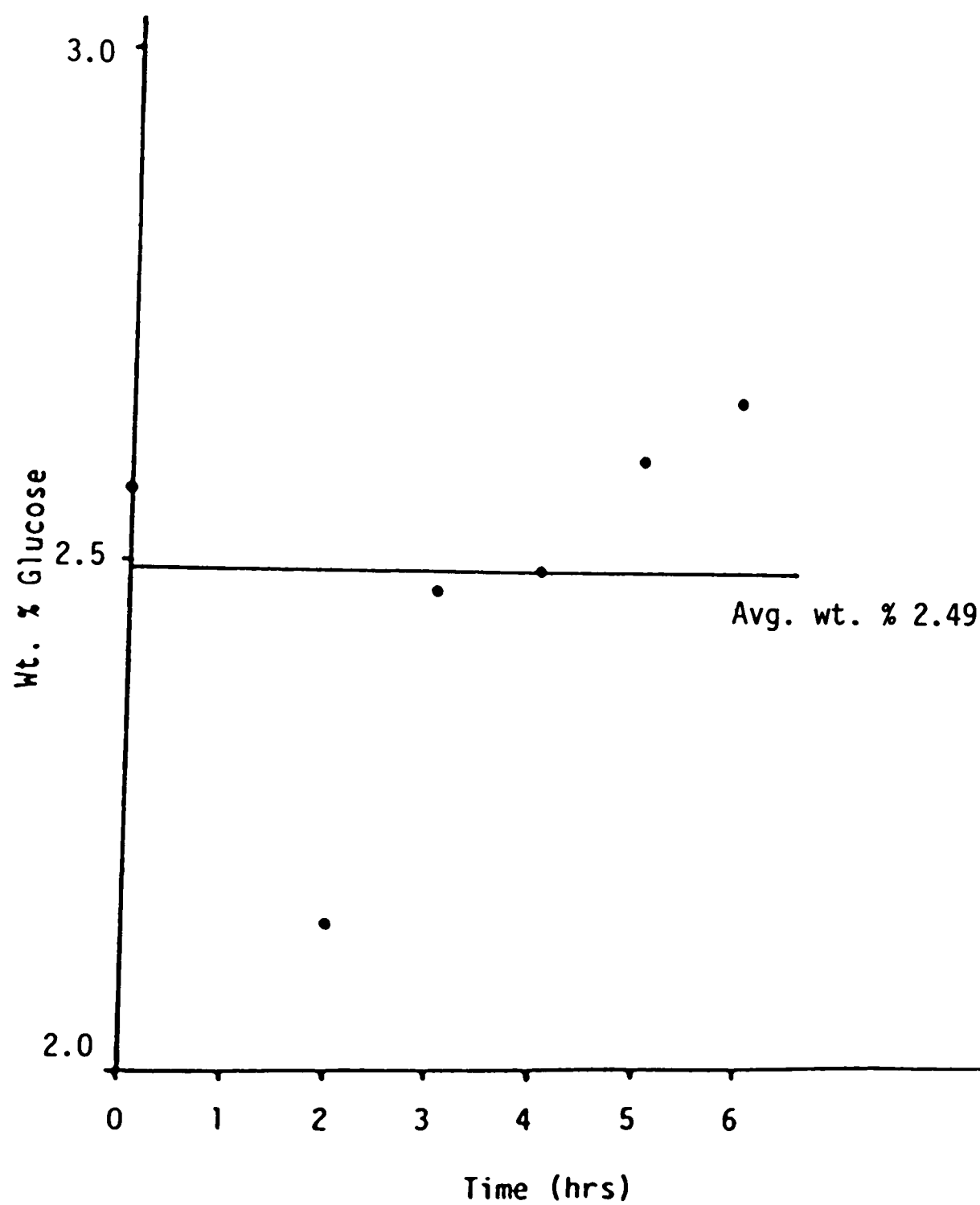


Figure G.18. Weight Percent Glucose versus Time for $T_1 = 41^\circ\text{C}$, $C_i = 23.1 \text{ g/l}$, $\text{pH} = 5.0$ and $\mu = 0.0 \text{ hr}^{-1}$

